STUDIES ON FREQUENCY SELECTIVE SURFACES FOR WIRELESS COMMUNICATION APPLICATIONS

A Dissertation Submitted in Partial Fulfilment of the Requirement for the Award of the Degree of

MASTER OF ENGINEERING

In

Electronics and Communication Engineering

Submitted By

KOMALPREET KAUR

Roll No. 801761008

Under Supervision of

Dr. Amanpreet Kaur

Assistant Professor, ECED

ELECTRONICS AND COMMUNICATION ENGINEERING DEPARTMENT

THAPAR UNIVERSITY, PATIALA, PUNJAB

JULY, 2019

DECLARATION

I, Komalpreet Kaur hereby declare that the work presented in this thesis entitled "STUDIES ON FREQUENCY SELECTIVE SURFACES FOR WIRELESS COMMUNICATION APPLICATIONS" in fulfillment of the requirement for the award of degree of Master of Engineering submitted at Electronics and Communication department T.I.E.T, Patiala is an authentic record of work carried out under supervision of **Dr. Amanpreet Kaur** (Assistant Professor) Electronics and Communication department T.I.E.T, Patiala from 2018 to 2019.

The matter presented in this thesis has not been submitted either in part or full to any other university or institute for the award of any other degree.

Date: 12/7/2019

Komalpreet Kaur 12/7/19

Komalpreet Kaur

Roll no: 801761008

It is certified that above statement made by the candidate is correct to the best of my knowledge and belief.

Date: 12/7/19

Amanpreet Kaur

Dr. Amanpreet Kaur

Assistant Professor

Electronics and Communication Department

Thapar Institute of Engineering and Technology

(A Deemed To Be University), Patiala, Punjab

ABSTRACT

Wireless communication technology has covered many progressive paths and has upgraded performance and proficiency in the communication environment in term of removal of unwanted signal from the desired ones. To overcome or minimize the problem of interference of the unwanted signals from nearby frequency bands microwave special filters have been proposed that are called frequency selective surfaces (FSS). FSS is an array of periodically arranged of metallic patches or apertures on the dielectric substrate that shows total reflection and transmission, respectively. However, the transmission response of the FSS structures is basically a function of frequency, angle-of-incidence (AOI) and polarization of the incoming waves. Their inherent features that results from their specific design make them a potential candidate to use as spatial filters in variety of microwave applications such as radomes and satellite communication. In addition to this, the miniaturization as well as angular and polarization stability of the structure are the potential issues. Thus the research work presented in this thesis is based on design and simulated miniaturized FSSs that are less sensitive to both angle of incident and mode of polarization. In addition to this, presented work also include the utilization of FSSs to enhance the gain of CPW fed MPA antenna.

The research work starts with the design and simulation of a SSLFSS (Single Square Loop Frequency Selective Surfaces) structure that offers stop band properties for IEEE.802.11b (2.4 GHz) and a complementary unit cell of the proposed stop band unit cell that shows pass band properties for the same IEEE 802.11b band. Secondly a Fan shaped FSS structure for dual pass of S (1.44 GHz-4.64 GHz) and X (6.32 GHz-12.17 GHz) band is designed and a complimentary and optimized structure of pass band is designed that offers dual stop band transmission characteristics for S (2.06 GHz- 4.4 GHz) and X (7.93 GHz-12.45 GHz) bands respectively. Then the fractal FSS structure with ultra-wide stop band (3.48 GHz to 12.31 GHz) properties is designed that is placed behind the ultra-wide band CPW fed antenna (3.39 GHz to 12.98 GHz) to improve its gain by 2.5 dB approx. All the proposed FSS structures including CPW antenna design and simulated using CST microwave studio 2016. Two FFSs; one Fan shaped FSSs and second is complimentary of the Fan shaped FSSs are fabricated using photolithography process and tested using two horn antenna and VNA for transmission parameters. The measured results are quite matching with simulated ones, allowing the FSS prototype to be suitable to work as a special filters for satellite navigation, telecommunication, Aircraft surveillance, amateur radio, Bluetooth, Zig-Bee, communications satellites, microwave devices, mobile phones , WLAN, Wi-Fi etc.

ACKNOWLEDGEMENT

I wish to express my deep gratitude and sincere thanks to my Supervisor, **Dr. Amanpreet Kaur** Assistant Professor Electronics and Communication Department, Thapar Institute of Engineering and Technology Patiala, Punjab for her invaluable guidance, constant encouragement, constructive comments, sympathetic attitude, and immense motivation, which has sustained my efforts at all stages of this work. Her valuable advice and suggestions for the corrections modifications and improvement did enhance my work.

I would like to express my gratitude to **Dr. Alpana Agarwal**, the Head of Electronics and Communication Department, Thapar Institute of Engineering and Technology Patiala, Punjab for providing me with adequate environment in carrying out the work.

Also, I would give special thanks to **Dr. Rajesh Khanna,** Professor, Electronics and Communication Engineering Department for sharing his knowledge and allowing me to use the experimental facilities to test my fabricated FSS prototype.

My greatest thanks are to all who wished me success especially my parents. Above all I render my gratitude to the Almighty who bestowed self-confidence, ability and strength in me to complete this work for not letting me down at the time of crisis and showing me the silver lining in the dark clouds. I do not find enough words with which I can express my feelings of thanks to my dear friends for their help, inspiration and moral support which went a long way in successful competition of the present study.

Komalpreet Kaur

TABLE OF CONTENTS

LIST OF FIGURES

LIST OF TABLES

LIST OF ABBREVIATIONS

FSSs	Frequency Selective Surfaces
AOIs	Angle of Incidence
SSLFSS	Single square loop frequency selective surfaces
L	Inductance
C	Capacitance
EC	Equivalent Circuit
TE	Transverse Electric field
TM	Transverse Magnetic field
CST	Computer Simulation Technology
VNA	Vector Network Analysis
WLAN	Wireless Local Area Network
Wi-MAX	Worldwide Interoperability Microwave Access
B.W	Bandwidth
CPWA	Coplanar Wave Guide Antenna
MPA	Microstrip Patch Antenna
VSWR	Voltage Standing Wave Ratio
FBW	Fractal Bandwidth
THz	Terahertz
GHz	Gigahertz

CHAPTER 1

INTRODUCTION

Wireless communication technology has experienced different phases of progress since two decades of its emergence [1]. It has covered many progressive paths and has upgraded performance and proficiency in the communication environment in term of removal of unwanted signal from the desired ones [2].The EM signals while travelling through free space environment suffers from interference caused due to the signals travelling in nearby wireless communication bands. This interference from nearby wireless environment weakens the desired wireless signals and therefore it is an essential consideration when working with wireless networking [3]. To overcome or minimize the problem of interference of the unwanted signals from nearby frequency bands microwave special filters have been proposed by many researchers and are called frequency selective surfaces [4-5-6].

1.1 FREQUENCY SELECTIVE SURFACES

These microwave filters i.e. Frequency selective surfaces (FSS) are used as spatial filters in microwave, optical and infrared ranges. FSS allow the specific frequency bands to pass through and block or stop the unwanted electromagnetic signals from unwanted frequency band. FSSs are also used to diminish the volume and expand the capability of anti- jamming of some multiband- electronic systems[7].FSS can act as a Band Pass filter , Band reject filter but along with this it has some more applications like it can be used in high performance devices. The examples of these devices are beam splitter and polarizers. FSSs can be applied as absorbers, high impedance surfaces, electromagnetic band-gap materials, and electromagnetic shields in the microwave and millimeter wave regimes.

A frequency selective surface (FSS) structure is a two dimensional periodically arranged array of metallic patches or apertures/slots imprinted on a dielectric substrate and the resultant structure performs as a spatial filter for the incoming electromagnetic waves and offers selectivity in frequency for angle-of-incidence (AOI) and polarization of the incident waves [8]. The FSS can be mainly classified as high-pass, low-pass, pass band and stop band filters. Their inherent features that results from their specific design make them suitable to control the propagation of electromagnetic energy for a specific frequency and angle of incident for operation as a Microwave filters [8-9]. Some specific types of the FSSs are explained in next subsection.

1.2 TYPES OF FSS AVAILABLE

FSSs works as a spatial filter which offers either the pass band or the stop band transmission characteristics for numerous practical applications of electromagnetic scattering problems [10-11]. The smallest part of the FSS that contains one or more elements, is well known as a unit cell. These unit cells structure are organized periodically, in required dimension such as one or two, to construct the entire structure of FSS. Normally, the unit cell structure contains patch elements on substrate or maybe

it's complementary geometry i.e. aperture element of different shapes or size on a substrate [11-12]. The incoming EM impinging on the FSS structure either gets reflected or transmitted about its resonant frequency for which it has been designed. Transmission or reflection characteristics of the FSS depend upon its designed geometry. FSSs that contain conductive patch elements on substrate reflect the incoming EM wave of a specific frequency while it's complimentary i.e. aperture elements transmit the incoming EM waves of a certain frequency band [12].

Based upon the size and shapes of the unit cell elements FSSs may be classified as:

1) Low pass FSS
2) High pass FSS
3) Band pass FSS
4) Band stop FSS

Figure 1.1 depicts the basic responses (Band stop, Band pass, Low pass and high pass) of frequency Selective Surfaces.

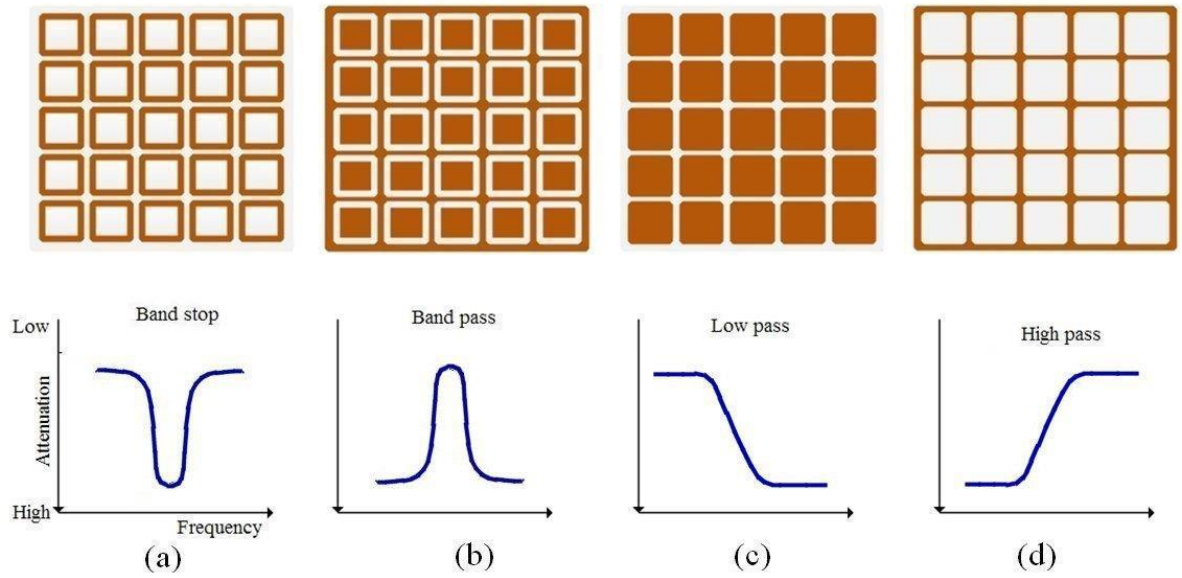

Figure 1.1 Characteristics response for (a) Band stop, (b) Band pass, (c) Low pass and (d) High pass [12]

In addition to these four conventional geometries there are some more different types of FSSs structure that have been proposed by many researchers for multiband, dual band, ultra wide band application.

1.3 PHYSICAL MECHANISM OF FSSs

The study of FSSs and their relationship with electromagnetic waves were first reported in the mid-1960s. Furthermore, there are numerous studies on FSS that have been recorded [13]. The patch and aperture type FSS geometries ideally demonstrate reflection and transmission characteristics, respectively, in the region of the fundamental resonant frequency. Various geometrical factors like its size, spacing between elements, periodicity of FSS structure, and parameters of dielectric substrate,

presence and absence of super substrate control the overall frequency response of FSS structure, its bandwidth, and dependency of output response on the angle of incident and polarization mode of incoming electromagnetic wave. Thus, in order to design an FSS structure for a desired frequency response; the selection of the substrate, shape and size of elements are the prime requirements. The patch geometry on dielectric substrate mainly decide the pass/stop band characteristics to be offered by it.

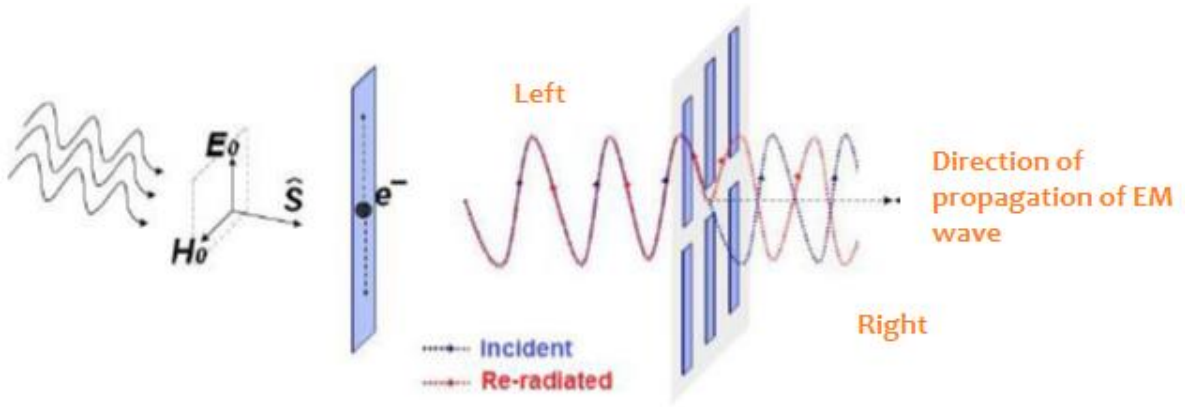

(a)

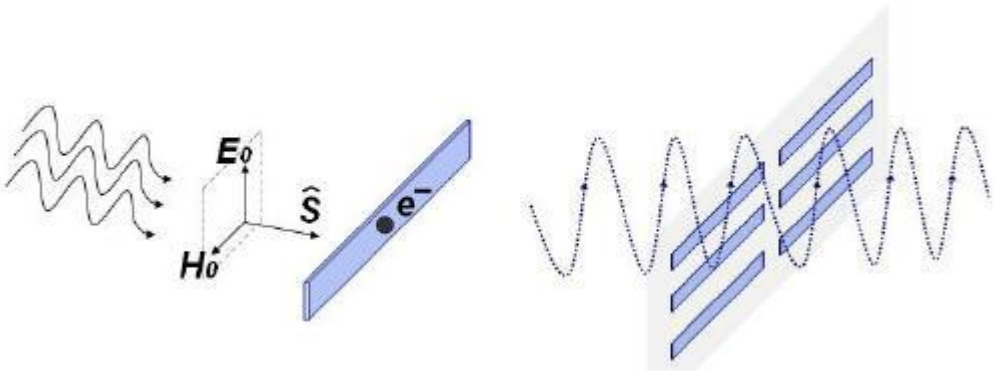

(b)

Figure 1.2. The basic filtering mechanism of FSS structure for E-vector (a) parallel and (b) Orthogonal to the metallic dipole [14].

In order to explain the physical mechanism of the FSS filtering characteristics, there are two scenarios of the incoming EM wave has been depicts in Figure 1.2. In the first set-up, a plane wave strikes on a metallic dipole of the FSS structure in such a manner that the orientation of electric field is along the height of dipole while FSS structure is oriented orthogonal to the Poynting vector [14]. As the vector of electric field is oriented toward the length of the dipole, it oscillates the electrons hence the percentage of incidence plane wave energy is converted into kinetic energy and gives rise to re-radiated waves/energy. Re-radiated waves/energy from the FSS structure cancels out the effect of incident waves which are at the left side of the FSS structure. This re-radiated energy on the left hand side of the FSS structure denotes the reflected waves and for this setup, low transmittance through the FSS filter is

shown [14]. In the second setup, the electric field vector is orthogonal to the parallel metallic dipole FSS, which is shown in Figure 1.2(b) [14]. In this case, the electrons do not re-radiate because of their inability to oscillate up and down. Therefore, the FSS structure remains invisible to the incident plane waves and total transmission occurs or transmittance will be higher for this case. Similarly different type of patch geometries used for FSS shows different pass band /stop band properties according to their resonant use. Some factors that affect the FSS performance and its response are explained in the next subsection.

1.4 FACTORS AFFECTING THE FREQUENCY RESPONSE OF THE FSSs

There are several factors, which affect the overall response and performance of the FSS structures, out of which the some important ones are:

1) Shape and parameters of the Unit cell element
2) Angle of incidence
3) Polarizations of the incident wave
4) Element conductivity

1.4.1 Shape and Parameter of the Element [8-15]

The shape and size of the unit cell structure of the FSS has the potential to provide the required frequency response for FSS operation [16-17]. The FSS structure consists of a conductive element pattern on the dielectric substrate whose shape depends upon the application for which the proposed FSS structure has to be used. Munk [8], defined the different shape of the conductive pattern of the Frequency Selective Surfaces into four simple parts:

1) Centre connected or N-pole type: These are one of the simple straight elements and include three legged elements such as dipoles, tri-poles, cross dipoles, anchor shaped elements and Jerusalem shaped cross elements etc.

2) Loop type: Such elements include square loop, circular loop and hexagonal loops for FSS structure.

3) Solid interior type: These type of FSS elements contain patch type geometry like square shaped meshes and circular shaped patches.

4) Combination type: Such type of FSS elements can be achieved effectively by combination of the above mentioned geometries.

Depending upon the application of FSS in the real world, each shape of unit cell structure of FSS has its own advantages and limitations. Some of the N-pole type shapes of FSS structure such as dipole, cross shaped dipole, tri shaped dipole etc. are more sensitive to angle of incidence. In addition to these shapes some more shapes of centre connected poles such as Jerusalem cross offer expressively wide range of operating frequency with polarization sensitivity also. These different shaped FSS structures have been reported in literature survey and it is fond that square loop and circular shaped elements of FSS are better candidates for various wireless communication application and offer polarization sensitivity also. For achieving the desired frequency characteristics response from the chosen FSS structure, some parameters such as periodicity (p), size (d), inter element spacing (g) and width of patch or slot (w) of the FSS structure have to be well optimized. The locality of the resonance peak of

frequency response of a FSS structure is influenced by its size, periodicity and width of the metallic patch used. Furthermore, angular sensitivity of the FSS structure is also influenced by its inter element spacing (g) [8-15].

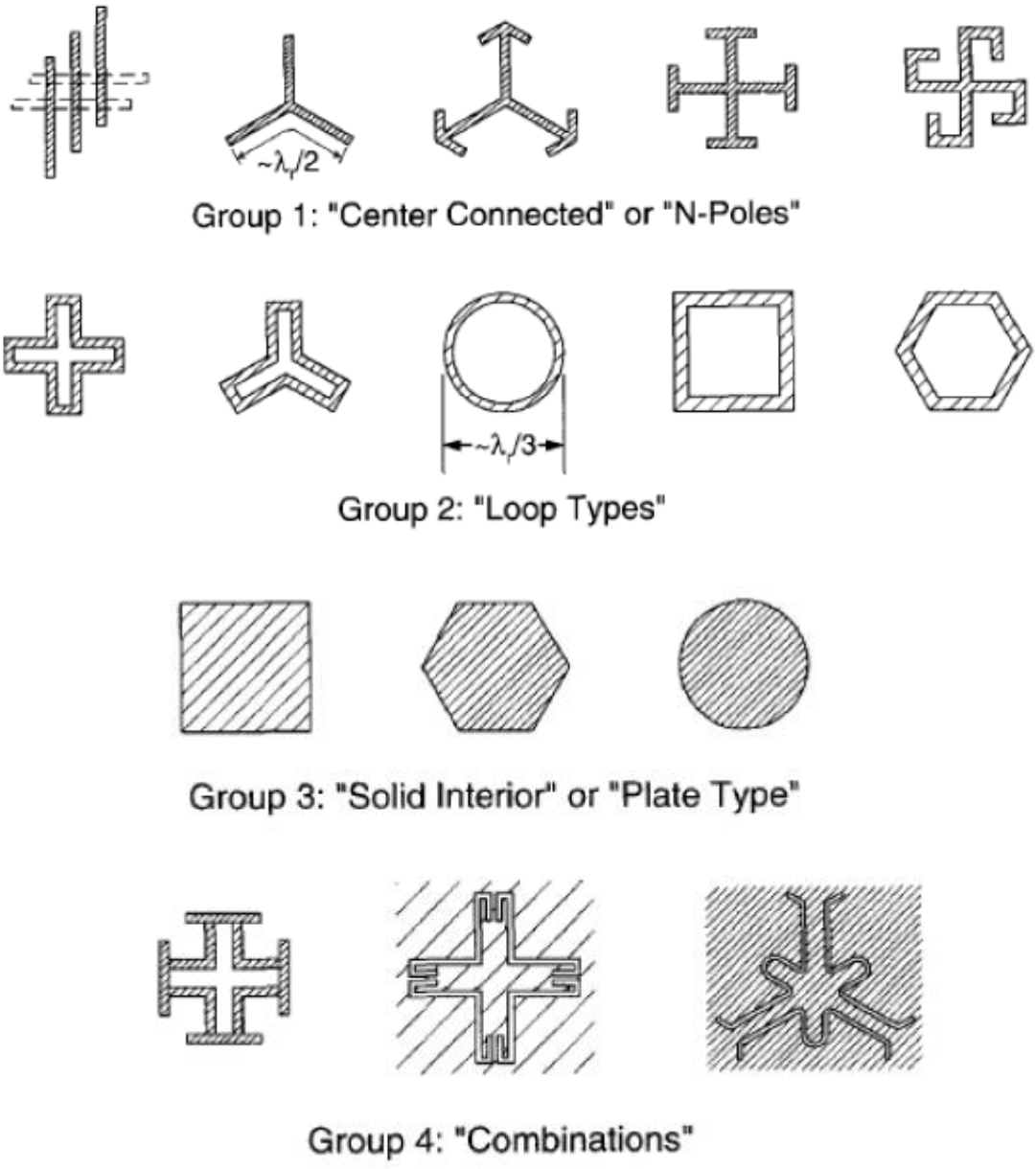

Figure 1.3. Some conventional shapes of FSS element [12].

1.4.2. Effects of Angle of Incident (AOIs)

When an incoming electromagnetic wave strike the surface of FSS structure at any oblique angle then width of the unit cell element of the conductive pattern and inter element spacing are reduced by the factor of cosθ, where θ is the oblique angle at which EM wave impinge on the FSS structure as depicted in Figure 1.4[18]. Hence, the designed parameters (p, d, w, g) are defined for the FSS structure geometries for oblique angle of incidence and normal angle of incidence. Moreover it also influences

the transmission/reflection characteristics of the FSS structure [19-20].The effect of different angles of incidence on the frequency response of the FSS structure can be observed by an equivalent circuit technique which governs the equivalent inductive and capacitive behavior of the FSS structure as a function angle θ [21]. For real life scenario, the incoming electromagnetic wave impinge on the FSS structure at different angle of incidences, hence the performance of the FSS structure depends a lot upon angle sensitivity. Thus the proposed research work concentrate on making the FSS filtering response insensitive to the angle of incidence of incoming EM wave [22].

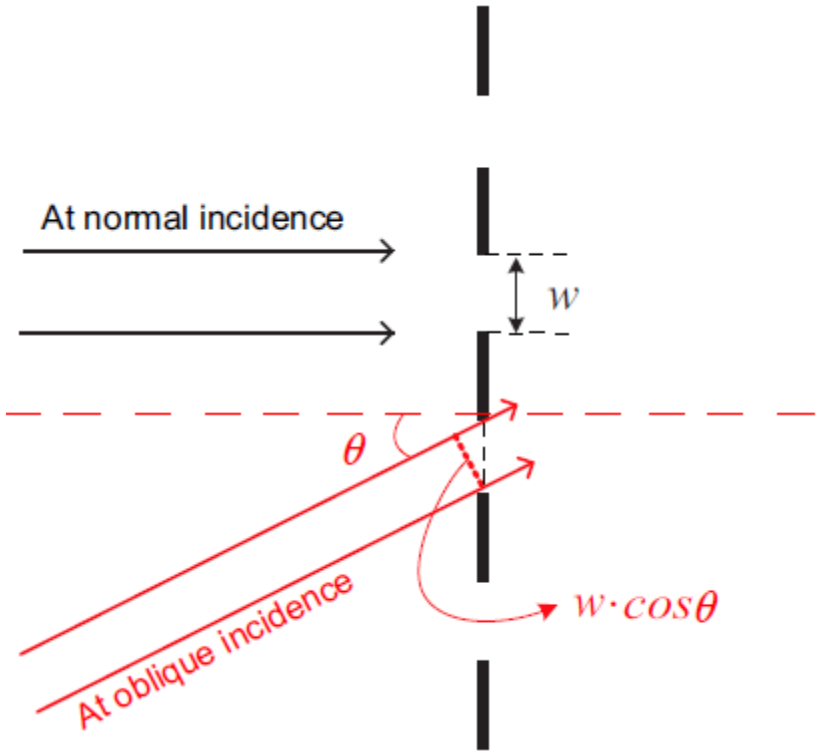

Figure 1.4. The effect of oblique angle of incidence on the geometrical parameters of FSS structure [22].

1.4.3 Effect of Polarization States:

The transmission\reflection characteristics of Frequency Selective Surfaces structure are also influenced by the polarization state of the incoming EM wave. By considering the Equivalent Circuit technique into consideration, the explanation of perpendicular and horizontal polarization state is available in the next subsection.

1.4.3.1 Perpendicular Wave Incidence:

For the incoming electromagnetic perpendicular polarized wave, the electric field vector E is perpendicular to the plane of the incidence as shown in Figure 1.6(a) [18]. When incoming perpendicular polarized EM wave impinging on the surface of the FSS structure, electric field E which is parallel to the vertical strip of the Square loop /dipole, becomes the reason for the oscillation of electrons, thus the surface current flows and hence offers an inductive behavior. Besides, the electric

field vector E that is in the perpendicular direction of the horizontal conductive strip offers a capacitor behavior due to the air gap between the two conductive strips as shown in Figure 1.5.

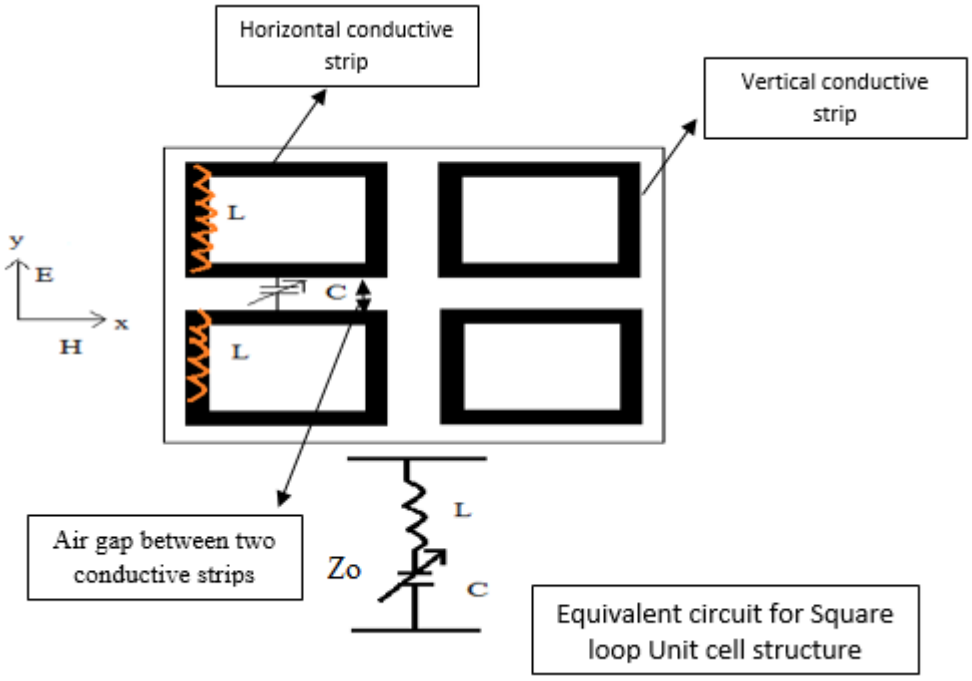

Figure 1.5 Equivalent circuit for square loop unit cell structure

1.4.3.2 Parallel Wave Incidence

For incoming parallel polarized EM wave, the electric field vector E is parallel to the plane of incidence as shown in Figure 1.6(b) [12-18]. When incoming perpendicular polarized EM wave impinging on the surface of the FSS structure, electric field E which is parallel to the horizontal strip of the Square loop/dipole, becomes the reason for the oscillation of electrons, thus the surface current flows and hence offers an inductive behavior. Besides, the electric field vector E that is in the perpendicular direction of the vertical conductive strip offers a capacitor behavior due to the air gap between the two conductive strips.

The conductive single square loop FSS structure is modelled as a series LC circuit while complimentary of the single square loop FSS structure modelled as parallel LC circuit connected across the transmission line having characteristics impedance (*Zo*) as shown in Figure 1.5.For both the polarization scenarios, the electric field vector 'E' is polarized parallel to the metallic strip of the dipole/square loop, thus offers an inductive component. Due to the oscillation of electrons the current induced on the strips of the dipole is different when electromagnetic wave impinging at different angle of incidence on the surface of the FSS structures. This is because for the perpendicular wave incidence state, the electric field vector 'E' is constantly parallel to the strip of the dipole and stimulates the full length of each metallic strip, nevertheless of the angle of incident for parallel wave incident state, the electric field vector 'E' arrives obliquely along the broadside of the strip, causing in a shorter projected metallic strip length as per the

angle of incidence increases. FSS with polarization insensitivity are preferred for many wireless communication application [23].

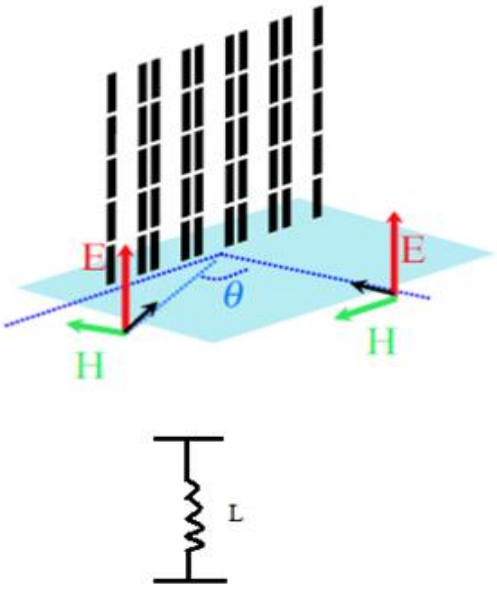

Figure 1.6 (a) Perpendicular wave of incidence and its equivalent circuit

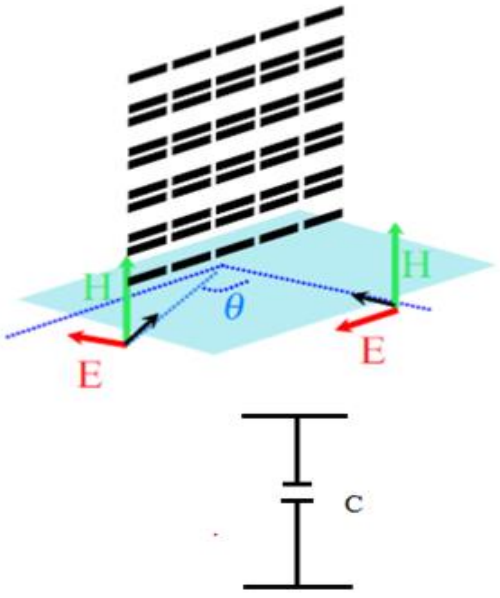

Figure 1.6 (b) Parallel wave of incidence and and its equivalent circuit

1.4.4 Element Conductivity

When incoming EM wave impinging on the surface of FSS structure, current is induced in the metallic strips. Resultant induced currents reradiate the EM wave from the conducting pattern in the similar manner as the metallic strips of dipole/square loop inside a rectangular waveguide [24]. By adopting an EC technique, the perfect electric conductor (PEC) conductive pattern, a single square loop unit cell structure of FSS is modelled as a series arrangement of inductor (*L*) and capacitor (*C*). Besides, for a lossy conductive pattern, the dissipation of power occurs, which have significant impact on the overall frequency response of the FSS structure and changes the equivalent circuit representation of the single square loop FSS structure, which has a resistor (*R*) in series with the *L* and *C* component. The presence of the resistive component (R) in the equivalent circuits diminishes the degree of attenuation in the band stop characteristics of FSS structure [25]. The silver coated paint (95% silver) shows better FSS filtering performance with reasonable manufacture cost as compared to the other conducting materials such as Al and Cu. Moreover, the silver coated paint itself having opaque property and to guarantee satisfactory transparency, the conductive strip of the metallic patch should not be very thin otherwise it arises the manufacturing issues [26].

1.5 Filter Geometries and Equivalent Circuits

Here some conventional types of filters are presented in this section and they are: strip-grating filters, mesh filters, cross-mesh filter. Further, basic information and equivalent circuits of the basic FSS structures have been described in the following section.

1.5.1 Strip Grating filters

Strip grating filter and its equivalent circuit has been depicted in Figure 1.7 [27]. For the electric field vector that is perpendicular to the metallic strips offers the capacitive reactance as depicted in Figure 1.7 (right).while when E-field vector that is parallel to the metal strips excite the whole strip and surface current flow that offer inductive strip-grating filter effect as depicts in Figure 1.7 (left).

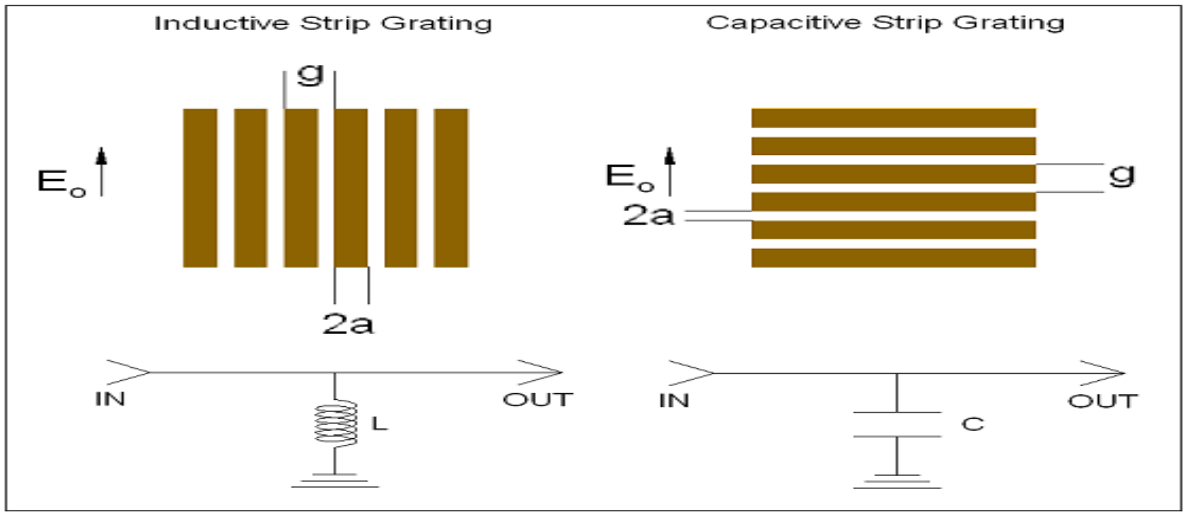

Figure 1.7 strip-grating filters and its equivalent circuit

1.5.2 Mesh Filters:

Figure 1.8 depicts the inductive and capacitive mesh type filters. The capacitive mesh type filters contain grid of metal squares whereas complementary structure of the capacitive mesh represents the inductive mesh filter. Such filters offer the characteristics of low pass and high pass filters along with the advantage of polarization independency [27].

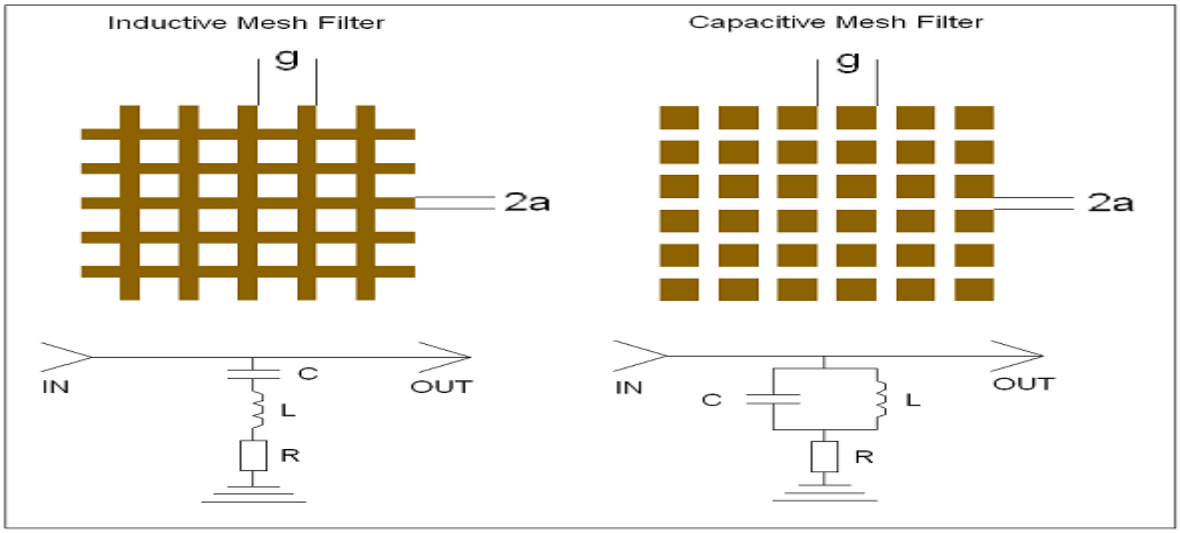

Figure 1.8 Mesh filters and its equivalent circuit

1.5.3 Cross-Mesh Filters:

Cross-Mesh filters are comparable to that of mesh filters excluding that the repeated elements for cross mesh filters are crosses instead of squares. The dimension of length and width of crosses adjust the resonant frequency and bandwidth of the transmission\reflection characteristics of the FSS structure. The resonant wavelength, for capacitive cross type mesh filters, shows a transmission zero (Band Stop Filter) while inductive cross mesh type filtering offers full transmission i.e. Band Pass Filter as depicted in Figure 1.9 [27].

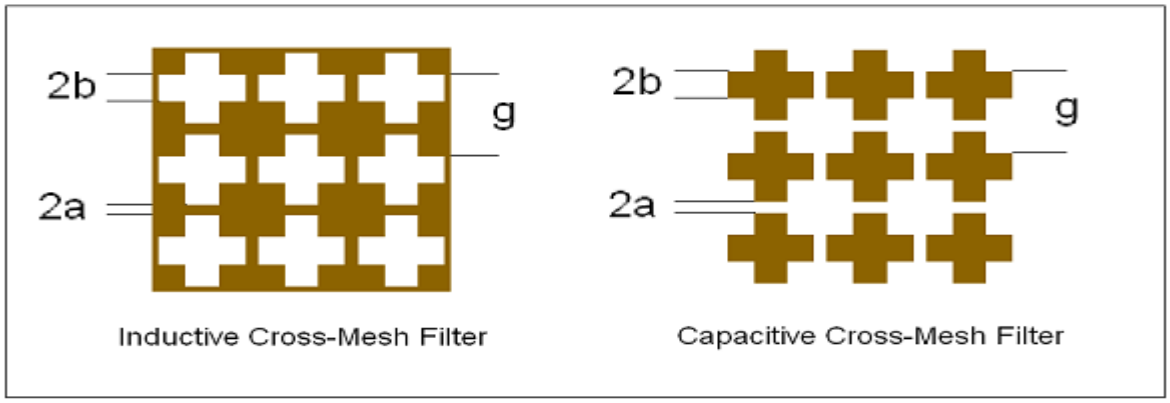

Figure 1.9 Cross-Mesh filters

1.6 ADVANTAGES AND DISADVANTAGES OF FSSs

1.6.1 Advantages of FSSs:

- Frequency Selective Surfaces are work as microwave filters for many wireless communication applications.
- Isolation of undesirable and unsafe radiation from microwave frequency band such as L and S bands in hospitals, schools or domestic environments.
- Frequency Selective Surfaces offers shielding effect for military and airport communication.
- Frequency selective surface scan also be work as reflector for enhancing the gain of antenna

1.6.2 Disadvantages of FSSs:

- Most of the FSS structures are sensitive to angle of incident.
- FSS structures are also sensitive to polarization of the incoming wave.

1.7 MATHEMATICAL ANALYSIS FOR EQUIVALENT CIRCUIT OF FSSs

The unit cell structure of FSS consists of metallic pattern placed on dielectric substrate. For the required transmission coefficients for wireless bands starts with the selection of substrate dimensions for the unit cell which is calculated using equation (i) for a resonance of centre frequency of the lower pass band/stop band [28]:

$$L = \frac{c}{4f_r\sqrt{(\frac{\varepsilon+1}{2})}} \ldots\ldots\ldots\ldots\ldots\ldots\ldots\ldots\ldots\ldots\ldots\ldots\ldots\ldots\ldots\ldots\ldots\ldots\ldots\ldots\ldots\ldots \text{(i)}$$

Where, 'L' is side of square shaped substrate, c is speed of light in vacuum in mm, f_r is centre frequency of lower pass/stop band.

For the dimensions of square loop equivalent circuit (EC) technique has been adopted where the mathematical expressions (ii to vii) are used:

$$\frac{\omega_r L}{Z_0} = \frac{d}{p} cos\theta \times F(p, w, \lambda, \theta) \ldots\ldots\ldots\ldots\ldots\ldots\ldots\ldots\ldots\ldots\ldots\ldots\ldots\ldots\ldots\ldots\ldots\ldots\ldots\ldots \text{(ii)}$$

Where

$$F(p, w, \lambda, \theta) = \frac{p}{\lambda}[\ln cosec\left(\frac{t\pi}{2p}\right) + G(p, t, \lambda, \theta)]$$

and

$$\frac{\omega_r C}{Y_0} = 4\frac{L1}{\lambda} sec\theta \times F(p, g, \lambda, \theta) \ldots\ldots\ldots\ldots\ldots\ldots\ldots\ldots\ldots\ldots\ldots\ldots\ldots\ldots\ldots\ldots\ldots\ldots\ldots\ldots \text{(iii)}$$

Where

$$F(p, g, \lambda, \theta) = \frac{p}{\lambda}[\ln cosec\left(\frac{g\pi}{2p}\right) + G(p, g, \lambda, \theta)]$$

Where L,C, $Z_0, Y_0, \theta,\ \varepsilon_{eff}, G(p, t, \lambda, \theta), G(p, g, \lambda, \theta)$ are the inductance, capacitance, free space characteristic impedance, free space characteristic admittance ,angle of incidence, effective dielectric permittivity of the medium, correction factors for both inductance and capacitance respectively.

To simplify the calculations for L1 at the cost of very small sacrifice in accuracy, some parameters are avoided from equation (ii) and (iii) and can be rewritten as

$$\frac{\omega_r L}{Z_0} = \frac{L1}{p} cos\theta \times \frac{p}{\lambda}\left(\ln cosec\left(\frac{t\pi}{2p}\right)\right) \ldots\ldots\ldots\ldots\ldots\ldots\ldots\ldots\ldots\ldots\ldots\ldots\ldots\ldots\ldots\ldots\ldots\ldots\ldots\ldots \text{(iv)}$$

$$\frac{\omega_r C}{Y_0} = 4\frac{L1}{\lambda} sec\theta\ \frac{p}{\lambda}\ln cosec\left(\frac{g\pi}{2p}\right) \times \varepsilon_{eff} \ldots\ldots\ldots\ldots\ldots\ldots\ldots\ldots\ldots\ldots\ldots\ldots\ldots\ldots\ldots\ldots\ldots\ldots\ldots\ldots \text{(v)}$$

By assuming air as dielectric substrate and multiply equations (iii) and (iv) and rewriting them we get

$$\omega_r{}^2 LC = 4\left(\frac{L1}{p}\right)^2 \times (\frac{p}{\lambda})^2 \ln cosec\left(\frac{t\pi}{2p}\right) \times \ln cosec\left(\frac{g\pi}{2p}\right) \ldots\ldots\ldots\ldots\ldots\ldots\ldots\ldots\ldots\ldots\ldots\ldots\ldots\ldots\ldots\ldots\ldots\ldots\ldots\ldots \text{(vi)}$$

$$\omega_r{}^2 LC = 4\left(\frac{L1}{p}\right)^2 (\frac{p}{\lambda})^2 \times \ln(\frac{1}{\sin\left(\frac{t\pi}{2p}\right)}) \times \ln\left(\frac{1}{sin\left(\frac{g\pi}{2p}\right)}\right) \ldots\ldots\ldots\ldots\ldots\ldots\ldots\ldots\ldots\ldots\ldots\ldots\ldots\ldots\ldots\ldots\ldots\ldots\ldots\ldots \text{(vii)}$$

For ideal case of FSS at resonance; $\omega_r{}^2 LC = 1$

Assumptions for simplifying the equations are w << 2p and g << 2p as g > w, so the ratio of $\frac{w\pi}{2p}$ dominant over $\frac{g\pi}{2p}$ hence equation vii can be simplified as

$$1 = 4\left(\frac{L1}{\lambda}\right)^2 \times \ln\left(\frac{2p}{t\pi}\right) \quad \text{(viii)}$$

Therefore the length L1 of square loop of unit cell can be calculated [29]:

$$L1 = \sqrt{\lambda^2}/4\,(\ln(2p/\pi t)) \quad \text{(ix)}$$

Where, λ is the higher wavelength of band. In addition to avoid this scenario and also the grating lobes condition at different angle of incidences, the periodicity of the FSS is related to wavelength of operation governed by the equation (x) [28-30].

$$P\,(1 + \sin\theta) < \lambda \quad \text{(x)}$$

1.8 THESIS OBJECTIVE

In order to allow effective wireless communications to take place and prevent the interference of the wireless signals from nearby frequency bands, some latest technologies which reduce the interference of the unwanted signal to the required signal band are adopted. For example while communicating through X and S bands, other frequency bands such as L, C or K band produce interference by leaking their nearby frequencies into the required band and should be avoided to keep SNR high. Therefore the main aim of this thesis is to design, simulate and develop FSS for pass and stop bands of the S and X wireless communication bands.

Two FSS geometries are proposed; one that shows pass band characteristics for S and X communication bands. Then its complimentary geometry is proposed that shows the stop band for same S and X bands. Another FSS with fractal geometry and ultra-wide Stop band is proposed. The research work is further extended to the design and simulation of an UWB CPW fed antenna. Since the gain is inversely proportional to antenna's bandwidth, the proposed FSS with an Ultra wide stop band is used to improve the gain of CPW fed antenna by placing the fractal FSS behind it. This FSS acts as a reflector and reflects the antenna's back lobe in the forward direction, thereby improving its average gain by around 2.25 dB approx.

The proposed FSS are fabricated and tested using a two port VNA to validate the transmission parameter results.

1.9 THESIS ORGANISATION

This thesis is basically divided into following five chapters

- Chapter 1: Brief introduction about the Frequency Selective Surfaces and their equivalent circuit. Moreover, the mathematical analysis of the Unit cell structure of Frequency Selective Surfaces and also their advantages and disadvantages are also explained.

- Chapter 2: A brief literature survey about Single layer Frequency Selective surface, multilayer Frequency selective surfaces, Frequency Selective Surfaces based on fractal geometry, multi band and wide band FSS, UWB FSS, Coplanar Wave guide antenna and FSS as reflector for enhancing the gain of antenna.
- Chapter 3: Theoretical analysis and simulation of transmission characteristics of Single Square Loop and its complimentary FSS for lower frequency application, Dual band pass and band stop Frequency Selective Surfaces for X and S band application and enhancing the gain of CPW antenna using FSS reflector.
- Chapter 4: The optimized Dual band Pass and band Stop Frequency Selective Surfaces designs are fabricated and tested.
- Chapter 5: Conclusion and future work.

CHAPTER 2

LITERATURE REVIEW

In order to carry out the research work in context to the design and development of different FSS; an extensive literature survey was carried out to study the development phase of FSS since 1999.

Some research gaps that were found between the presented research works are also outlined in this chapter that were forms the basis for defining the objective of proposed research work.

2.1 FSS DEVELOPMENT

In 1999 Alon S. Barlevy *et al.* presented a work that showed the effects of the orientation of the repeatable metallic elements of a frequency selective surface (FSS). Proposed work showed the existence of another degree of freedom that could be adopted to design the FSSs. Periodic green function and method of moment were adopted to analyse the FSS. It had been shown that the orientation of the dipoles at oblique angle caused a minor shift in the resonant frequency response of the FSSs and also reduce the bandwidth of the FSS frequency response. In addition to this the empirical formula that showed the relation between the bandwidth and oblique angle for was also given. Authors also explained that the oblique angle might cause extra resonance peak [30].

In 2000 Chen Guorui *et al.* proposed a paper of curved FSS radome design, the theoretical and experimental investigations had been made on frequency selective surfaces with square loop slots. Expressions of basis function and transmission coefficient T were given. Factors were discussed which affect significantly the transmission characteristics. The measured T is greater than -0.51 dB for normal incidence and T was greater than –l.0 dB at oblique incidence of 60°. The measured results were quite satisfactory [31].

In 2005 Chun Yu *et al.* proposed an integral-equation approach to analyse the transmission/reflection characteristics of finite and curved shaped FSS. These equations were established by applying the surface and volume equivalent principles. Proposed approach having the advantage of modelling arbitrarily shaped FSS structures. Scattering parameters of FSSs and their responses were also analyzed in detail [32].

In 2008 Ghaffer I. Kiani presented a paper on the topic of angle and polarization independence FSS for indoor wireless system. In this paper author described a novel band stop FSS that showed decent stability in transmission characteristics of the FSS for electromagnetics wave which imping on FSS sheet at normal (0 degree) or any oblique angle. To evaluate the perfection (independency in polarization and angle of incident) for the proposed FSS structure, it was compared with the

conventional FSS structure. On the basis of its transmission characteristics this was a better option to provide security to WLAN and indoor wireless systems [22].

In 2009 A. L. P. S. Campos *et al.* proposed a miniaturized FSS structure. The proposed prototype of FSS consisted of repeatable unit cell metallic elements in 2 dimension. The elements of this unit cell design were based upon Koch fractal geometry. The prototype of FSS structure were designed and simulated using the software Ansoft Design and a number of prototypes for different fractal geometries were built. RT-Duroid 3010 was used as a substrate for the fabrication of the FSS sheet. This article explained the reduction from the area of FSS unit cell elements using Koch geometry [33].

In 2009 Asim Egemen Yilmaz *et al.* presented a paper in which he explained about Particle Swarm Optimization for conventional FSS structure for example Single square loop, gridded square loop and dual square loop. For this optimization, equivalent circuit technique was adopted. Then based on the transmission coefficients, an objective function for numerous frequencies of the pass/stop-bands, was defined. The multi-dimensional search operation was used in a systemic manner for swarm intelligence [34].

In 2010 Ghaffer I. Kiani *et al*. proposed an electrically switchable FSS that switched between its reflective and transmission characteristics responses. It could be used to provide a spatial filter solution to reconfigure the electromagnetic architecture of buildings. The measurements of the prototype of FSS validate its independency from angle of incident and mode of polarization. The unit cell of FSS structure consisted of a single square loop and 4 PIN diodes across the aperture at every 90˚ intervals. From the measured results it was found that there was nearly 10 dB additional transmission loss could be fimilirized on average at the resonance frequency, for both mode of polarizations, by switching the PIN diodes [35].

In 2012 Y. Yang *et al.* proposed a dual band FSS structure with miniaturized elements. Two concentric square loops which were separated by, two different slots, were constructed. Slot were etched in between these two square loops to realized double pass band transmission characteristics. Each pass band was realized by a slot and thickness of the slot had been taken very small to miniaturise the elements. The proposed FSS structure design offered stable transmission characteristics at various incident angles up to 45 degree and different polarizations mode of incoming waves and this allowed it to be appropriate for shipboard communication [36].

In 2013 In-Gon Lee *et al.* proposed the reconfigurable blind structures with FSS for the wireless security applications. The transmission parameters of the suggested FSS unit cell structure were inspected and verified through simulated and measured results. In addition, FSSs were investigated for

different angle of incident. There were two type of proposed FSS unit cell structure i.e. cross dipole and circular ring [37].

In 2014 Filippo Costa *et al.* presented a review paper to explain the circuit analysis of FSS for validity of dissimilar models and their benefits in terms of simplicity and physical insight. This circuit approach was based on an equivalent circuit demonstration of the FSSs with series or shunt connections of inductances and capacitances. Here author mathematically explained the equivalent circuits of various conventional FSS unit cells [38].

In 2014 M. W. B. Silva *et al.* proposed a design of an electromagnetic absorber for both narrow and wide band reflection characteristics. For the proposed work, author adopted a method of equivalent-circuit and used it for calculating the lumped parameters of the proposed FSSs unit cell metallic elements. Thus, the procedure was applied to high-impedance surfaces to drive the required absorbers. The absorbers were simply realised by placing the unit cell structure over a dielectric substrate and a metal layer on the back side of the dielectric [39].

In 2015 David Ferreira *et al.* adopted equivalent circuit (EC) model technique for optimized the parameters of the square loop and a square slot FSSs. More attention was given to the physical features of FSS i.e. physical dimension of the unit cell elements, inter element spacing of unit cells, thickness of dielectric substrate, effects of angle of incidence on the frequency response of the FSSs. A complete examination of the physical parameters of FSS on its frequency response was also presented [40].

In 2015 Mohamad Zoinol Abidin Abd. Aziz *et al.* proposed a FSS structures for single, double, triple bands that were design and simulated using CST Microwave Studio software. Here dielectrics (FR-4 and glass) were used for the FSS structures. Six different type of configurations were used for analysis of the reflection and transmission responses of the FSS unit cells. All configurations were simulated with the similar size of the FSS structure. It was observed that the hybrid materials such as FR4 and glass affected the transmission and reflection coefficients or characteristics of the Frequency selective surfaces (FSS) which led to the denser FSS unit cell structures [41].

In 2015 Ic-Pyo Hong presented a letter on the angle insensitivity wide stop band FSS fabricated on paper substrate of thickness .180 mm using ink jet printing. From the simulated results it was verified that the proposed structure of FSS offered same transmission characteristics at the different angle of incidence. Verification of the simulated results was done by comparing these results with measured ones. Author highlighted its advantages such as insensitivity for both angle of incidence and polarization, thus it could be significantly used for the application of Ku band satellite communication [42].

In 2016 Kartal *et al.* proposed a FSS based absorber for reducing the interference and improving the performance of unlicensed ISM bands. The author offered a well-organized method to solve this problem of interference in ISM band by of transforming a building wall to a FSSs, which filters out the unwanted signals, but permitted electromagnetic signals from other devices such as mobile phones, radios and televisions (ISM band only). The absorber characteristics were achieved by employing a second layer of FSS including lossy periodic FSS elements for absorber characteristics [43].

In 2016 Sanjeev Yadav *et al.* proposed a novel FSS structure for the application of Wi-MAX. Authors described that the proposed FSS structure allowed to pass the signals of frequency range of 2.5 GHz and 3.5 GHz and stops the other signals to pass through them. But these bands suffered from the problem of path loss, so a band pass FSS was proposed in this paper which led to augmentation in the transmission of Wi-MAX signal to combat the effect of path loss. In the proposed unit cell structure of FSS, a single sided FR-4 substrate was incorporated with two loops and a cross element that offers dual band (2.5 GHz and 3.5 GHz) characteristics [44].

In 2017 Yun. Junsik proposed a stop band FSS for X-band applications. The proposed FSS unit cell structure had a geometry with planar array of hexagonal ceramic prisms with a honeycomb-shaped structure. From the simulated results it was investigated that it had three resonant dips. These were combined to offers a fractional bandwidth (FBW of 210 %) with a broad stop-band. Analysis of cylindrical cavity mode that were based on the cylindrical wave functions were also used for verifying the resonant characteristic modes [45].

In 2017 Varittha Sanphuang *et al.* proposed a special filter for temperature sensing. For this purpose author offered a frequency selective surfaces (FSS) incorporated with bi-material actuator .The actuator consisted of two materials that had different thermal expansion rates and controlled based on temperature tuning. Author also established reconfigurable filters functioning in the frequency range of THz band. The filter was fabricated using printing of gold on silicon substrate. SiO2 and Al were used as bi-material actuators. The equivalent circuit of the FSS was also demonstrated [46].

In 2017 Hou Zhang *et al.* proposed a compact and spiral loop based FSS with the miniaturized elements, spiral loops were connected end-to-end, via-holes. The spiral loops formed a complete closed loop in the unit cell structure of FSS. For the validation of its miniaturisation, authors compared the results of the proposed FSSs with the earlier FSSs. In addition, the centre frequency did not show any deviations for incoming waves that were impinging on it at different angles of incidence and different modes of polarizations [47].

In 2018 Mahdiye Rahzaani *et al*. presented a method for designing a unit cell element of FSS. A double slot square loop (DSSL) that had double resonant frequencies, was nominated for a primary unit cell element of FSSs. In addition the frequency bandwidth of the FSS structure was enhanced by using proposed method. Equivalent circuit technique was adopted to investigate the effect of the proposed method on the frequency response of DSSL unit cell. To validate the enhancement in the bandwidth of FSSs prototype, it was fabricated and tested. Moreover, its measured return loss verified that the enhancement in the bandwidth of proposed FSS was about 50% in X band. The proposed FSS structure had some specific characteristics such as it had high frequency bandwidth with low fabrication complexity and stable angular response that made it appropriate for its usage in microwave filters [48].

In 2018 Sanjeev Yadav *et al*. proposed a polarization independent double pass band FSS. This FSS unit cell consisted of metallic structure of modified concentric plus shaped structure inside a square ring imprinted on one side of epoxy FR4 substrate. The geometrical dimensions of metallic structure of FSS unit cell were optimized in such a manner that the proposed structure realized the double pass band characteristics for Wi-Max applications. The proposed FSS structure offered a stable frequency response for oblique angles of incidence for both mode of polarizations (TE and TM). An equivalent circuit technique was adopted for modelling the equivalent circuit of the FSS unit cell and its response was verified by using Advanced Design System tool [28].

In 2018 V. P. Silva Neto *et al.* proposed a design of Active FSS that was based on a non-uniform distribution of finite array of square loop metallic patches that were imprinted on a dielectric substrate .The reconfigurability of the FSSs was verified by altering the polarization of PIN diode (from OFF to ON state and vice versa) that were connected in between the slots of square loop of the FSS array. This simulation of the FSS unit cell were performed by using the wave concept iterative procedure and HFSS package. Prototypes of the proposed FSS were fabricated for validation of reconfigurability purposes. Besides this measured results of the FSS structure showed that proposed FSS had dual band transmission characteristics and also validated the insensitivity of FSS structure for angle of incidence and polarization [49].

2.2 FSS USING FRACTAL GEOMETRY

Fractal FSS have been a choice of researchers because of their multiband properties. Some literature survey on these designs presented below.

In 2010 Antonio Luiz P. S. Campos *et al.* presented a paper that was based on the simulation and experimental investigation of a FSS using a fractal geometry. The design of unit cell structure of FSS was achieved by adopting the Minkowski island fractal. Two unit cell structures were designed for level 1 and 2 of Minkowski island fractal, which offered stop-band transmission characteristics with resonant frequencies of 9 GHz and 10 GHz, respectively. Both simulation and experimental investigations were conducted and verified [50]**.**

In 2013 Davi B. Brito *et al*. investigated the properties of FSSs with fractal patch elements. Predominantly, with the main aim of the paper was to design a FSS unit cell that offered the band reject filtering response with high angular stability. Proposed design was based on a simple Minkowski fractal element shapes. The selected FSS geometry consisted of a periodic array of metallic patches on a one side of dielectric layer. It was found that the proposed FSSs had very simple design with independent of angular stability. In addition to this, the very small changes in terms of resonant frequency and bandwidth results for different values of the incident wave angles [51].

In 2013 Amanpreet Kaur *et al.* proposed various types of fractal geometries such as koch fractal, Square patch fractal antenna, sierpinski fractal antenna, fractal tree type antenna each having its own pros and cons and having various wireless applications. Authors explained many approaches for fractal antenna designs and considered the different attributes related to performance parameters of an antenna as like multi frequencies, wide bandwidth, low VSWR, high gain, high radiation efficiency and small size etc. [52].

In 2013 Clarissa de Lucena Nóbrega *et al.* proposed a simple design based on Sirpinski fractal geometry that offers band-stop filters for microwave applications. The main objectives of the design were to its miniaturization, angular stability with dual-band frequency response and polarization independency in performances. The proposed FSS structure was consists of the periodic arrangement of fractal metallic patches that etched on a layer of dielectric substrate. A parametric study of the FSS was achieved to verify the effect of the size of the fractal patch and iteration level on the frequency response. It was found that as the iteration level of patches increased the more tuning possibilities of the FSS structure were detected at the resonant bands [53].

In 2014 Anshika Khanna *et al.* proposed the design of a microstrip patch antenna that based upon the fractal geometry and gap coupled modified square. The proposed antenna was designed to overcome the problem of narrow band width. The antenna had an impedance bandwidth of 85.42% around the resonant frequency. This antenna could be simultaneously used for some wireless applications such as Bluetooth, WLAN and Wi MAX etc. [54].

In 2018 Roman Kubacki *et al*. presented a paper on fractal geometry based MPAS. Proposed design used planar arrangement of periodic geometries to provide the enhanced frequency response. The advantages of the fractal geometries were incorporated in a single-fractal layer design and also in the antenna design, which employed fractals on both the upper and bottom layers of the antenna. The final double fractal layer based structure was optimized to improve the bandwidth and gain of the microstrip antenna. The proposed geometry significantly improved antenna performance [55].

Apart from the fractal geometry, some other designs are also used for multiband and wide band applications. Some of them are explained in the next section.

2.3 FSS FOR MULTIBAND AND WIDE-BAND

In 2000 Jordi Romeu *et al.* presented a paper to design multiband FSS structure based on Sierpinski dipole geometry. Proposed FSS was examined and measured results show remarkable dual-band performance. Moreover, a near-field measurement technique was applied to illustrate the performance of FSS at different angles of incidence. The dual-band response was eventually the cause of the self-similarity properties of the Sierpinski geometry based FSS [56].

In 2012 J. - Y. Kim *et al.* presented a paper for design a notched ultra-wideband (UWB) antennas by using FSSs. The proposed antennas significantly utilized the band stop characteristics of unit cell structure of FSS. In suggested design of FSS unit cells and UWB antenna were on the same plane. Proposed antenna with FSS unit cell structure designed to reduce the interference from the WLAN band, 5.15–5.825 GHz in the UWB band, 3.1–10.6 GHz. The measured peak gain of the UWB antenna with FSSs was more than 2dBi and miniaturized and plane in size. Thus, it could be used for commercial purposes such as small mobile applications [57].

In 2013 Clarissa de Lucena Nóbrega *et al*. proposed a compact FSS structure based on sierpinski fractal geometry for dual band application. In this paper author explained sierpinski geometry up to second iteration. A parametric examination of the FSS transmission coefficients response was proficient to find out the influence of the element's cell size of fractal patch and number of iteration or level. To authenticate the used approach, three prototypes were built and measured. Along with this the insensitivity of proposed FSS design with simulated and measured results was verified [58].

In 2015 Syed Irfan Sohail *et al.* proposed a dual layer wide band FSS, that was printed over commercially available epoxy FR-4 substrate, that exhibits a wide stop-band of 9.5 GHz from frequency range of 4.91-14.41 GHz. Resonant peaks of reflection coefficients were more than 35 to 45 dB hence it could be effectively used for shielding applications and also shield the X band satellite signals. Author verified that dual layer FSS exhibited better response than the single layer FSS structures. It was also observed from the article that proposed dual layer FSS structure were not polarization independent and it also showed angle sensitivity [59].

In 2016 Rabia Yahya *et al.* proposed a compact ultra-wide band FSS with stable performance for different angles of incidence. It was observed that the element size of the proposed FSS unit cell was miniaturized which was sandwiched between two dielectric substrates. Simulated results of the FSS validated the insensitivity of FSS unit cell structure for both angle of incidence of the incoming

electromagnetic waves and modes of polarization. As FSS offered stop band transmission characteristics it could be used as a reflector for UWB antenna to enhance the gain of the antenna [60].

In 2017 Wei Li *et al.* proposed a dual stop band FSS. The FSS element consisted of metal criss-cross elements with four loops etched on commercial available epoxy FR-4 dielectric substrate. It was observed that the stop band transmission characteristics were justifiable for a wide range of angle of incidence. Moreover, the structural parameters were identified for the adjustment of flexible band separation. In this work, an equivalent circuit of the FSS in term of circuit model was established for explaining the electrical property of the band stop FSS as special filter [61].

In 2017 Zhenzhen Zhao *et al.* presented a paper for wide pass band FSS. It consisted of four layers of metals separated from each other by three layers of substrate. Authors validated its insensitivity for both angle of incidence (0 to 60 degree) and polarization (both TE and TM mode). Authors proposed that FSS with stability (both angle of incident and polarization) could be used for applications in radomes [62].

In 2018 Qingya Li *et al.* proposed a unique FSS with miniaturized-elements which offered a second-order pass band characteristics response. The proposed FSS was made up of inductive wire grids and a hybrid resonator. Where hybrid resonator was a 2D periodic arrangement of Jerusalem slots imprinted into a ground plane, hence formed miniaturized unit cell elements. The equivalent circuit model of the FSS unit cell was also established. A prototype of the repeatable FSS sheet was fabricated using a PCB technique and tested in free space measurement setup. The simulated results of the proposed FSS were validated by comparing these with measured results and a remarkable stability in the performance of FSS up to angle of 45 degree was observed [63].
Apart from providing pass band and stop band filtering property for microwave bands, FSS can be used to increase the gain of an antenna. The literature review in this content is presented in next section.

2.4 FSSs FOR INCREASING THE GAIN OF ANTENNA

In 2012 Y. Ranga *et al.* presented an article to demonstrate the enhancement in gain of stotted antenna using FSSs as reflector. Complete theoretical analysis of the proposed antenna with FSSs as reflector was mentioned in the article. Proposed FSSs offered a complete liner phase transmission coefficients, therefore it could be used as reflector for slotted antenna. The minimum gain enhancement was about 2.5 dB and maximum gain enhancement of 4 dB had been observed at frequency of 4.2 GHz. The gain variation was approx. ± 1.5 dB from frequency range of 3-10 GHz [64].

In 2014 Moufida Bouslama *et al.* proposed a FSS design for enhancing the gain of conventional MPAS that operates on 5.2 GHz frequency range. Here authors used FSSs as a superstrate for micro strip antenna. The main attention of this arrangement was to design low profile compact size micro strip

antenna with improved gain. Radiation pattern of the antenna were explained. Proposed FSSs with antenna were used to improve the gain of antenna up to 9.2 dBi without altering the reflection coefficients of the antenna much [65].

In 2015 Ayan Chatterjee *et al*. proposed method to enhance the gain of wide slotted antenna using dual pass band FSS. Here FSSs were used as a superstrate for the antenna. The proposed stacked FSSs offered in phase transmission of waves that radiated from the proposed antenna. The suggested arrangement of the FSSs and antenna enhanced the gain of antenna up to 4 dBi over the entire frequency range of 5 GHz to 8 GHz. In addition the compound structure of antenna with FSSs offered impedance bandwidth of 65% and average antenna gain between 6 dBi to 8 dBi over the entire frequency range .Measurement results of the proposed prototype were well matched with it simulated results [66].

In 2016 Rabia Yahya *et al.* proposed a technique to enhance the gain of coplanar waveguide antenna using FSSs as reflector behind the proposed antenna. Moreover proposed arrangement of FSS sheet behind the antenna also provided a constant gain of .5 dBi for overall ultra-wide band without much altering its reflection characteristics and merits. To validate the technique the measured results were compared with and without FSS reflector behind the coplanar antenna [67].

In 2016 Mohamed Aly Aboul-Dahab *et al.* proposed a technique to enhance the gain and efficiency of the micro strip patch antenna by placing a FSS reflector sheet behind the antenna to enhance the gain of antenna without much altering its merits. For this purpose author designed an FSS unit cell at the operating frequency of antenna. From the measured results, it was verified that there was an increment of 48% in antenna gain and 97% improvement in the efficiency of antenna at the operating frequency of 10 GHz [68].

In 2016 Ayan Chatterjee *et al.* proposed a dual band FSSs that worked as reflector for enhancing the gain and directivity of the antenna. Proposed FSSs had multilayer miniaturized unit cell elements that cascaded with air gap in between and offered a linear phase transmission characteristics. Besides FSSs also used as a superstrate for any antenna to enhance the gain of antenna. To validate its insensitivity at different angles of incidence, simulated results were checked and verified with measured results [69].

In 2017 Mahdi Ghorbani *et al.* presented an article for compact size, high gain wave guide fed aperture antenna. Authors proposed a FSSs that was placed in front of antenna as a superstrate to enhance the bandwidth and gain of antenna. From the measured results it was observed that such arrangement could enhance the maximum gain of the antenna up to 16.03 dBi at frequency of 15.5 GHz, high gain bandwidth of 29.9% for frequency range of 13.42-18.13 GHz and 3dB gain bandwidth of 19.7% over the frequency range of 14.25–17.35 GHz. Proposed antenna was compared with the earlier designs [70].

Based upon the extensive literature survey carried out in the field of design and development of frequency selective surfaces for wireless applications, a few gaps were outlined. These are presented in the section below.

2.5 RESEARCH GAPS

Based upon the literature survey carried out in content to FSS for pass band and stop band filter properties, a few gaps left untouched by researchers are mentioned as:

1) It was found that the FSS structures performance depends upon angle of incidence. When the incoming signals were incident at any angle other than 0˚, there was a shift of resonant frequency peaks. So work can be done to design FSS independent of angle of incidence of incoming EM wave.
2) It was also found that at higher angles of incidence, the effect of grating lobs on filtering goes on increasing. Therefore angle sensitivity is also an open topic for research.
3) Size miniaturization of FSS structures without effecting its characteristics of operation is also an open topic of research to allow these to fit in ant handheld device.
4) It was found that FSS structure performance depends on polarization mode. FSS does not give the same transmission response for both TE and TM mode of polarization at oblique angle of incidence.
5) It is found that very less work is available for UWB and Wide band applications for pass and stop band FSS structures.
6) It was found that in case of dual or multiband FSS, the effect of angle of incident was even more at smaller angles, so work can be done to avoid it.

2.6 OBJECTIVE OF RESEARCH

Based upon the research gaps identifies; a few objectives for the proposed research work are presented in the next subsection.

1. To design and simulate a FSS unit cell for stop and pass band microwave filters application of WLAN (IEEE 802.11b)
2. To design and simulate a miniaturized Fan shaped unit cell element for pass band microwave filter applications of S and X wireless communication bands.
3. To design and simulate a complimentary unit cell structure of the Fan shaped unit cell (one proposed in objective 2) to get a stop band of operation for S and X wireless communication bands.
4. To design and simulate a FSS with ultra-wide stop band properties.
5. To design and simulate an UWB CPW fed MPA and implementation of the proposed ultra-wide stop band FSS as a reflector with this MPA to improve its gain properties.
6. Fabrication and testing of two proposed FSSs in objectives* 2 and 3.

CHAPTER 3

DESIGN AND SIMULATION OF THE UNIT CELLS STRUCTURE OF FREQUENCY SELECTIVE SURFACE

3.1 INTRODUCTION

This chapter presents the research work carried out to cover the first five objective of FSS designing and simulation. The presented work starts with the design and simulation of a FSS unit cell for stop band properties for IEEE.802.11b (2.4 GHz).A complementary unit cell of the proposed stop band unit cell is then design and simulated that shows pass band properties for the same IEEE 802.11b band. Then the FSS structure for dual pass and stop band of S and X band are designed and simulated. Then the fractal FSS structure with ultra-wide stop band (3.48 GHz to 12.31 GHz) properties is designed and simulated. A CPW fed antenna is then designed and simulate to excite an ultra-wide band operation. This proposed fractal UWB FSS is placed behind the antenna to improve its gain by 2.5 dB approx. All the proposed FSS structures including CPW antenna design and simulated using CST microwave studio 2016. The proposed FSS structures and the CPW antenna are designed on commercially available epoxy FR-4 substrate of thickness 1.57mm with permittivity 4.4 with the loss tangent of 0.24. The next section of this chapter present the detailed research work carried out to cover the first five objective of thesis work.

3.2 BAND STOP AND BAND PASS FREQUENCY SELECTIVE SURFACE WITH MINIATURIZED ELEMENT IN LOW FREQUENCIES:

Here in this section a single square loop FSS (SSL FSS) equivalent circuit technique is used to extract the circuit lumped parameters such as inductance (*L*) and capacitance (*C*) associated with the structure. For designing a FSS unit cell, it is required to having its parameters such as its periodicity (p) of FSS, width (w) of single square loop FSS ,length (L) of single square loop FSS and for finding all these parameters we use equations from (i) to (x) as mentioned in section 1.7. After finding all above parameter for 2.4 GHz frequency the single square loop FSS is optimized using CST to miniaturize its size on FR-4 substrate. Figure 3.1(a) and Figure 3.1(b) show the top view of the FSS structure for both band stop and band pass property respectively. The FSS structure for band stop is a single-layer structure with no metal on the back of the substrate FR-4. A single square patch of copper arranged periodically on a dielectric substrate which transmits or reflects 2.4 GHz frequency response for the two cases and can be used as spatial filter. Dimensions of the proposed FSSs are mention in the Table 3.1.

Table 3.1 Optimize parameters of FSSs:

specification	Dimensions (mm)
Substrate length (periodicity) (p)	25
Length of Square loop (L_2)	22.5
Thickness of loop (L_2-L_1)	1

This square shaped patch structure with substrate at bottom works as a stop band filter while its complimentary structure ,which has a slot where metal was there on the stop band FSS and metal where slot was there on FSS, is work as pass band. The two proposed FSS unit cells behave as stop band and pass band for the IEEE 802.11b WLAN band. In figure 3.1(b) where white portion shows substrate and black portion shows copper.

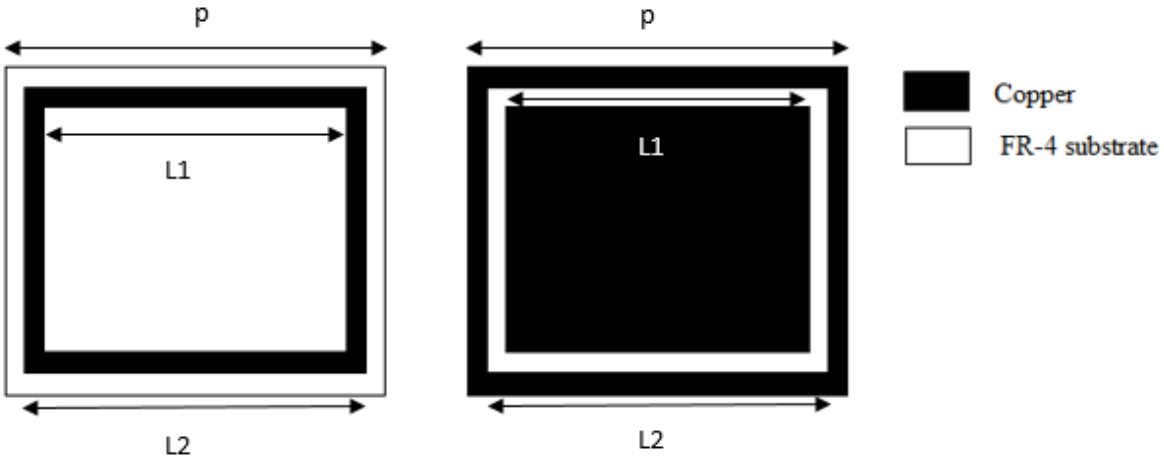

Figure 3.1(a) Front view of stop band unit cell Figure3.1 (b) Front view of pass band unit cell

3.2.1 Equivalent Circuit of Square Loop FSSs

The admittances of the SSL-FSS for band stop and band pass characteristics can be calculated by using the equivalent circuit models for Figure 3.2 (a) from Figure 3.2(b) and equivalent circuit model of Figure 3.3 (a) from Figure 3.3(b) [25]:

$$Y = \frac{1}{X1+B1} \text{…….. (6)}$$

Where X1 is inductive reactance and can be write as $X1 = \omega L1 = \frac{d}{p}F(p, w, \lambda)$ and B1 is capacitive susceptance and can be write as $B1 = \omega C1 = 4\frac{d}{p}\varepsilon F(p, 2g, \lambda)$

Similarly admittance for pass band can be found from equation 7 as:

$$Y = \frac{X1+B1}{X1.B1} \text{…….. (7)}$$

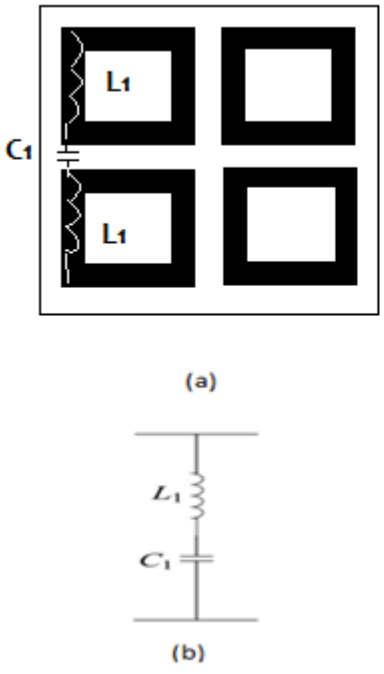

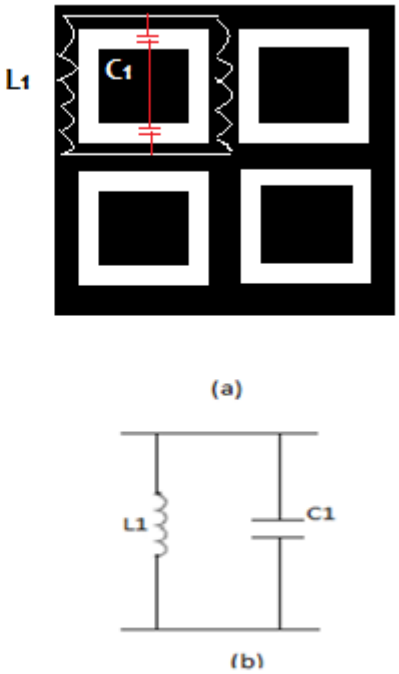

Figure 3.2(a) 2×2 band stop FSS array

Figure 3.2(b) Equivalent circuit for band stop FSS

Figure 3.3(a) 2×2 band pass FSS array

Figure 3.3 Equivalent circuit for band pass FSS

3.2.2 Simulated Results

The proposed FSSs are design and simulated using CST Microwave Studio version 2016 using unit cell boundary conditions and floquet ports. The band stop and band pass square loop structures are shown in Figure 3.1 and their corresponding transmission parameters behavior are shown in Figure 3.4 and Figure 3.5 respectively. Here it is seen that a return loss below -10 dB is observed for a frequency band of 1.88 GHz to 2.89 GHz. This shows that this frequency band will be supported by the proposed FSS structure for incident EM waves on it. The resonance peak occurs at 2.4 GHz and this stop band FSS structure allows frequency below 1.88 GHz and frequencies above to 2.89 to pass through. For band pass FSS structure as shown in figure 3.5 frequencies from 1.08 GHz to 4.5 GHz are allowed to pass through but frequencies below to 1.08 GHz and above 4.5 GHz are blocked by FSS structure. It is important to note that resonance for pass or stop band occurred at same frequency which is 2.4 GHz.

It can be concluded that by making complimentary structure, pass and stop band properties of an FSS structure unit cell can be reversed.

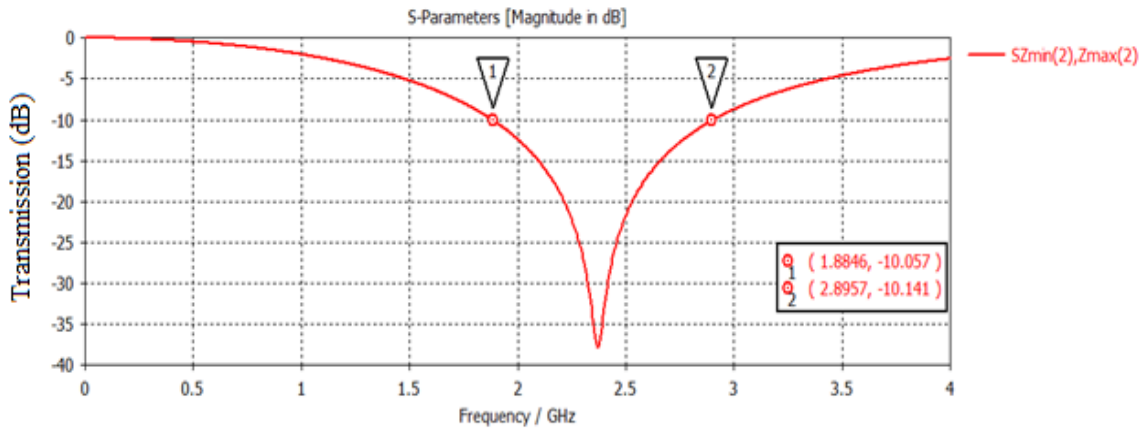

Figure 3.4 Transmission parameters response of proposed FSS band stop

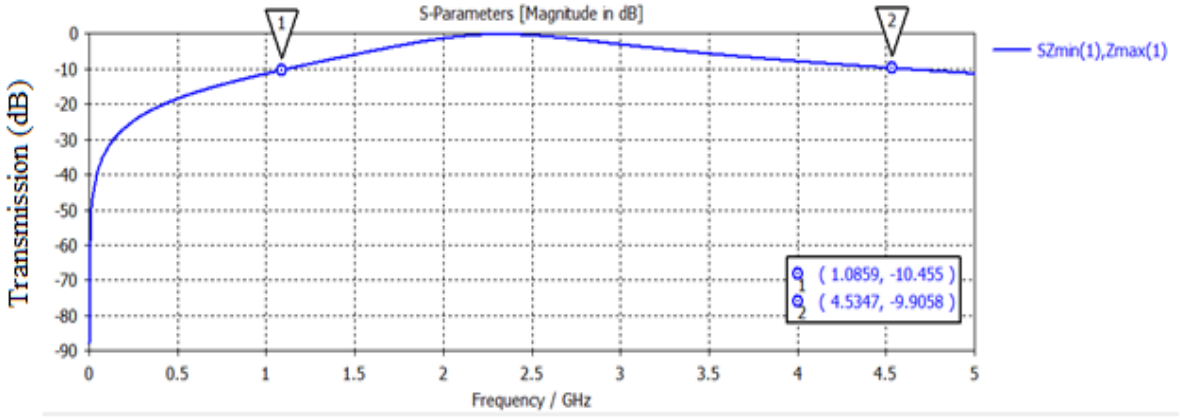

Figure 3.5 Transmission parameters response of proposed FSS band pass

3.2.2.1 Effect of variation in angle of incidence

As illustrated in Figure 3.6 and Figure 3.7, incident angle (theta) of incoming EM wave has been varied from 0º to 80º to see the behavior of transmission characteristics of the proposed FSS structure. At 0º maximum signal is transmitted and with the increase in angle of incidence transmission is less and absorption is more. Also at larger incidence angles (80º), undesired resonating frequencies are introduced. Similarly, for pass band FSS structure, variation in angle of incidence from 0º to 80º are also shown in Figure 3.7 .This shows that if there is an increase an angle beyond 50 º, the effect of grating lobs on filtering goes on increasing. This effect can be tolerated since this has a minor effect on the S_{21} parameters and can be neglected. From equation (x) that explained in subsection 1.7, we find that for maximum AOI the relationship between wavelength and periodicity is established as long as inequality is satisfied. To avoid the grating lobs on higher angle of incidence, periodicity of FSSs have to obey the equation (x).

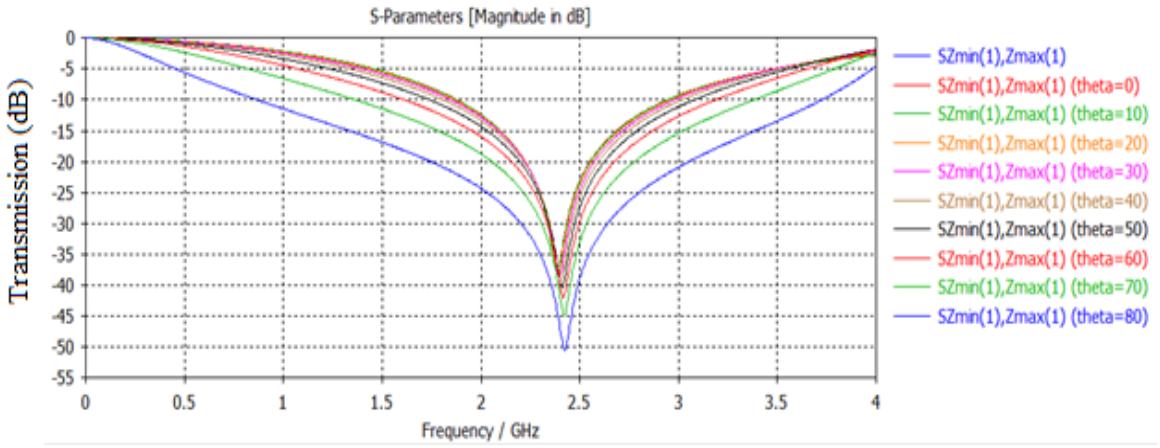

Figure 3.6 Incidence angle variation of stopband unit cell in TE mode

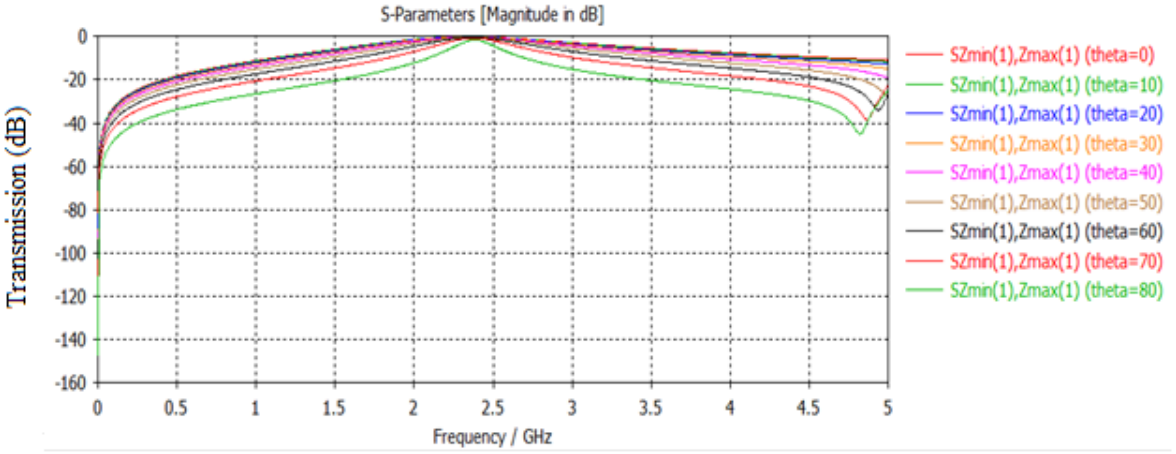

Figure 3.7 Incidence angle variation of pass band unit cell in TE mode

Table 3.2 Effect of variation in angle of incidence (Stop band)

Varying parameter Angle of incidence theta (degree)	Return loss (dB)	Bandwidth(GHz)	Resonance Frequency (GHz)
0˚	-37.536	1.059	2.40
10 ˚	-37.543	1.059	2.40
20 ˚	-37.544	1.059	2.40
30 ˚	-37.558	1.121	2.40
40 ˚	-37.701	1.187	2.41
50 ˚	-39.763	1.374	2.41
60 ˚	-41.61	1.607	2.41
70 ˚	-44.756	2.004	2.42

80 °	-50.145	2.906	2.42

From table 3.2 it is clear that effect of angle of incidence on resonance frequency is negligible while band width and return loss goes on increasing as angle of incidence increases. This is because at higher angle, periodicity of FSS structure gets reduced and FSS structure behaves as a densely packed structure.

3.2.2.2 Polarization Independent Behavior

The proposed unit cell for passband and stopband of IEEE 802.11b shows a polarization independendent behavior.From Figure 3.8 it is verified that proposed FSS stucture is independent of modes of polarization. The Proposed FSS depicts the same transmission charecteristics for both TE and TM polarization modes. The reflection and transmission perameters (TE) for FSS are represented by SZmax(1),Zmax(1) and SZmin(1),Zmax(1) respectively.Similarly for TM mode reflection and transmission coefficient are represent by SZmax(2),Zmax(2) and SZmin(2),Zmax(2).It is seen that the transmission and reflection coefficient for both TE and TM modes overlap each other at each and every point showing a polarization independent behavior for the stop bands of 1.888 GHz to 2.89 GHz and 1.08 GHz to 4.53 GHz for pass band.

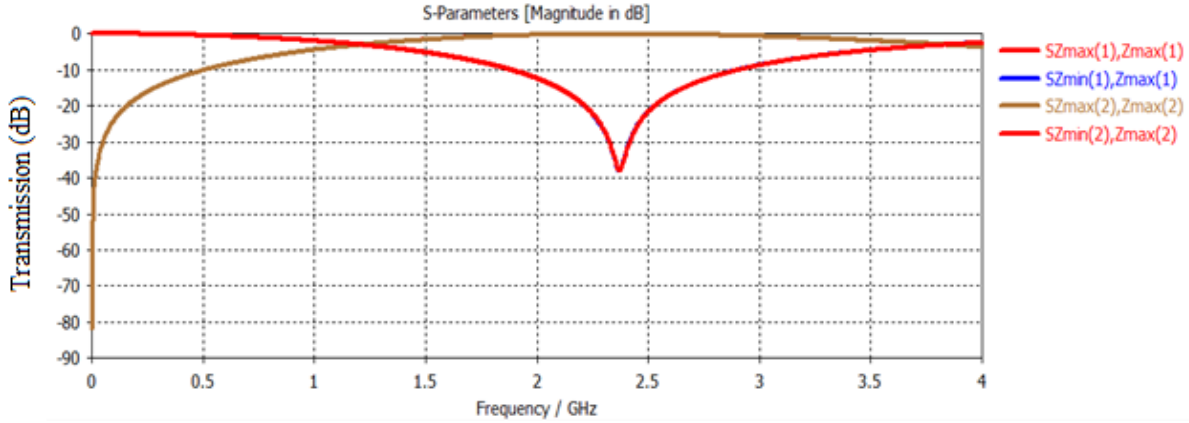

Figure 3.8 TE and TM reflection and transmission response for stop band

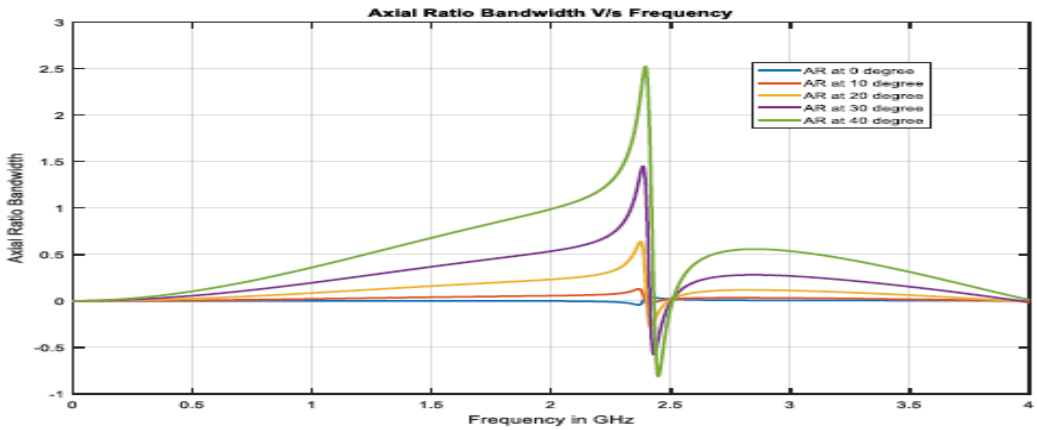

Figure 3.9 Axial ratio bandwidth for stop band chracteristics

In order to verify the polarization independent behavior of the proposed system the simulated axial ratio bandwidth [9] as depicted in Figure. 3.9. This shows that proposed FSS design is independent of polarization as axial ratio bandwidth is below 3dB for the desired stop and pass band of operation.

3.2.2.3 Effect of Change in Loop Width of SSL-Stop Band FSS:

Here we see that if there is change in the width of patch w (L2-L1) from 1 mm to 6 mm there is shift in transmission null point from 2.4 GHz to 5.6 GHz this means that the resonance is shifted from lower to higher frequencies. It can be observed from the Figure 3.10 that transmission null point is downshifted and transmission null point bandwidth is increased as we change width of single square loop structure. This is because an increasing the width, inductive effect reduces which causes the increase in width of stop band response parameters. It is clear that by varying the value of the 'w' the desired band of rejection of the signal is achievable and therefore width of SSL FSS is optimized to 2.5 mm.

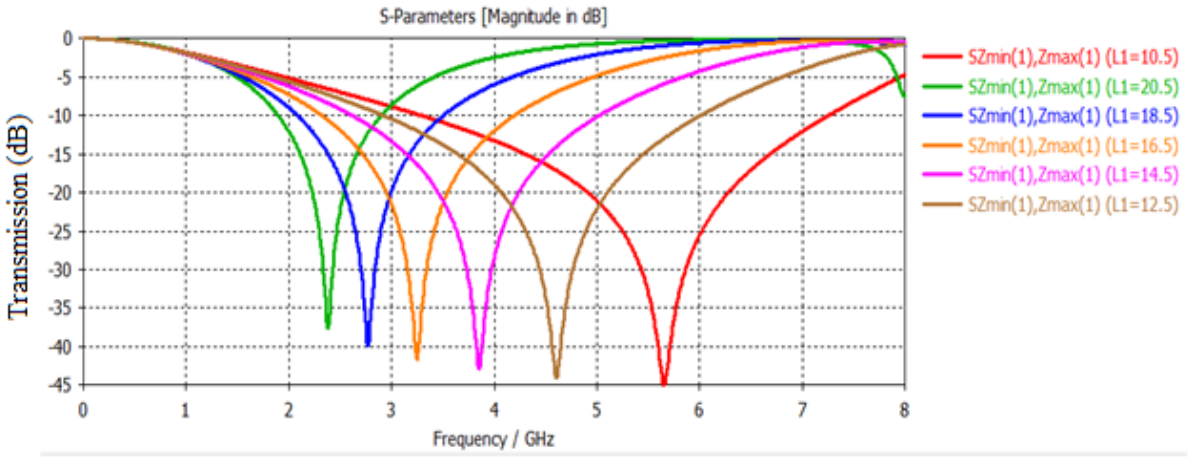

Figure 3.10 variation in width of single square loop FSS structure (stop band)

Table 3.3 shows the variation in return loss and bandwidth of the stop band of proposed FSS unit cell for Figure 3.2(a).

Table 3.3 Effect of varying width of Unit cell Structure of FSS

Varying Parameters Width of Square Loop (mm)	Return loss (dB)	Bandwidth(GHz)	Resonance Frequency (GHz)
1	-37.296	1.038	2.400
2	-39.67	1.426	2.776
3	-41.52	1.847	3.248

4	-42.84	2.395	3.856
5	-44	3.086	4.612
6	-44.884	4.093	5.666

3.3 DESIGN AND SIMULATION OF A MINIATURIZED UNIT CELL ELEMENT FOR PASS BAND MICROWAVE FILTER APPLICATION FOR S AND X WIRELESS COMMUNICATION BANDS

A polarization independent frequency selective Surface (FSS) with pass band characteristics for the 'S' and the 'X' wireless communication bands respectively has been explained in this subsection. This sub section also explains the design of unit cell of proposed FSS structure. The simulation results in terms of transmission parameters, axial ratio bandwidth and output response with variation in angle of incidence and current distribution results of the proposed unit cell (when it is taken as a periodic structure) are presented.

3.3.1 Design of Unit cell Structure of FSS

The design of FSS structure begins with the design of a unit cell structure. Figure 1(a) depicts the top view of the proposed unit cell of FSS structure. The design a unit cell structure of FSS starts with the dimensions of the substrate that is calculated by using the equation (i) that explained in section 1.7 for a resonance of 3GHz i.e. centre frequency of the lower pass band. The proposed FSS is designed on an FR4 dielectric substrate with dielectric constant of 4.4 and height of substrate is 1.57mm. The dimensions of the inner square loop of the proposed Unit cell structure have been calculated using equation (ix) that is mentioned in subsection 1.7.The unit cell design of FSSs contains two concentric square loops of dimension mention in table 3.4. To control the transmission coefficients of incident wave, two sets of orthogonal stubs are interleaved at the centre of the inner edges of the wide square loop. These stubs have an input impedance that shows purely reactive properties that is either capacitor or inductor, which depends upon electrical length of stubs. Optimization of both length of inner square loop and length of stubs are explained in section 3.3.2.4.

Table 3.4 Specified and optimized parameters of unit cell of FSSs

Specifications	Dimensions (mm)
Substrate(W×L)	13×13
Outer Square loop(W×L)	13×13
Thickness of outer loop	0.25
Inner Square Loop(W1×L1)	11.5 ×11.5
Thickness of inner loop(t)	1.5

Stubs (w × l)	0.5 × 2.875
Spacing between two loops (s)	0.5

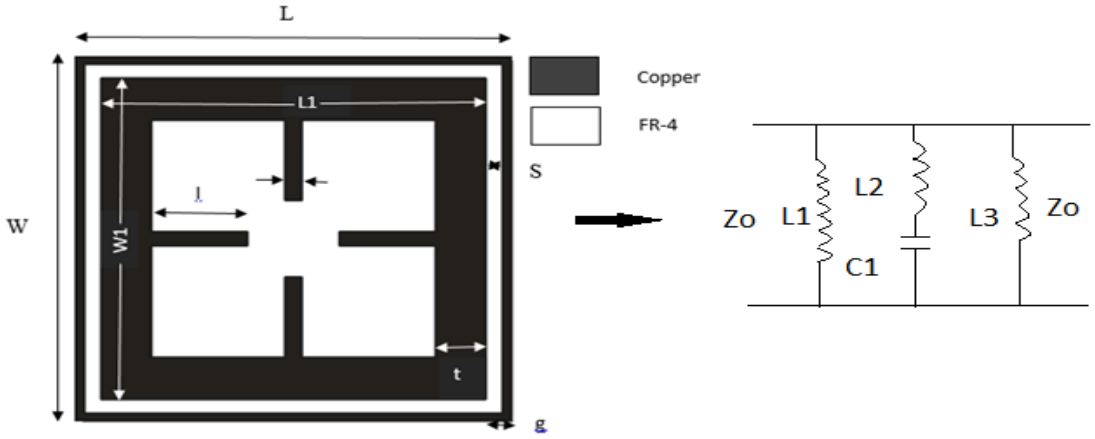

Figure 3.11(a): Top view of unit cell

Figure 3.11(b): Equivalent circuit for unit cell of FSS

Figure 3.11(b) shows the equivalent circuit of the proposed FSS. Here L1 inductor exist because of the inner square loop, L2 exist because of outer square loop while L3 occur because of set of stubs. One capacitor C1 exist in series with L2 because of the air gap between the inner and outer loop as depicted in Figure 3.11(b).

3.3.2 FSS Simulated Results

The proposed FSS is designed and simulated using CST Microwave studio version 2016 using unit cell boundary condition and floquet ports. Figure 3.12 shows the transmission characteristics of the proposed unit cell structure of FSS. It depicts two pass bands from1.44GHz to 4.64 GHz and from 6.3GHz to 12.1GHz for both TE (Szmin (1), zmax (1)) and TM (Szmin (2), zmax (2)) modes of operation. From the simulated transmission parameters, it is perceived that at normal angle of incidence both TE and TM transmission coefficients overlap each other showing that at this incidence, the proposed FSS design is independent of polarization of the incoming waves.

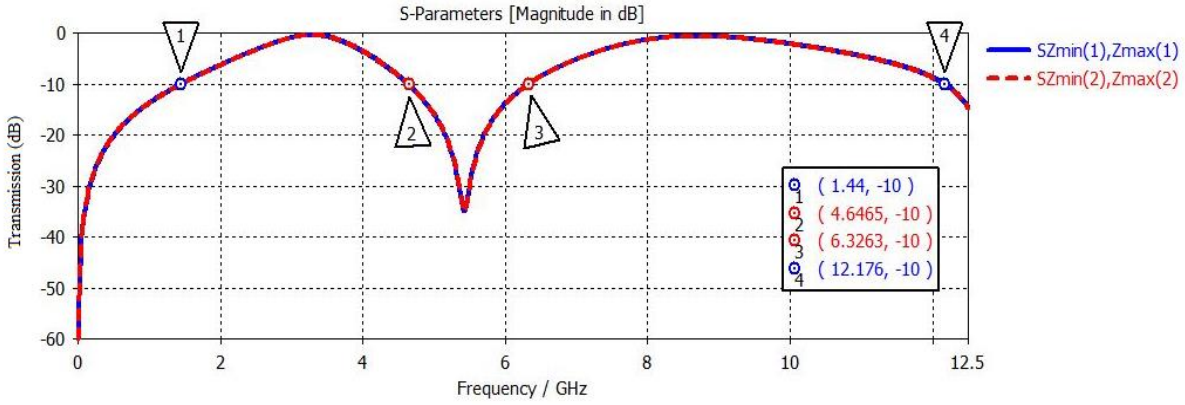

Figure 3.12: Transmission parameters of TE and TM mode

3.3.2.1 Axial Ratio Bandwidth

In order to validate the polarization independent behavior of the proposed FSS structure, the axial ratio bandwidth has been shown in figure 3[9] for the entire S and X band. It is verified from the simulated axial ratio bandwidth that the proposed FSS design has an axial ratio < 3dB for the entire S and X bands. This depicts the polarization independent nature of the FSS for the entire frequency band of S and X bands [71].

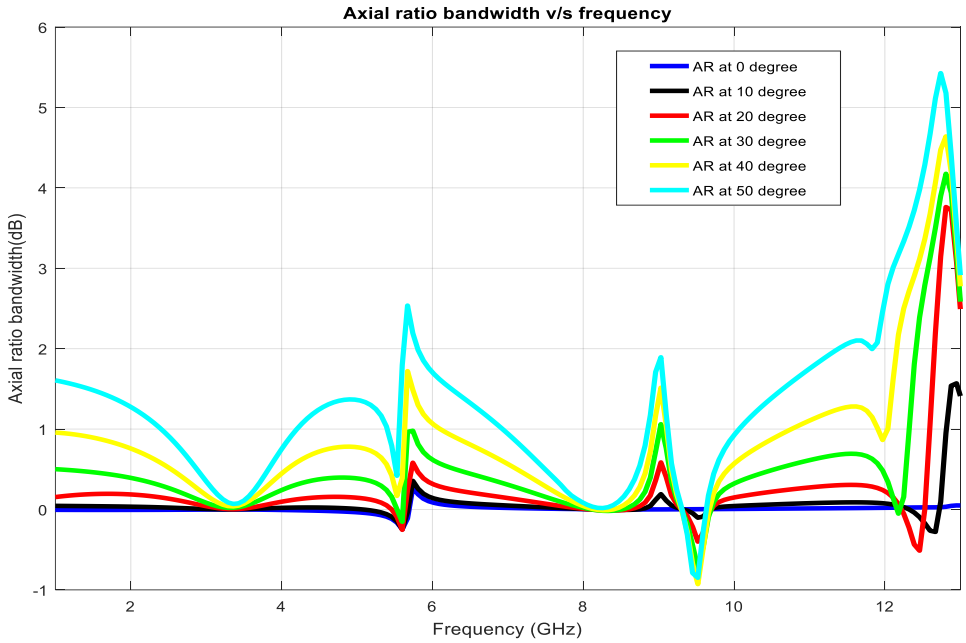

Figure 3.13: Axial Ratio V/s Frequency

3.3.2.2 FSS Response to Variation in Angle of Incidence

Figures 3.14 and 3.15 depict the variation in transmission characteristics of the proposed FSS with respect to the angle of incidence from 0˚ to 60˚ for both TE and TM modes. It can be seen that a pass band from 1.44GHz to 4.64 GHz in both TE and TM modes demonstrate the harmonic free transmission for all the angles of incidence. For the second pass band from 6.3GHz to 12.1GHz also offers a harmonic free transmission at normal incidence but as angle of incidence increases from 0 to 60 degrees, the signal offers a low magnitude of harmonics in transmission which is above -10 dB in the pass band hence is acceptable. The complete frequency response of FSS unit cell structure at different angles of incidence on the bandwidth of the two pass bands for both TE and TM mode is also mentioned in table 3.5.

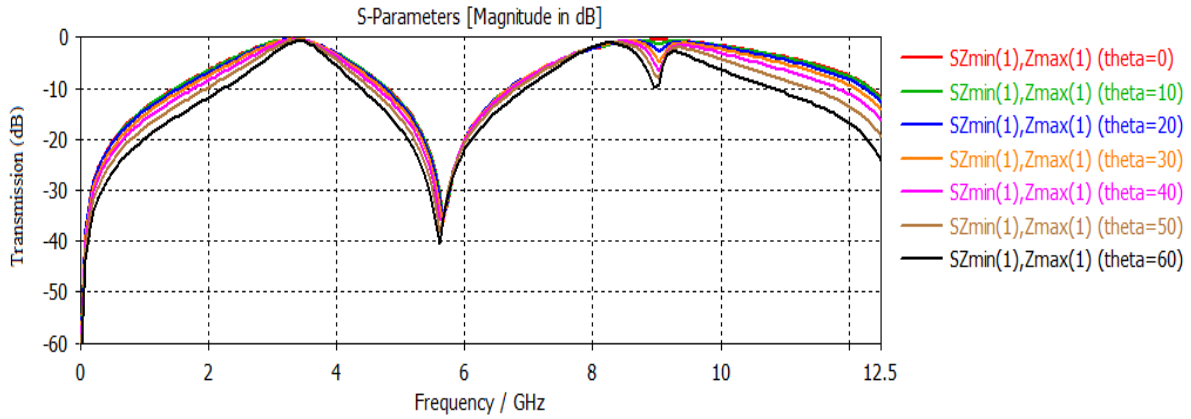

Figure 3.14 Transmission coefficients for TE mode at different angle of incidence

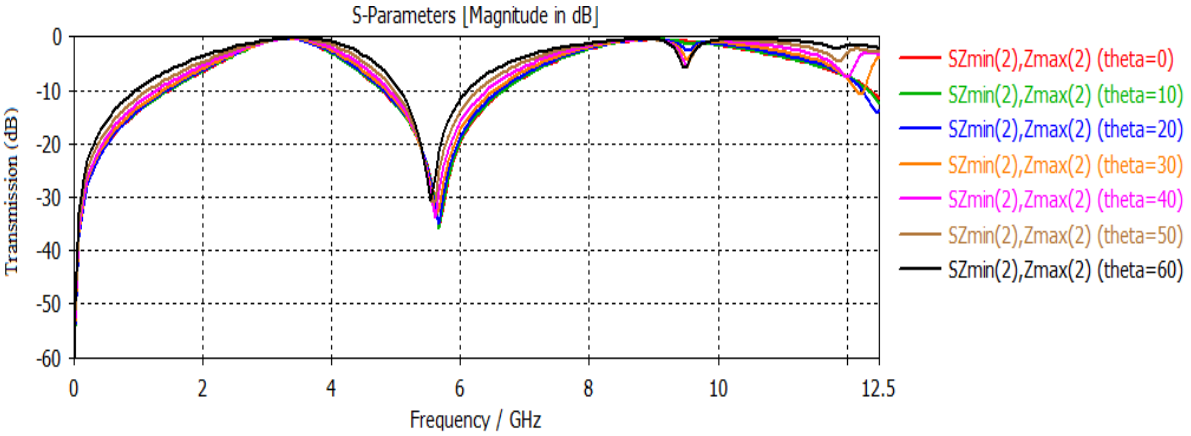

Figure 3.15 Transmission coefficients for TM mode at different angle of incidence

Table 3.5 Variation in bandwidth of the pass bands (TE and TM) at different angle of incidence

Angle of incident	Bandwidth in GHz for First pass band (TE)	Bandwidth in GHz for Second pass band (TE)	Bandwidth in GHz for First pass band (TM)	Bandwidth in GHz for Second pass band(TM)
0˚	3.2	5.85	3.2	5.85
10˚	3.18	5.85	3.21	5.86
20˚	3.12	5.74	3.28	5.85
30˚	2.99	5.57	3.40	5.84
40˚	2.79	5.21	3.53	7.78
50˚	2.52	4.71	3.75	7.85
60˚	2.09	3.97	3.99	7.87

3.3.2.3 Effect of Stubs on the FSS Performance and Current Distribution

To improve the transmission characteristic response of the unit cell FSS structure, a set of orthogonal stubs are interleaved at the centre of the inner square loop. This is illustrated in Figure 3.16 that shows the transmission characteristics of the proposed FSS (TE mode) for two cases that are with and without the use of stubs. Each stub length is optimized to the 0.115λ. The horizontal stubs control the transmission characteristics of TM mode while vertical stubs are responsible for sharpen the transmission characteristics of TE mode. From Figure 3.16, it is perceived that a resonance frequency for both TE and TM mode (12.17GHz) is excited only when theses stubs interleaved at the inner edges of the inner square loop. Surface current distribution on the metal part is shown in both the TE and TM modes at a resonance of 12.17GHz in Figure 3.17. It specifies that for TE mode, stubs that are parallel to electric field vector stimulate a resonance at the frequency of 12.17GHz and likewise stubs that are alongside the direction of incident wave are control for excitation of resonance for TM mode. Figure 3.17 shows a maximum current distribution of 170 A/m for both vertical stubs for TE mode and horizontal stubs for a TM mode.

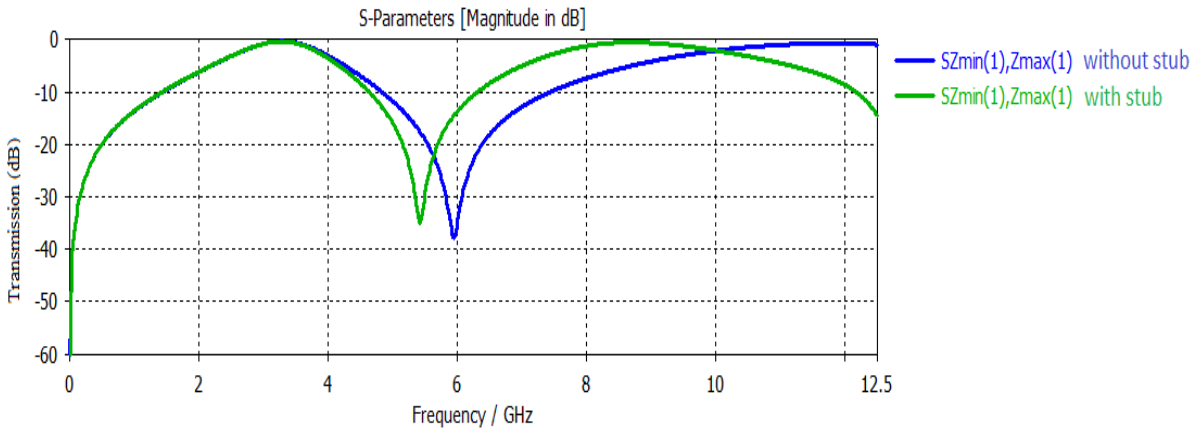

Figure 3.16 Transmission coefficient for TE mode with and without stubs

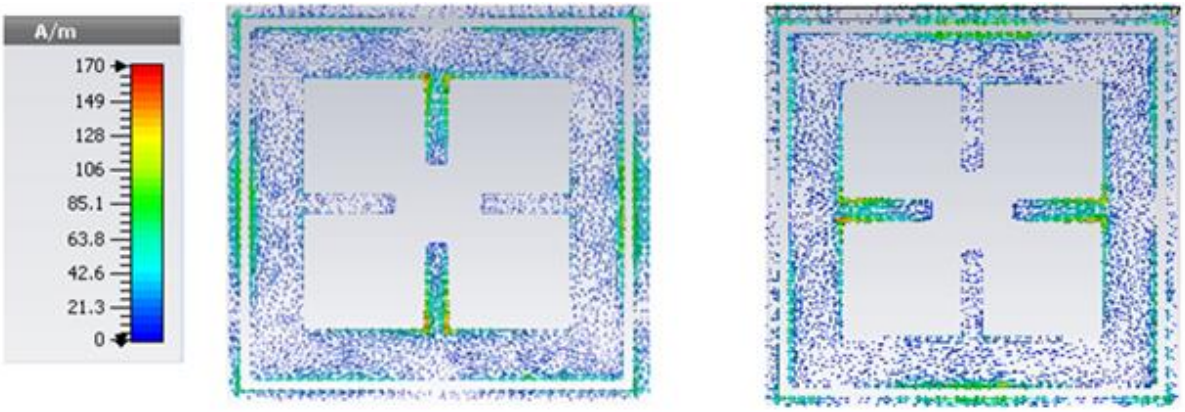

(a) (b)

Figure 3.17 Surface current distribution of the FSS at 12.17GHz (a) TE mode (b) TM mode

3.3.2.4 Parametric Study

From equation (ix) it is observed that the length of inner loop interlinked with its thickness. Table 3.6 depicts the influence of the thickness of the inner square loop on its length. Figure 3.18 shows the effects of variation in length and thickness of the inner square loop on the transmission characteristics of the proposed FSS. From the simulated results of the proposed FSS structure (at different thickness and different length of inner square loop) it is verified that thickness of the inner square loop also effect the transmission characteristics of the proposed FSS structure.

Table 3.6 Effects of thickness of inner loop on its length

s.no	Thickness of inner loop (mm.)	Length of inner loop (mm.)
1.	.5	8.95
2.	.75	9.68
3.	1	10.32
4.	1.25	10.91
5.	1.5	11.5
6.	1.75	12

As the thickness of the inner square loop change from .5 mm to 1.75 mm. It is observed that there is shift initial resonance peak towards lower frequency because as thickness increases, length of inner square loop also increases that offers more inductive effect hence resonance frequency moves towards lower frequency side.

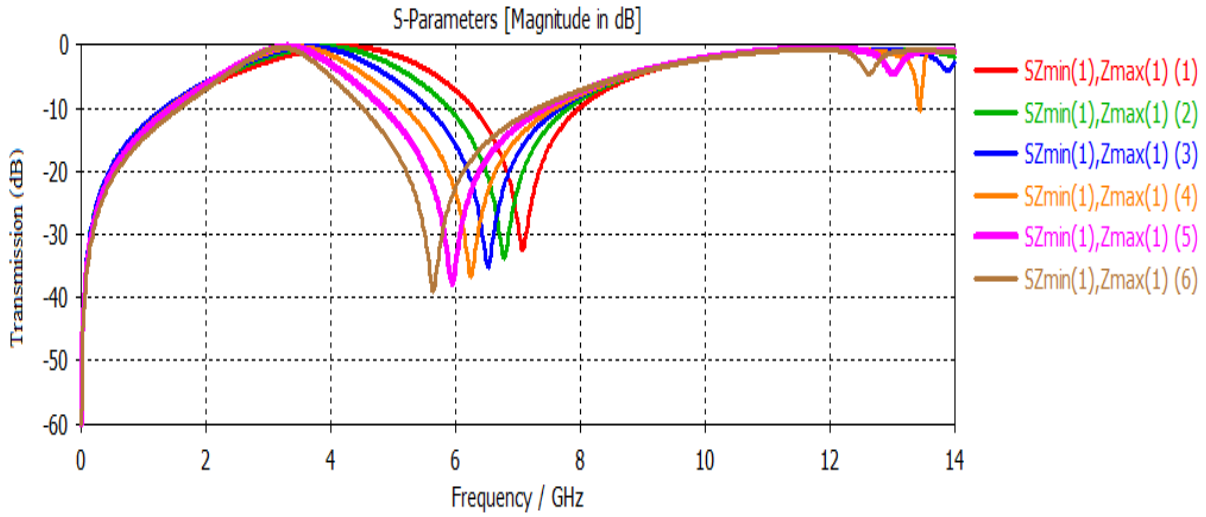

Figure 3.18 Transmission coefficient for TE mode at different lengths and thickness of inner loop of FSS unit cell

3.3.2.5 Effect of length of stubs on resonance

From Figure 3.19 it is observed that as the length of the stub from 1.35 mm to 2.875mm, resonance peaks shifted towards higher frequency because as we increase the length of the stubs inductance effect decreases simultaneously and resonance peak gets shifted to higher frequencies. In addition to this, an increase in length of stub X band effects the most because its sharpness decreases as length of stubs increase. The best results are found at length of 1.375 mm.

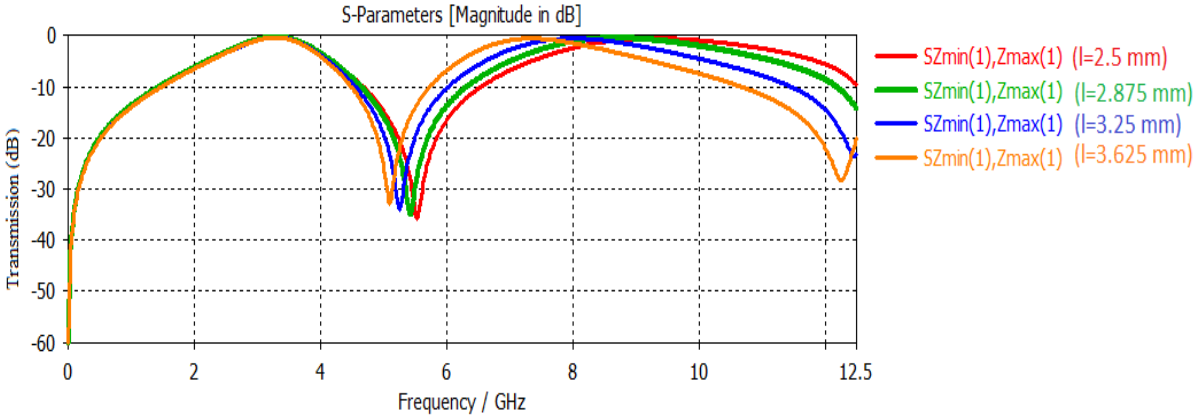

Figure 3.19 transmission coefficient for TE mode at different lengths of stubs

The proposed unit cell shows dual stop band properties for S and X wireless communication band and also shows a polarization independent behavior. The incoming waves from 0˚ to 60˚ angles of incident do not affect the output performance of the proposed FSS structure.

3.4 REALISATION OF A DUAL STOP BAND FOR 'S' AND 'X' BANDS FROM THE COMPLIMENTARY GEOMETRY OF THE DUAL PASS BAND (S AND X BAND APPLICATION) FSSs

In this section, the realisation of stop band unit cell structure of FSS from the one that is proposed in section 3.3 using its complimentary geometry is done. As it is well known that transmission characteristics of complimentary structure of FSS unit cell, will be complimentary of the original FSS transmission characteristics. Therefore the stop band transmission characteristics from pass band can be realized by simply replacing the metal elements of FSS unit cell structure by slots/aperture of the same size and geometry (i.e. complimentary of the original FSS unit cell structure). But here it is important to mention that resultant frequency response of the complimentary structure will not be exactly opposite to that of frequency response of original structure. Therefore the FSS unit cell is optimized to get the desired stop band response for S and X bands.

3.4.1 Design of FSS Unit Cell Structure:

In this subsection, the design procedure and optimization of the complimentary FSS unit cell structure for dual pass band to realise the dual stop band characteristics for S and X band is presented. Step by step changes in the complimentary structure to obtain the dual stop band frequency response has been shown in Figure 3.20.

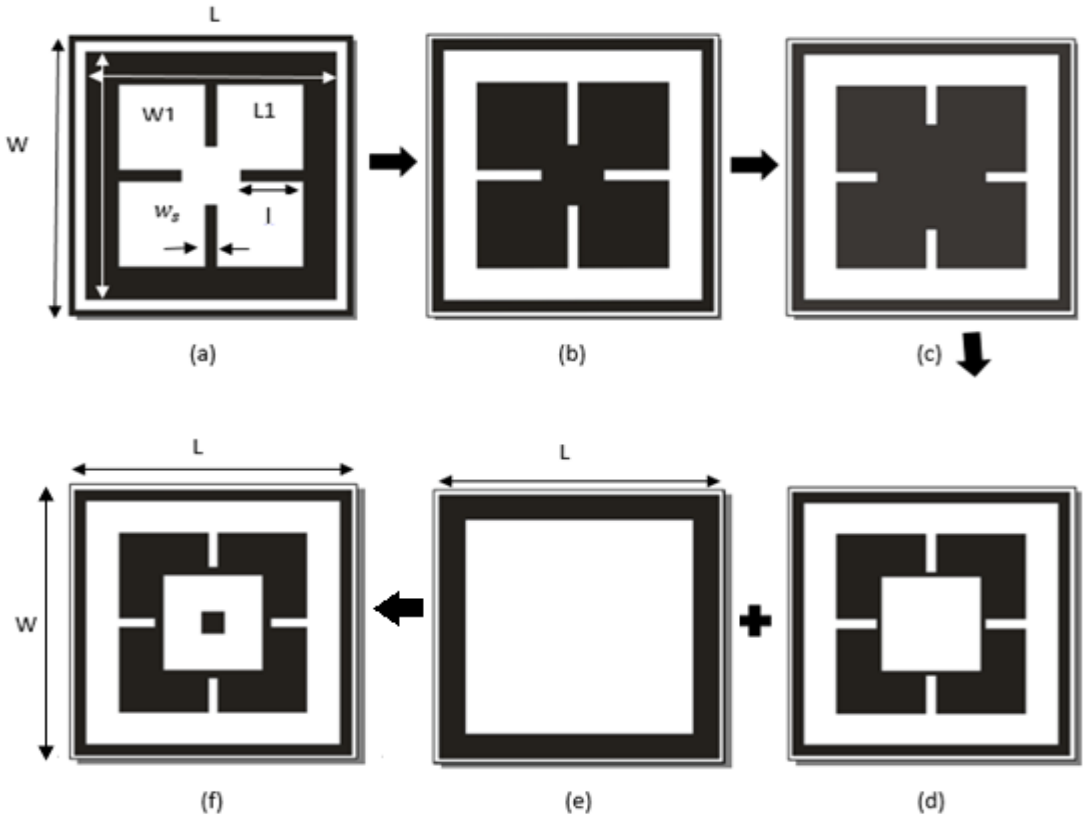

Figure. 3.20 Step wise development of the final unit cell structure of FSS

Figure 3.20 depicts the different steps for the realisation of required stop band FSS from the pass band FSS that is proposed in section 3.3. The steps include to replacing the metal part of the pass band unit cell element with slot/aperture and slotted part with metal one to get the complimentary structure as depicted in Figure 3.20(b). For obtaining the required stop band transmission response the centre square of the complimentary unit cell (b) is made wider as depicted in Figure 3.20(c). In addition to it a wider slot is cut from centre square that offers better results for X band without effecting the S band transmission response. Then one single square loop element on the back side of the substrate is added that increases the bandwidth of both S and X wireless bands, as depicted in Figure 3.20(d) and 3.20(e) respectively. Finally, one small patch of dimensions 0.5 mm × 0.5 mm is added at the centre of the square slot that offers smoothened transmission response for both S and X bands. The optimized parameters of the proposed FSS are mentioned in table 3.5. Moreover final Optimized FSS unit cell for stop band characteristics is also depicted in Figure 3.21.

Table 3.7 Specified and optimized parameters of unit cell of FSSs

Specification	Dimension (mm)
Substrate length (L)	13
Substrate width (W)	13
Length of outer square (Lo)	12.5
Width of outer Square (Wo)	12.5
Thickness of outer loop	0.25
Length of Flower shaped structure (L1)	8.44
Width of Flower shaped structure (W1)	8.44
Slot thickness (t1)	0.44
Length of inner patch (Li)	1
Width of inner patch (Wi)	1

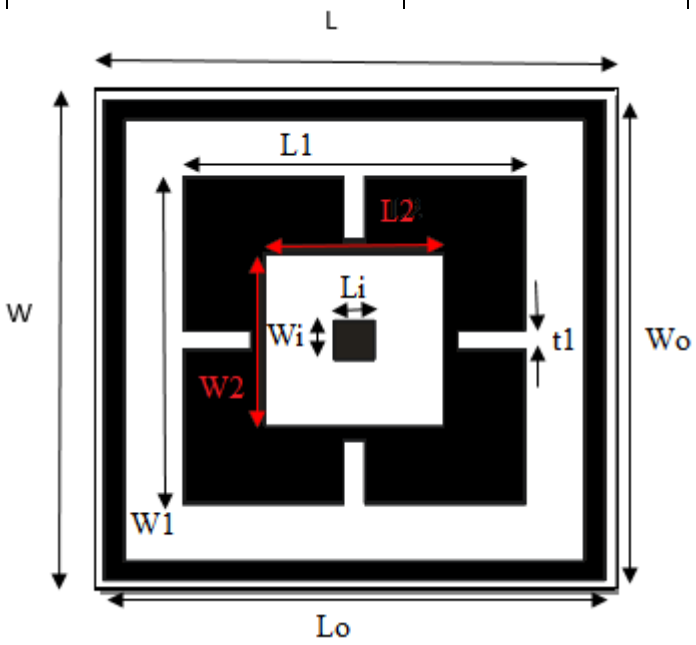

Figure. 3.21 Top view of the unit cell structure of FSSs

3.4.2 Simulation Results

The transmission characteristics of the required stop band have been shown in Figure 3.22. From here it is observed that to realise the band stop transmission characteristics from pass band, Unit cell of FSSs has to go through different stages, as shown in Figure 3.20, where every parameters of the unit cell structure effects the transmission characteristics. Figure 3.22 shows the first stage complimentary structure of the Unit cell that is shown in Figure 3.20(a). It is seen that the transmission characteristics are complimentary of the pass band but do not cover the entire S and X bands. Therefore optimized complimentary structure of FSS is obtained for stop band characteristics that covers the entire S and X bands. At the second stage, the broadened centre square of the inner Flower shaped structure, gives the transmission characteristics that do not alter the stop band response for S band but shifts the resonance frequency of X band towards the higher frequency as shown in Figure 3.22 (dotted blue curve). At third stage, a slot is cut from the inner square and single square loop of metal pattern on the back side of substrate is added. It is seen that it again do not alter the S band frequency response but broadens the bandwidth of X band frequency response. At the final stage, when add a small metallic patch at the centre of slot is added the bandwidth of S band and X band frequency responses becomes wider and now offers the required transmission stop band characteristics for the entire S(2.06 GHz-4.44 GHz) and X (7.9 GHz-12.4 GHz) bands.

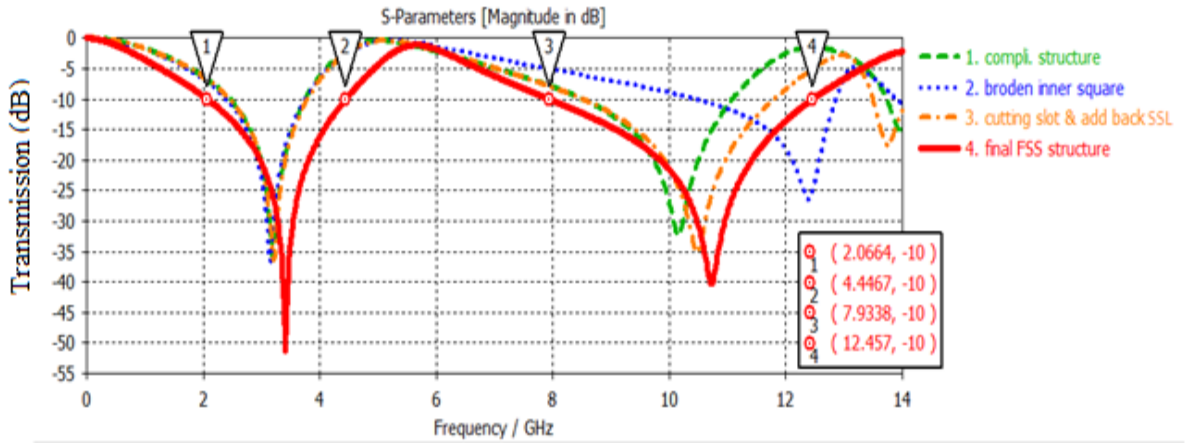

Figure 3.22 Transmission characteristics (stop band) of FSSs

3.4.3 Parametric study

To obtain the required stop band characteristics from complimentary structure of the proposed pass band FSS mentioned in section 3.3, various parameters of the Unit cell structure of FSS such as length (L1) of inner flower shaped structure, it's slots thickness (t1), length (L2) of the inner slot and small inner patch (Li) have been optimized and effect of each parameter on the performance has been explained in this section.

3.4.3.1 Variation in the Length of Inner Flower Shaped Structure

Figure 3.23 depicts the effect of variation in length of the flower shaped structure of FSS unit cell element. It is observed that smaller length (L1) of inner flower shaped structure offers more effects on the S band of the transmission characteristics without much effecting the X band. As the length L1 goes on increasing from 8.42 mm to 8.46 mm, change in the transmission characteristics of both S and X band is observed. It is observed that best results are found at L1 =8.44 mm and is therefore selected.

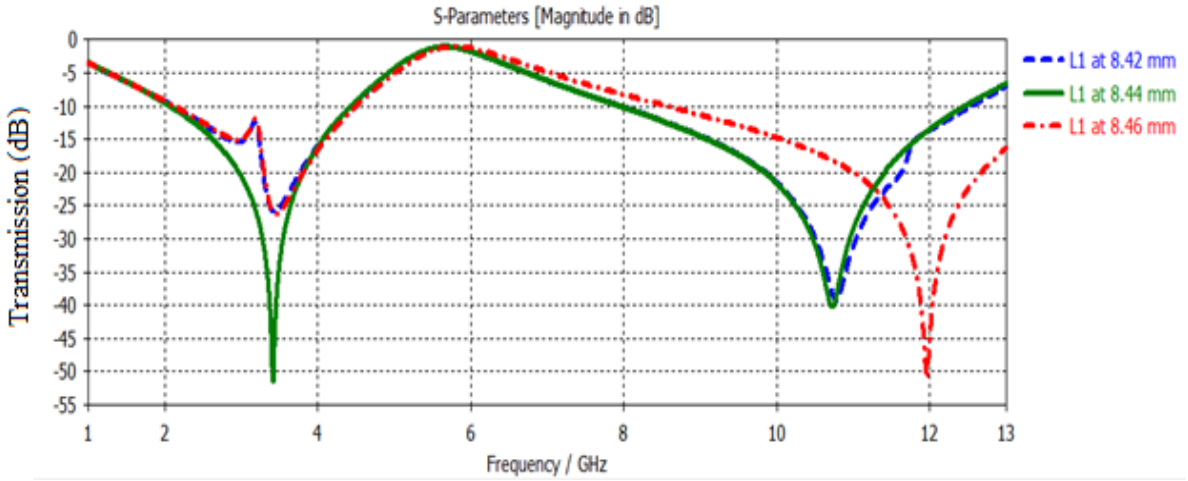

Figure 3.23 Variation in the length of inner flower shaped structure

3.4.3.2 Variation in the Thickness (t1) of the Slot of Inner Flower Shaped Structure

From Figure 3.24 it is shown that thickness of rectangular slot 't1' effects the S band characteristics without much effecting the X band characteristics. As the thickness changes from 0.42 mm to 0.46 mm, it is observed that, lower value of t1 alter the X band frequency response while higher value 0.46 mm alters the S band frequency response of the FSS unit cell structure. It is observed that the better result at t1=0.44mm and is therefore selected.

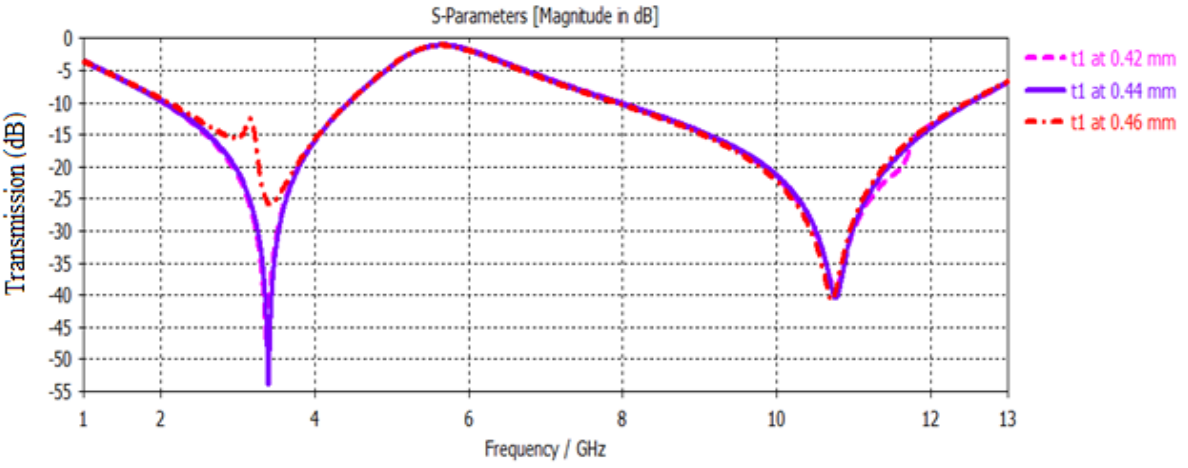

Figure 3.24 Variation in the thickness (t1) of the slot of inner flower shaped structure

3.4.3.3 Variation in the Length (L2) of the Square Slot of Inner Flower Shaped Structure

Figure 3.25 depicts the effect of length (L2) of inner square slot on the frequency response of FSS structure. As size of the slot increases from lower (3 mm) to higher (5 mm), it is observed that the resonant peaks of the X bands moves towards lower frequency. In addition to this, the frequency response of S band of FSS structure is also affected. Better results are found in terms of transmission characteristics at length of 4.5 mm and is therefore selected.

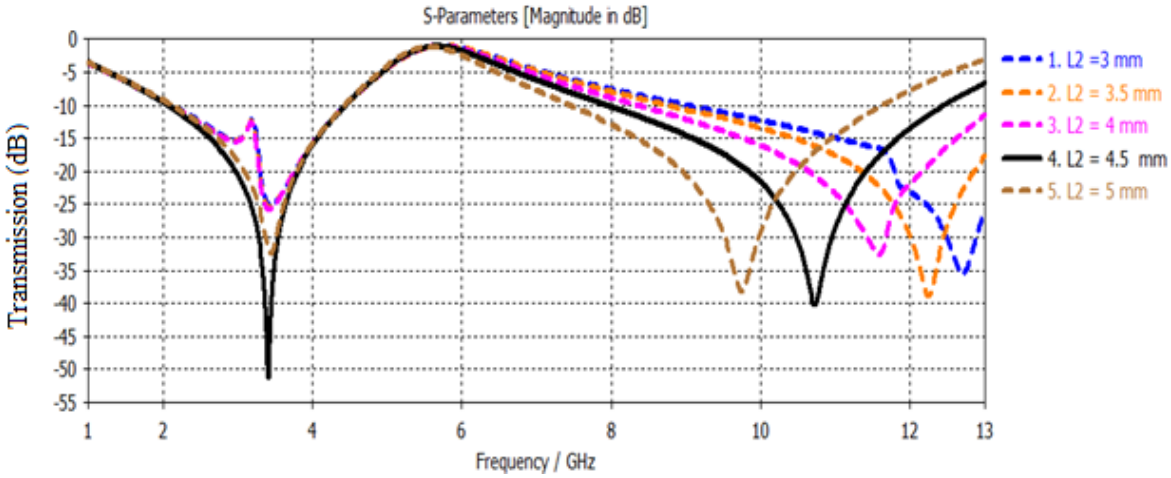

Figure 3.25 Variation in the length (L2) of the square slot of inner flower shaped structure

3.4.3.4 Variation in the Length (Li) of the Small Inner Metallic Patch of FSS Structure

From Figure 3.26 it is observed that the inner patch effect the S band frequency response more without much effecting the frequency response of X band. Best results are found at Li=1 mm and is therefore a selected parameter.

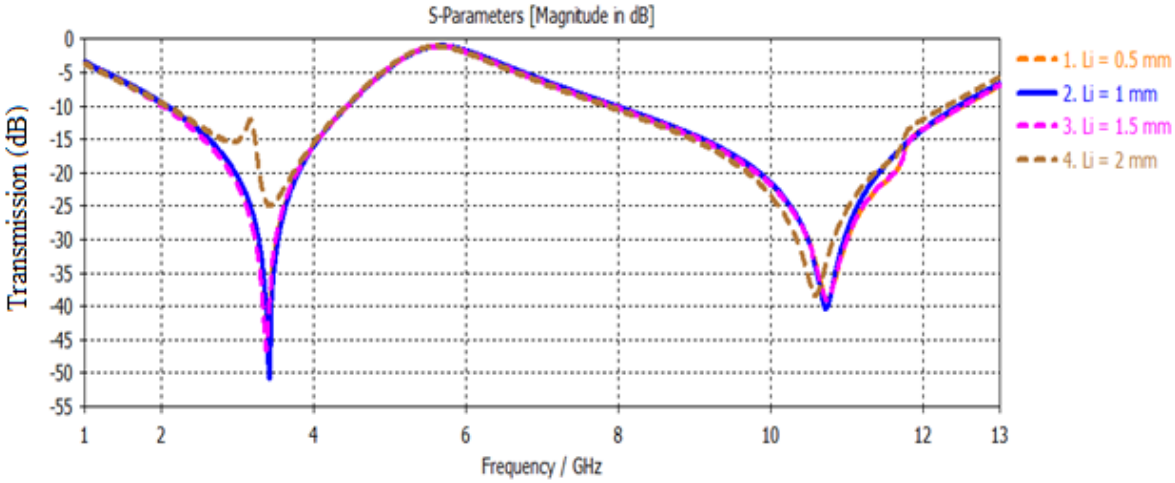

Figure 3.26 Variation in the length (Li) of the small inner metallic patch of FSS structure

3.5 FSS FOR ULTRA-WIDE STOP BAND CHARACTERISTICS USING FRACTAL GEOMETRY

In this subsection we propose a fractal geometry based FSS for ultra-wide stop band characteristics. This subsection also explains the design of unit cell structure of FSS, its simulation results in terms of its transmission characteristics and the effect of variation in angle of incidence with respect to the incoming EM waves.

3.5.1 Geometry of Unit cell of the Proposed FSSs

Proposed Ultra wideband FSS is a 2D array of periodic distribution of Unit cell elements that are printed on the dielectric substrate (FR4). This FSS structure works as a reflector that reflects the incoming EM waves for the frequency of 3.4 GHz to 12.31 GHz. The dimensions of proposed FSS unit cell is 14 mm × 14mm × 1.605mm. When the periodic array of the proposed unit cell is replicated on the FR-4 sheet,the final FSS sheet dimensions are 42mm× 42mm×1.605mm. Figure 3.27 depicts the iteration wise geometry of the proposed flower shaped unit cell. The flower shaped patch is printed on FR-4 substrate with relative permittivity of 4.4, loss tangent of 0.24 and thickness substrate is 1.57 mm. To achieve this flower shaped geometry, five square slots each of dimension 4mm×4mm are etched from the copper sheet (12mm×12mm×0.035mm) that is printed on the dielectric substrate to obtain the required Unit cell structure of FSS as depicted in Figure 3.27. Further for the second iteration, two stubs of L2/9 are interleaved at the adjacent sides of each of the four slots of the FSS unit cell structure. Here L1 and W1 are the length and width of the unit cell elements. Periodicity of the unit cell P=L1=W1=14mm.

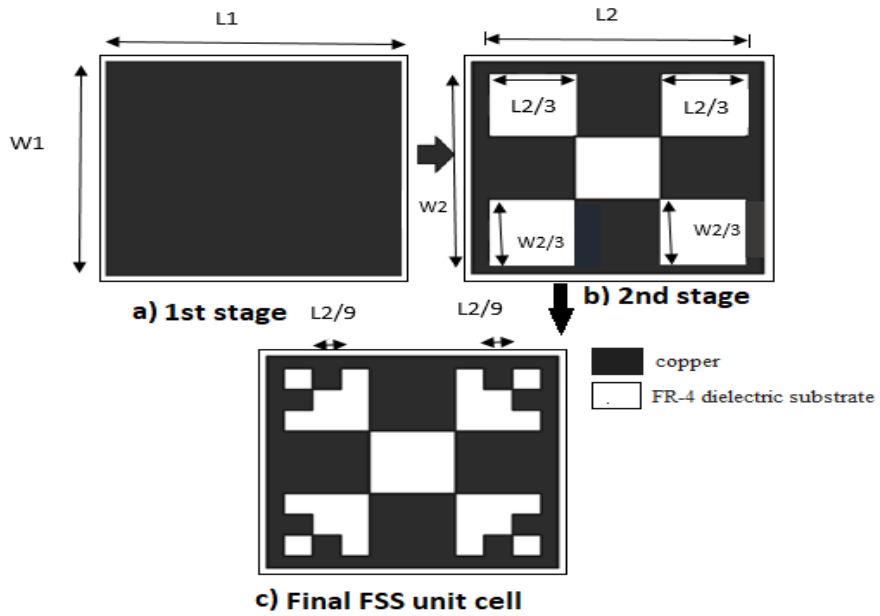

Figure 3.27 Step wise geometry of FSS unit cell

3.5.2 Simulation Results

The unit cell of the proposed FSS is designed and simulated in microwave CST 2016 version in frequency domain using unit cell boundary condition along X and Y direction and floquet ports. The transmission coefficients for the first iteration of the proposed FSS unit cell depict that it has achieved an ultrawide wide stop band for the frequency range of 3.45 GHz to 11.82 GHz.For further enhancement in the bandwidth of the FSS, one more iteration has been done and its transmission coefficients, now cover a frequency band from 3.48 GHz to 12.31 GHz as shown in Figure 3.28.Hence with 2nd iteration there is an overall approximate enhancement in bandwidth by 5 % and is therefore the proposed geometry.

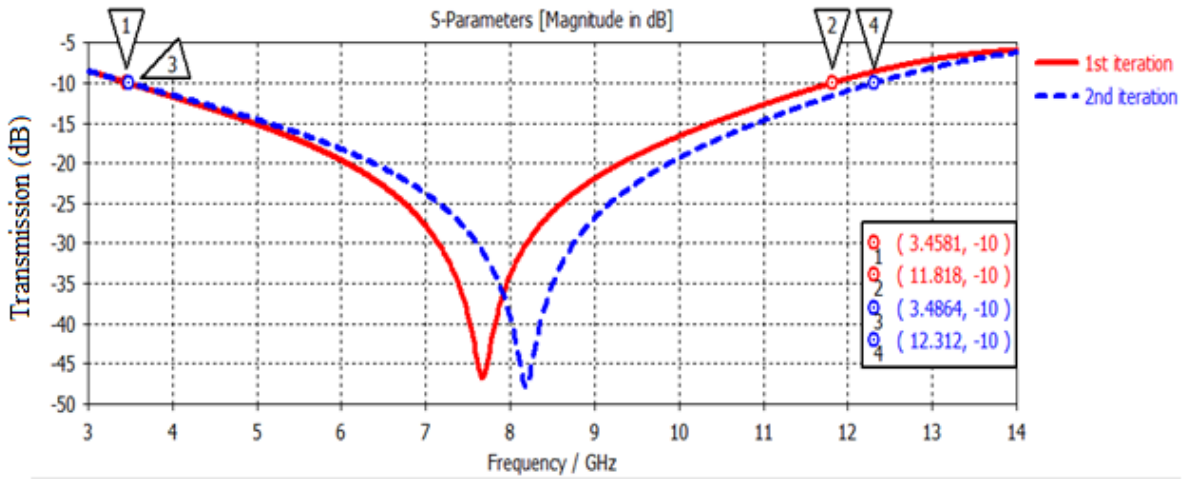

Figure 3.28 Transmission coefficients for FSS unit cell for 1st and 2nd iteration

3.5.3 Effect of the Incidence on the Transmission Characteristics of the Proposed FSS:

Figures 3.29 and 3.30 depict the variation in transmission characteristics of the proposed FSS with respect to the angle of incidence from 0˚ to 60˚ for both TE and TM modes respectively. It can be seen that an ultra-wide stop band, from 3.48 GHz to 12.312 GHz and 3.51 GHz to 12.319 GHz for TE and TM modes, demonstrate the harmonic free transmission for normal angle (0˚) of incidence. The proposed fractal FSS structure offers harmonic free transmission characteristics (TE mode) just at normal incident but the same FSS structure offers harmonic free transmission characteristics (TM mode) for all angles till 30˚as shown in Figure 3.30. It is observed that angle of incident (> 30˚) FSS offers harmonic transmission characteristics for TM mode.

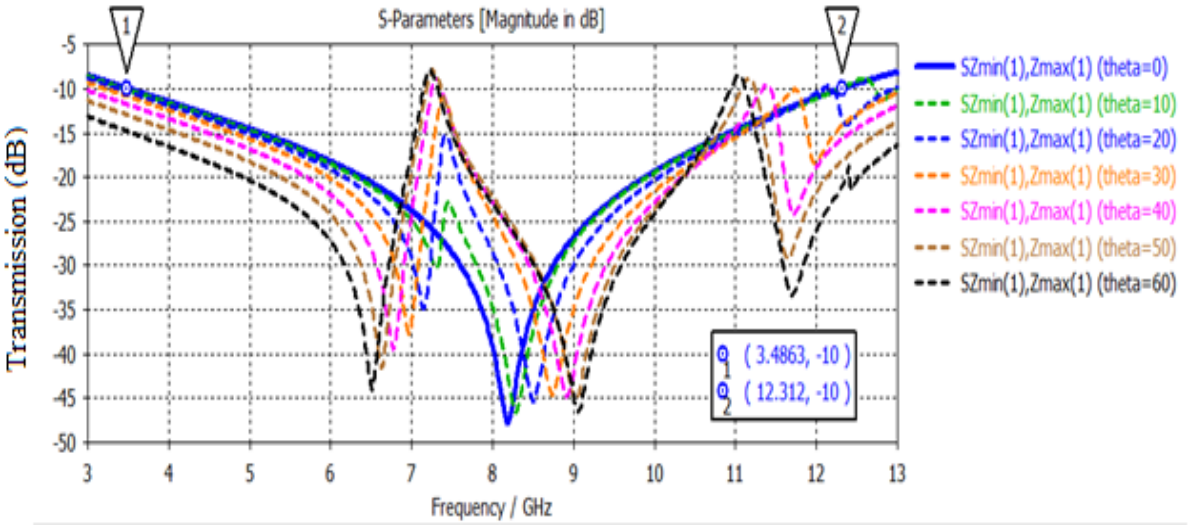

Figure 3.29 Transmission coefficients for TE mode at different angle of incidence

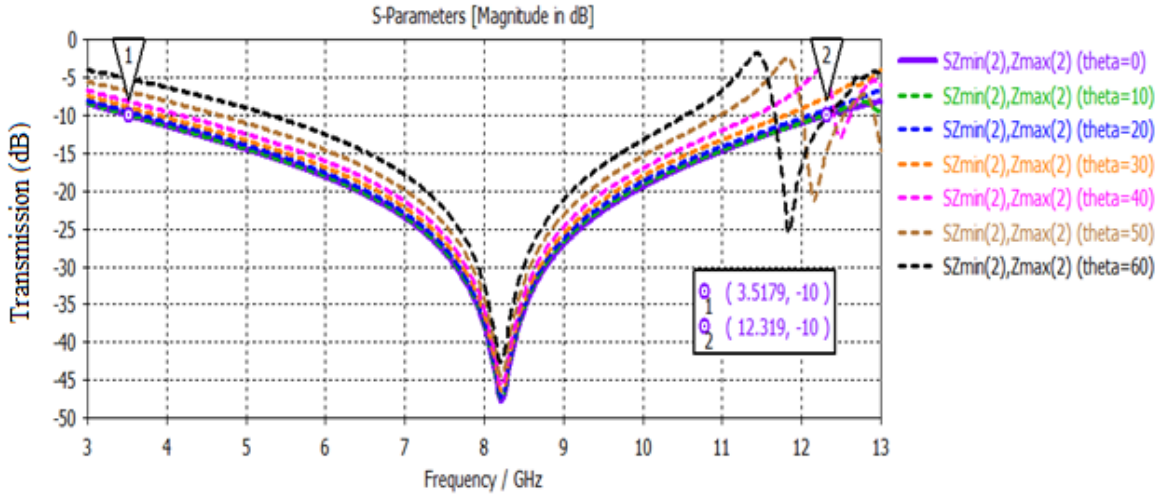

Figure 3.30 Transmission coefficients for TM mode at different angle of incidence

The proposed FSS unit cell structure offers ultra-wide stop band transmission characteristics. Because of its ultra-wide band characteristics, this FSS can be used as a reflector for UWB antenna having resonance nearly equal to the resonance of proposed FSS structure that explained in next sub section.

3.6 DESIGN AND SIMULATION OF AN UWB CPW FED ANTENNA AND IMPROVE IN ITS GAIN BY USING THE FRACTAL FSS AS ITS REFLECTOR

In this section, an ultra-wide stop band FSS has been proposed to be used as reflector with a CPW antenna to enhance the gain for UWB applications. Simulation results of antenna are carried out using CST Microwave Studio 2016 version in the time domain. A fractal FSS unit cell designed and simulated using periodic boundary conditions and floquet ports that presented in section 3.5 is used as a reflector with the proposed antenna to achieve an improvement in the antenna gain by around 2.25 dB.

3.6.1 Coplanar Wave Guide Antenna Design and Geometry

The antenna is designed using transmission line equations [11].The design steps are depicts in figure 3.31(a-d).The proposed antenna with dimension 38 mm× 38 mm× 1.605 mm is presented in this section. As the antenna is co-planar so its radiation patch, ground, feed line all are printed on the same dielectric substrate of FR-4 material as shown in Figure 3.32. The substrate has dielectric constant 4.4 and the thickness as 1.57 mm. CPW fed MPA is preferred as it has superiority of small size and ease of integration. In this section, a slotted rectangle with stubs is used for the antenna geometry. Two stubs are interleaved at the outer edges of the rectangle for achieving ultra-wideband characteristics and a slot has been etched from the rectangular patch for enhancing the bandwidth as shown in Figure 3.31(a-c). Two inverted right angle triangles each of the base 3 mm and perpendicular height of 1 mm have been added to the lower part of the slotted rectangle for achieving impedance matching and Ultra wideband characteristics as shown in Figure 3.31(d). The reduced ground layer is made on both sides of the coplanar feed line for better impedance matching and bandwidth improvement. Coplanar feed line has been optimized using a parametric sweep option in CST microwave studio 2016. A difference of 0.5mm is maintained between the reduced ground and feed line which is optimized for obtaining strong coupling of antenna to the feed network. The feed network is coplanar to avoid the surface waves. Table 3.6 gives the optimized dimension of antenna labelled in Figure 3.32.

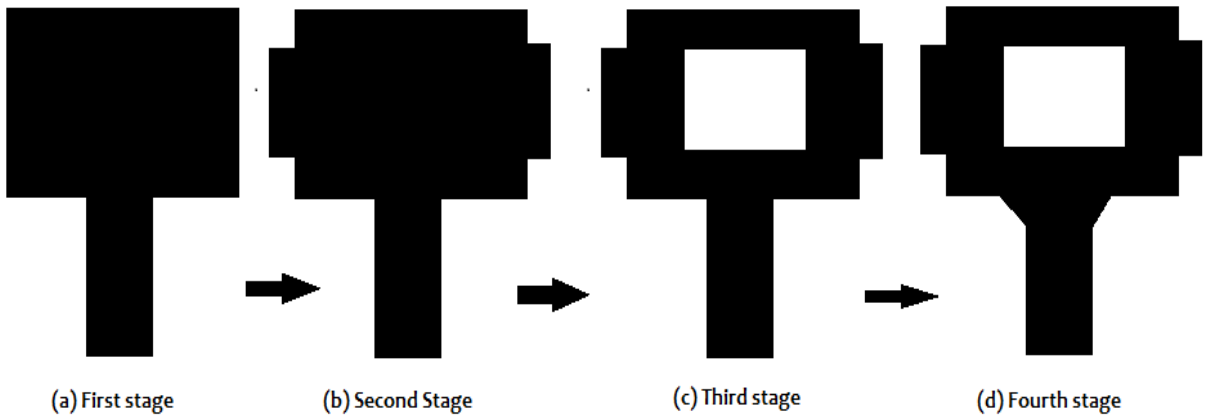

Figure 3.31 Different antenna configuration

Table 3.31 Specified and optimized parameters of coplanar waveguide antenna

Specification	**Dimension (mm)**
Substrate(L×W)	38 × 38
Patch (l1×w1)	12.25×16
Stubs($l_s \times w_s$)	7×2.25
Slot(b × a)	8×6
Ground ($l_g \times w_g$)	14.5 × 12

Feed line ($l_f \times w_f$)	15×4

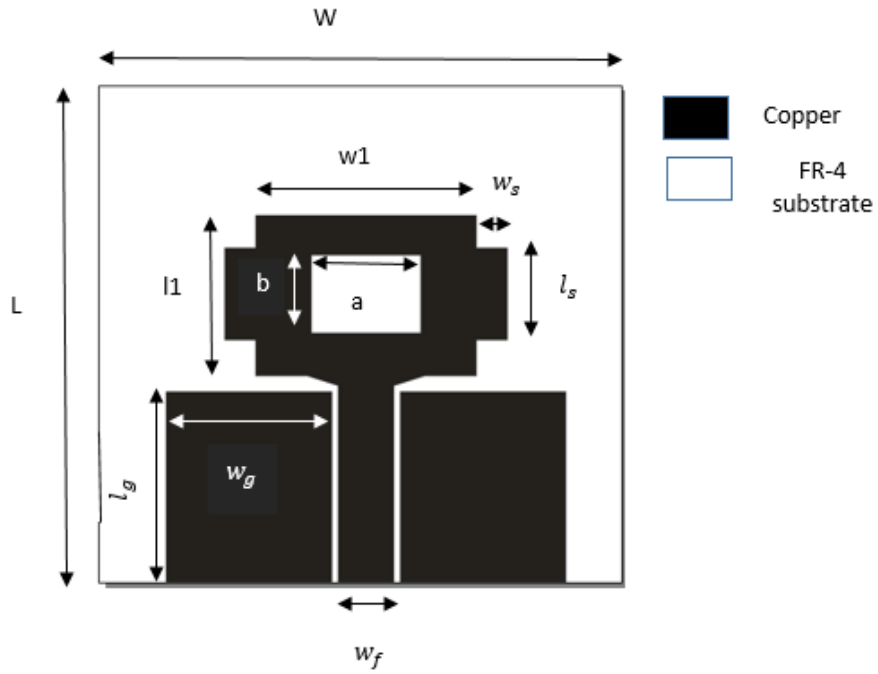

Figure 3.32 Front view of the coplanar waveguide antenna

3.6.2 Simulation Results

This subsection presents the simulated results of proposed CPW fed antenna. Then the proposed ultra-wide stop band fractal FS is placed behind this antenna to act as a reflector that reflects its back lobe towards the major lobe and hence improve the gain of the antenna by around 2.25 dB. The simulated results in terms of its reflection coefficient and gain have been shown to observe the effect of the FSS sheet on the antenna performance.

3.6.2.1 S Parameters Results:

The performance results of the proposed UWB CPW fed antenna for various design steps are shown in Figure 3.33. It is found that an optimized reflection coefficient for the antenna which resonates at 5.52 GHz and 8.91 GHz with return loss 33.93 dB and 27.94 dB respectively and covering the frequency range from 3.39 GHz to 12.89 GHz with impedance bandwidth of 9.5GHz. Figure 3.31 (d) shows the final optimized selected geometry and shows an UWB from 3.39 GHz to 12.89 GHz.

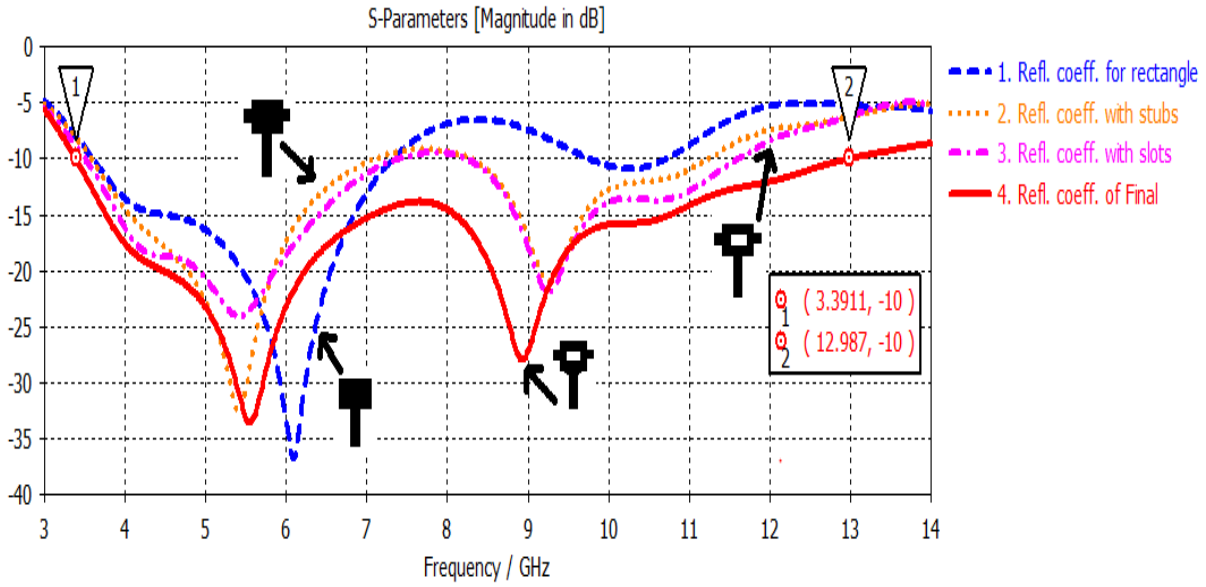

Figure 3.33 Reflection coefficients for Co planer wave guide antenna

3.6.2.2 Effect of Variation In Width of Reduced Ground

The effects variation in the width of reduced ground on the bandwidth of the antenna has been depicts in Figure 3.34. From the figure, it is verified that with the increase in the width of the ground, reduction in the bandwidth of the antenna takes place. For an optimized width of antenna ground w_g =12 mm is best result in terms of bandwidth are seen. Therefore it is selected parameter for ground width.

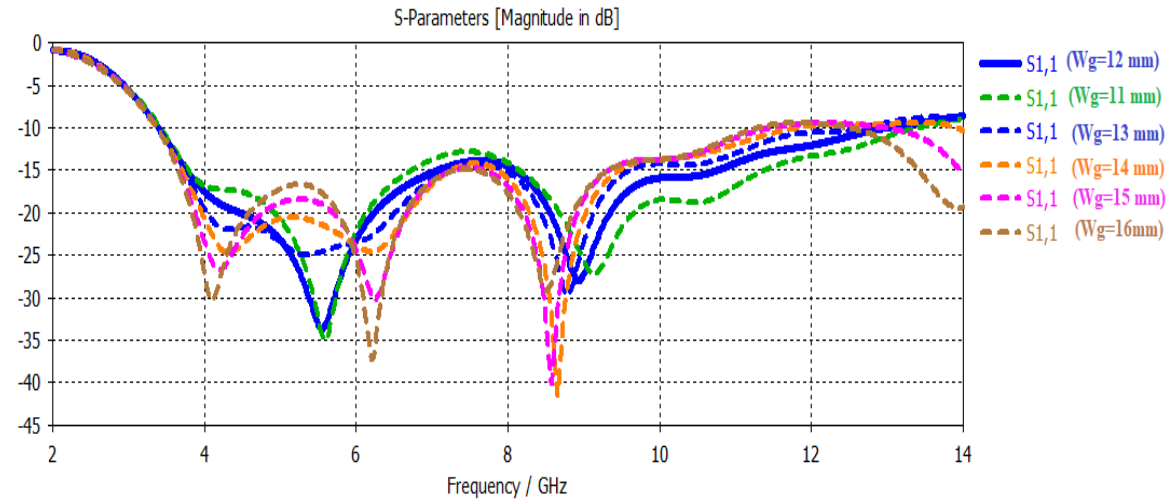

Figure 3.34 Variation in the width of the ground

3.6.2.3 Effect of Variation in the Width of the Feed Line

The effect of variation of width of the feed line on the performance of the proposed UWB CPW antenna has been shown in Figure 3.35. It is verified from the simulated results that at different width of the feed line, there is variation in bandwidth as well as impedance matching.For thinner feed line (w_f=2.5mm) impedance matching is very poor. Improvement in the impedance matching has been

observed for thicker feed line (w_f=4mm)as shown in the Figure 3.35. Therefore 'w_f=4mm' is optimized selected width of feedline for UWB antenna operation.

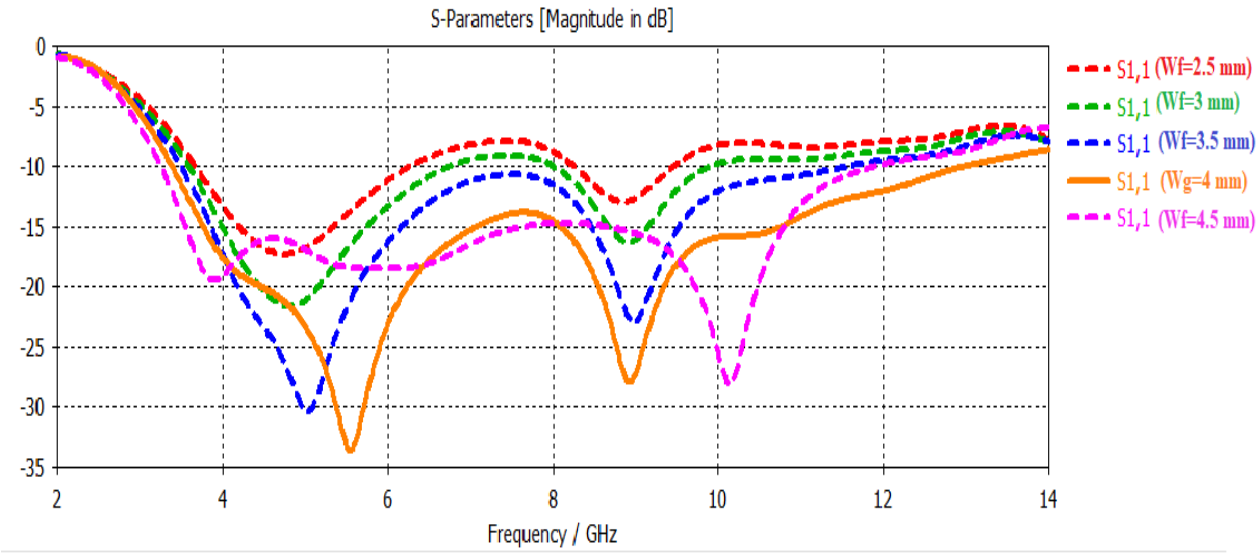

Figure 3.35 Variation in the width of the feed line

3.6.2.4 Improvement in Proposed UWB Antenna Gain with Fractal FSS as a Reflector

Since the fractal FSS proposed in section 3.5 has ultra-wide stop band properties; it can be used as a reflector behind the proposed CPW fed antenna to improve its gain. This is because that the fractal FSS will stop\ reflect the UWB frequency from 3.48 GHz to 12.31 GHz. If a reflection of this kind is placed behind the UWB antenna which radiates 3 dimension the back lobe of the radiation pattern will get reflect from the FSS and will get merged into the major lobe to improve the proposed antenna gain property. The simulated results for antenna with FSS in terms of reflection parameter, bandwidth and gain have been mentioned in this section. Figure 3.36 shows that for improving the performance of the antenna in terms of its gain, an array of FSS unit cell elements is placed behind the UWB coplanar waveguide antenna, so the electromagnetic waves after striking with a reflector/FSS will form unidirectional beam towards major lobe therefore improve the gain of the antenna.

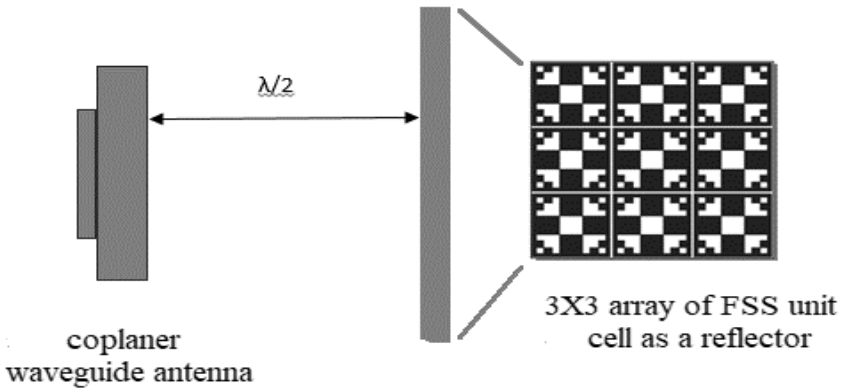

Figure 3. 36 side view of the Set up for antenna and FSS reflector for simulating results

Moreover, Figure 3.37 depicts the comparison of the simulated results of the reflection coefficient of the CPW antenna with and without FSS reflector. The presence of the array of FSS reflectors behind the coplanar antenna does not affect the reflection coefficients of the antenna much significantly and also maintains a proper impedance match over the entire band. For the frequency of 8.9 GHz the return loss of coplanar antenna in the presence of FSS reflector is significantly improved from -27.9 dB to 37.3 dB and it is also observed that enhancement of 1.33% in the bandwidth of the antenna is there. Figure 3.38 depicts the comparison of the gain for both cases (presence and absence of FSS reflector). With the use of an array of FSS as a reflector, the gain of the antenna enhances over the entire frequency band from 3.2GHz to 12.47 GHz. The maximum observed gain is 8.14 dB at a frequency of 12.47 GHz while the minimum gain is 4.98 dB at a frequency of 3.285 GHz which previously (without FSS reflector) was 1.866 dB. Hence with the presence of FSS reflector, there is an overall enhancement in the gain of the antenna by 2.25 dB (average) without much significantly affecting its ultra-wideband characteristics. Minimum gain enhancement is 0.8 dB at a frequency of 12.81 GHz while maximum gain enhancement is 3.7 dB at a frequency of 4.63 GHz and an average gain enhancement for the entire band is 2.25dB.

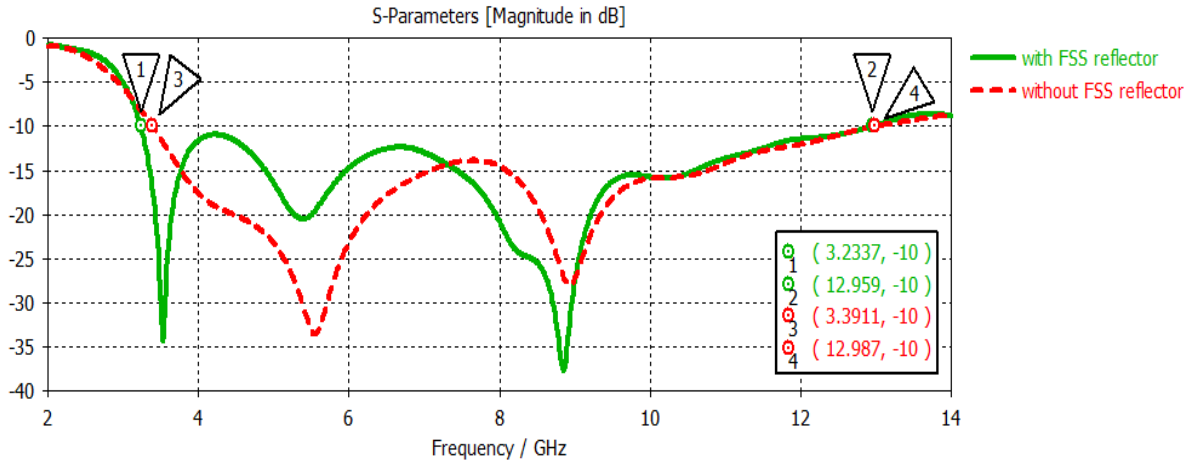

Figure 3.37 comparison of reflection coefficients of CPW with and without FSS reflector

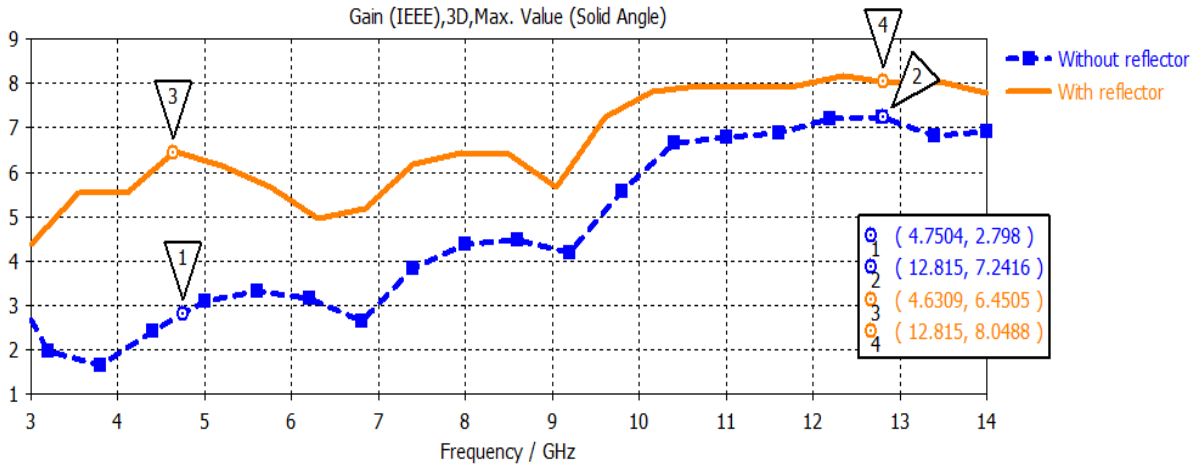

Figure 3.38 comparison of gain of CPW antenna with and without FSS reflector

3.6.2.5 Radiation pattern of CPW fed antenna with and without FSS reflector:

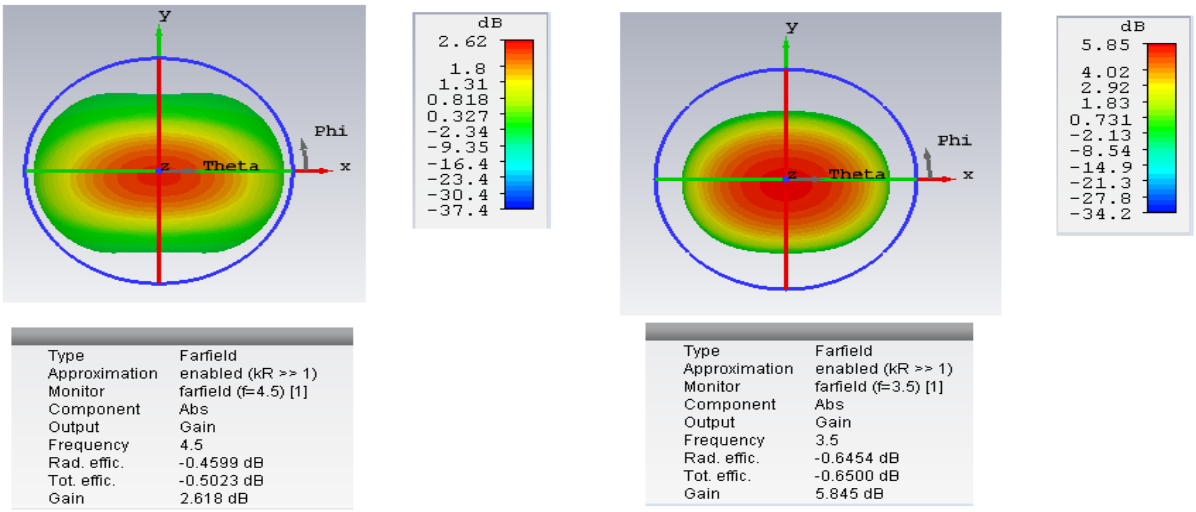

(a) (b)

Figure 3.39 (a-b) Radiation pattern of CPW antenna with and without FSS reflector respectively

Figure 3.39 (a) depicts the 3D radiation pattern of a CPW fed antenna without a use of FSS reflector. A single CPW antenna without FSS reflector having gain of 2.618 dB at frequency of 3.5 GHz is seen. In the presence of FSS reflector side lobes and back lobes merge into main lobe and hence an enhancement in the gain of antenna to 5.845 dB is seen as shown in Figure 3.39(b).

3.7 CONCLUSION

In this chapter a unit cell FSS for IEEE 802.11b stop and pass bands is designed and simulated foe transmission parameters. Then a Fan shaped FSS with polarization independent property for dual pass band of S and X band is designed and simulated. The basic fundamental of using complimentary geometry to obtain stop band behavior is utilized for getting a stop band response for S and X band respectively. A fractal ultra-wide stop band FSS is designed and simulated and applied as a reflector for a CPW fed antenna to improve its gain property. Next chapter presents the fabrication and testing of the proposed FSS to validate the simulated results.

CHAPTER 4

FABRICATION AND TESTING OF THE FREQUENCY SELECTIVE SURFACES

4.1 INTRODUCTION

This chapter presents the fabrication and testing of two FSSs that are designed and simulated in chapter 3. This chapters explains the fabrication process and testing of the prototype of two FSS using a VNA E5063 (Agilent) to evaluate the performance of the proposed FSS as band pass and band stop filters for S and X wireless communication bands.

4.2 FSS FABRICATION PROCESS

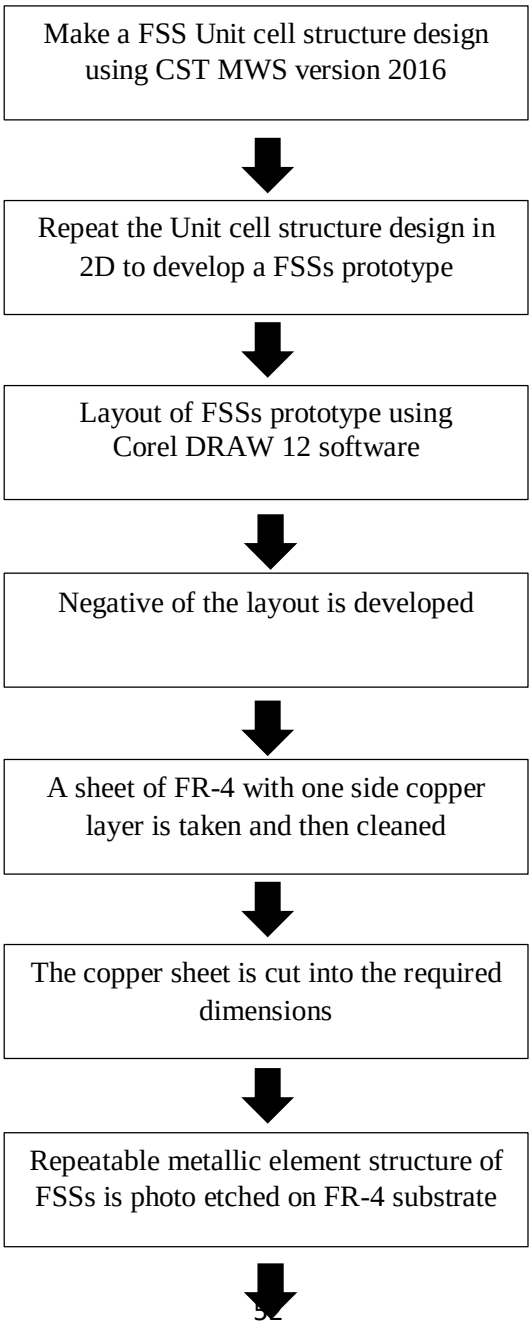

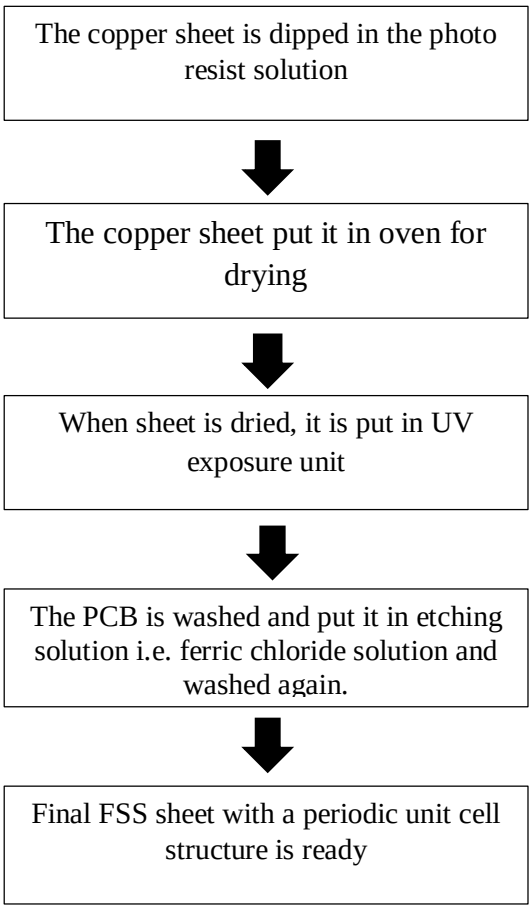

Figure 4.1 Flow Chart of Fabrication Process

4.3 INSTRUMENTS USED FOR FSS FABRICATION AND TESTING

The hardware used to design the prototype of the proposed FSS required two processes: Fabrication of the prototype and testing of the proposed prototype. The following steps are used to fabricate the prototype of FSS.

- Initially simulate the unit cell design of FSS in CST microwave studio version 2016.Then repeat the unit cell in 2D to form an array structure of FSS.
- Develop a layout of the FSS prototype using corelDRAW 12 software. Negative of the prototype is designed using same above software.
- A cleaned copper sheet is cut in required dimensions using PCB cutter as shown in Figure 4.2.
- Photo printing of FSS prototype is made on dielectric substrate.
- Then copper sheet is put in photoresist solution and after that it is placed in oven for drying span of 3-4 minutes at the temperature of 140-150 degree. Oven unit is shown in Figure 4.3
- Dried sheet of FSS is put in UV exposure unit. At last PCB is washed and put in ferric chloride solution and finally washed the PCB properly.

Figure 4.2 PCB cutter

Figure 4.3 Oven unit used for drying process

Testing of the FSS is done using VNA and two horn antennas operating from 20 KHz to 20 GHz. The FSS prototype that shown in Figure 4.4 is tested for S_{12} and S_{21} transmission parameters. Two highly calibrated horn antenna (with gain 12 dBi)having frequency range from 20 KHz to 20 GHz are connected to the two ports of the Agilent's VNA E 5063 . Prototype sheet of proposed FSS structure is placed in between the two radiating horn antennas for testing of transmission characteristics (S_{12} and S_{21}) of the proposed FSS sheets.

4.4 FABRICATED PASS BAND FSS PROTOTYPE

The layout of proposed FSS prototype is prepared by using corelDRAW 12 software and the PCB of prototype is prepared using the process mentioned in flowchart 4.1. Figure 4.4 (a) shows the unit cell structure of the pass band FSS for S and X wireless communication bands which is fabricated as a periodic FSS sheet of 13× 13 mm^2 using the process mentioned in section 4.2.

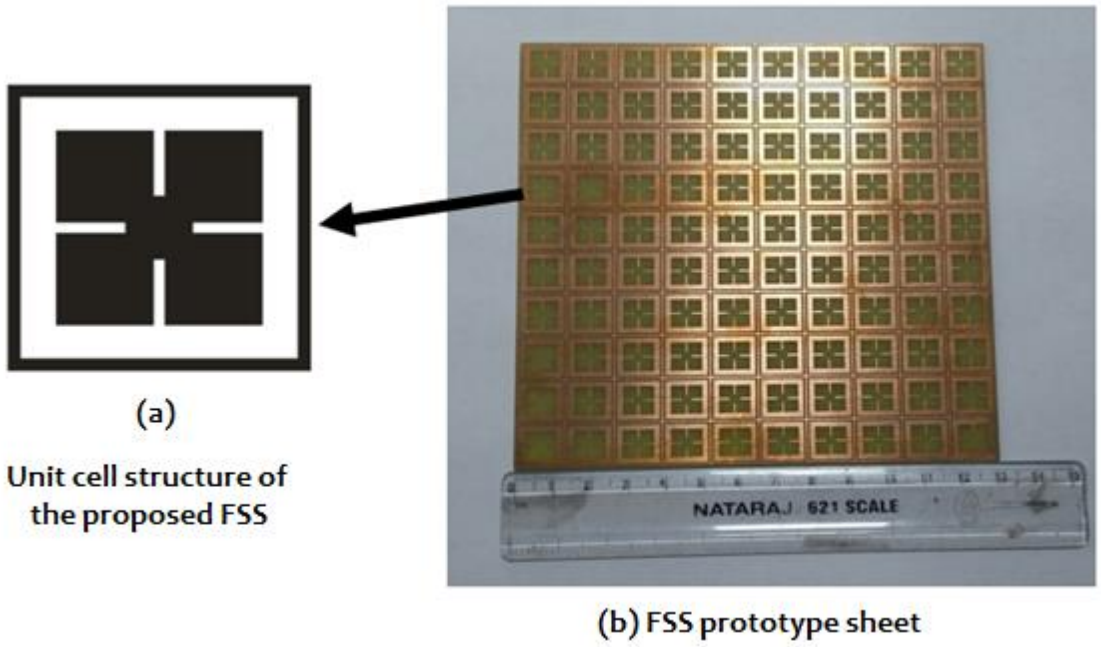

Figure 4.4 (a-b) Unit cell structure of FSS and Snapshot of the FSS prototype respectively

4.4.1 Measured Results of Pass Band FSS

Figure 4.5 depicts the comparison between the simulated and measured results in terms of transmission parameters of proposed FSS. It can be observed from Figure 4.5 that a satisfactory match between simulated and measured results is seen. The comparative detail of simulated and measured results are presented in table 4.1 from where we found that there is a very small variation in the simulated and measured results for first pass band while there is a variation of 1.27 GHz for higher frequency of the second pass band. Along with this resonance peak of stop band of measured results has been shifted from resonance peak of simulated results. These variation may be because of minor fabrication errors or because of reflection upon the environment near measuring equipment.

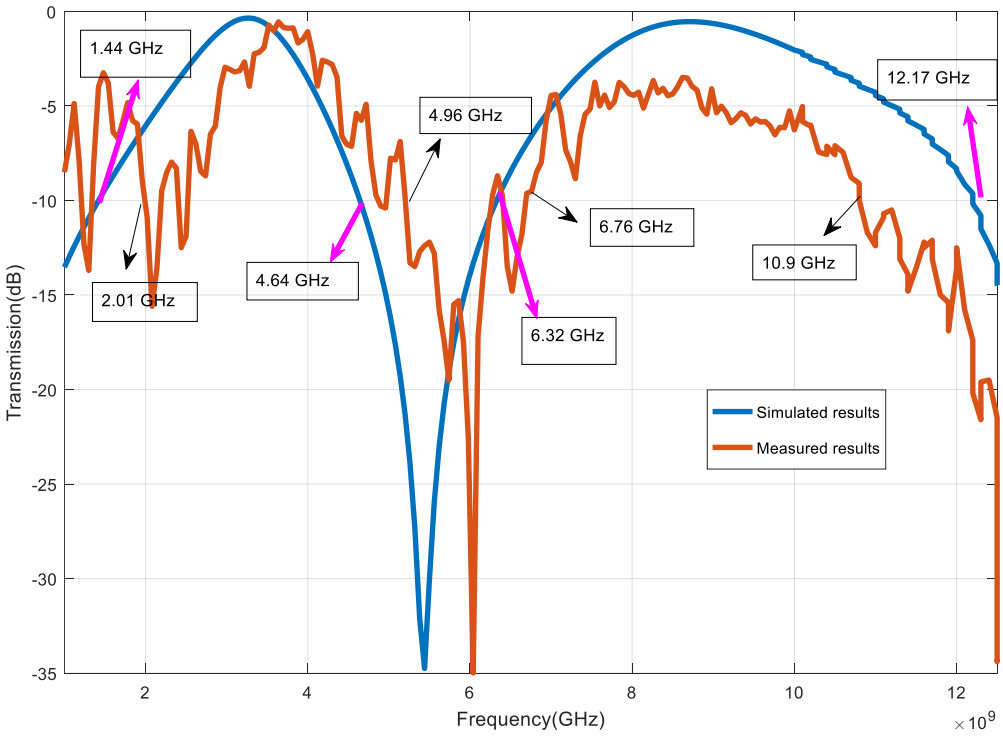

Figure 4.5 comparison between simulated and measured results

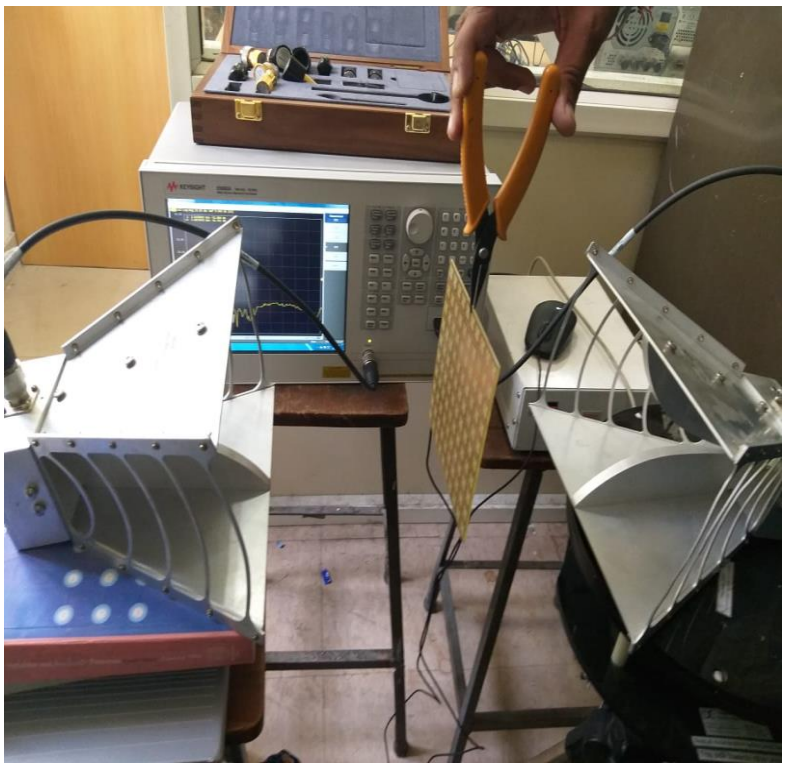

Figure 4.6 Set up for measurement of results

Table 4.1.Comparison between simulated and measured results

Results	First pass band (GHz)	Second pass band (GHz)	Band width for 1st band	Band width for 2nd band
Simulated results	1.44 GHz-4.64 GHz	6.32 GHz-12.17 GHz	3.2 GHz	5.85 GHz
Measured results	2.01 GHz-4.96 GHz	6.76 GHz-10.9 GHz	2.95 GHz	4.14Hz

It can be seen from table 4.1 that the simulated pass band for lower band is from 1.44 GHz to 4.64 GHz and measured results are from 2.01 GHz to 4.96 GHz. From table 4.1 we observed that bandwidth covers (simulated) for the first band is near about 3.2 GHz and for measured bandwidth for the first band is near about 2.95 GHz. In addition simulated and measured second pass band covers the frequency range from 6.32 GHz to 12.17 GHz and 6.76 GHz to 10.9 GHz respectively. Second pass band of the FSS for both simulated and measured covers nearly bandwidth of 5.85 GHz and 4.14 GHz respectively. Simulated and measured results are nearly matched.

4.5 **FABRICATED STOP BAND FSS PROTOTYPE**

The layout of proposed FSS prototype with dimensions of 195mm×195 mm×1.605 is prepared by using corelDRAW 12 software and the PCB of prototype is prepared using the process mentioned in flowchart Figure 4.1. Figure 4.7 (a) shows the designed unit cell for stop bands of S and X wireless communication bands. The prototype of the proposed FSS structure is shown in figure 4.7(b). Proposed FSS sheet is tested using two horn antennas and VNA for measurement of the FSS transmission parameters.

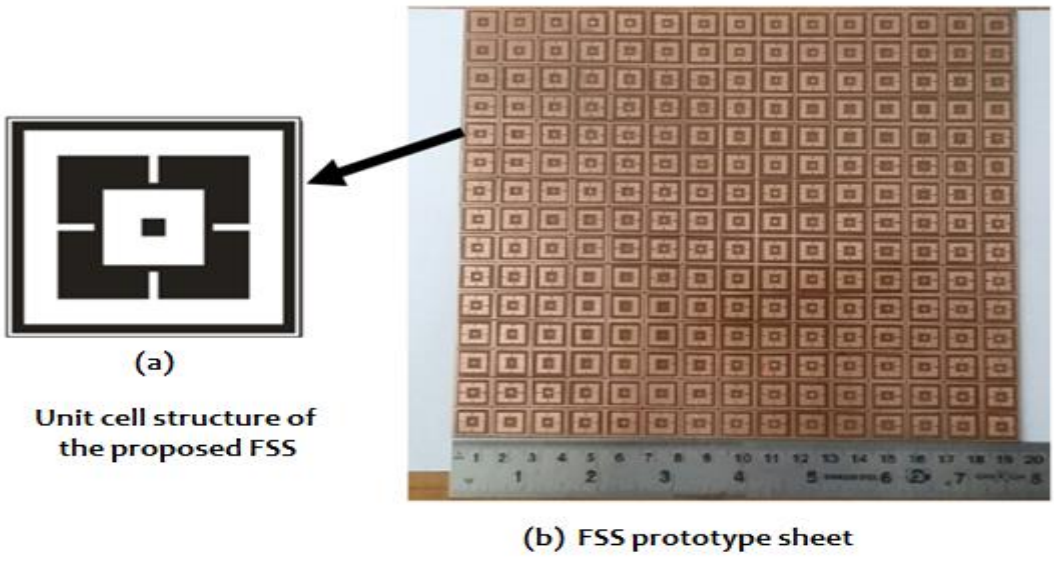

Figure 4.7(a-b) Unit cell structure of FSS and Snapshot of the FSS prototype respectively

4.5.1 Comparison between Simulated and Measured Results

Figure 4.8 depicts a comparison between the simulated and measured results in terms of transmission characteristics for the proposed stop band FSS. It can be observed from figure 4.8 that an acceptable match between simulated and measured results is seen. Table 4.2 also shows the comparison between simulated and measured results of the proposed FSS stop band filters for S and X bands. From Figure 4.8 it is seen that for first stop band i.e. 2.48 GHz to 4.8 GHz (measured) the return loss is different from simulated one and second stop band i.e. from 8.32 GHz to 12.45 GHz (measured) is nearly matched with simulated one.

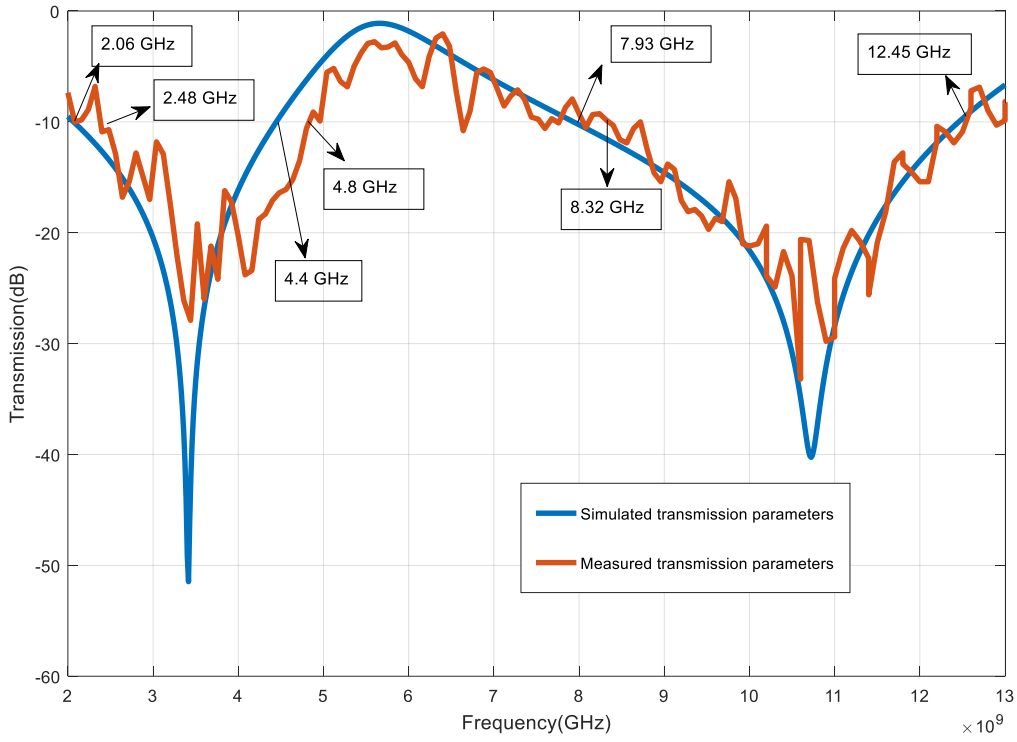

Figure 4.8 Comparison between simulated and measured results

Table 4.2 Comparison between simulated and measured results

Results	First pass band (GHz)	Second pass band (GHz)	Band width for 1st band	Band width for 2nd band
Simulated results	2.06 GHz- 4.4 GHz	7.93 GHz-12.45 GHz	2.34 GHz	4.52 GHz
Measured results	2.48 GHz-4.85 GHz	8.32 GHz-12.45 GHz	2.37 GHz	4.13 GHz

It can be seen from table 4.2 that the simulated stop band for lower band is from 2.06 GHz to 4.4 GHz and measured results are from 2.48 GHz to 4.85 GHz. From table 4.2. We observed that bandwidth

covers (simulated) for the first stop band is near about 2.34 GHz and for measured bandwidth for the first stop band is near about 2.37 GHz. In addition simulated and measured second stop band covers the frequency range from 7.93 GHz to 12.45 GHz and 8.32 GHz to 12.45 GHz respectively. Second stop band of the FSS for both simulated and measured covers nearly bandwidth of 4.52 GHz and 4.13 GHz respectively. Simulated and measured results are nearly matched.

4.6 CONCLUSION

The chapter presents the fabrication and testing of two proposed FSSs sheets (in chapter 3) for pass and stop bands of S and X wireless communication bands respectively. The variation of the simulated results of the proposed FSS sheets is done using a two port VNA with two radiating horn antenna connected at the two ports. The proposed FSS sheet is placed between them two horn to measure the transmission parameters S_{21} / S_{12} for the two sheets. A good match between the simulated and measured results allow the proposed FSS measured results allows the proposed FSS to be practically used as band pass and band stop filters applications for both the S and X communication bands respectively.

CHAPTER 5

CONCLUSION AND FUTURE SCOPE

5.1 CONCLUSION

In order to control the interference from nearby frequency bands in the wireless communication, it is essential to use some kind of filter in the antenna system that offer the filtering characteristics to specific wireless communication band. For this persistence, the FSS structures are the potential nominees. In order to carry out research on FSSs it is essential to study the state-of-the-art of design problems, band stop/band pass filtering performance and scattering characteristics mainly, the frequency response, bandwidth, and stability for angle of incident and different polarization modes of the structures. Therefore current thesis work presents the design, simulation and analysis of a few FSS structure based upon the gaps identified in the available literature. The application of the proposed FSS sheets to enhance the gain of a CPW fed antenna also proposed. The research work presented in this thesis is summarized as follow.

- The basic understanding and working of a FSS is explained and the mathematical analysis of the Unit cell structure of the FSS is carried out in chapter 1.With the help of analysis; Unit cell structures of the FSS are designed and simulated in CST MWS version 2016.
- The chapter 2 presents the literature review done in this thesis regarding four FSSs that are designed and two of them are fabricated and tested for practical applications. Based upon literature survey some research gaps has been find out and objective of thesis are also mentioned in this chapter.
- The chapter 3 presents the four antenna designs. In first design proposed a band stop SSLFSS at frequency 2.4GHz and further extended to design the band pass SSLFSS structure. As we seen from the simulation results that proposed FSS structure is miniaturized. Along with this proposed FSS structure is independent of angle of incident and polarization. Frequency range from 1.88GHz to 2.89 GHz is blocked by FSS structure and resonance peak occur at 2.4 GHz. This stop band FSS structure allows frequency from below 1.88 GHz and frequencies above the range of 2.89 GHz to pass through. For band pass FSS structure frequencies from 1.08 GHz to 4.5 GHz are allowed to pass through but frequencies before to 1.08 GHz and beyond to 4.5 are blocked by FSS structure. Proposed FSS is insensitive to angle of incident.

Table 5.1 Simulated results for Proposed SSLFSSs:

Band stop FSSs		Band pass FSSs	
Frequency range (GHz)	Bandwidth (GHz)	Frequency range (GHz)	Bandwidth (GHz)
1.88-2.89	1.01	1.08-4.5	3.42

- Objective 2 of the proposed research work was design and simulate (section 3.2) a Fan shaped FSS geometry imprinted on FR-4 substrate. The proposed FSS offers polarization independence to the incoming electromagnetic waves in both TE and TM modes. A simulated AR bandwidth for pass bands of 'S' (1.44GHz to 4.64 GHz.) and the 'X' (6.3GHz to 12.1GHz) bands is also observed. The simulated results also show a stable performance of the proposed FSS for variation in angle of incidence up to 30 degrees for lower band and up to 45degrees for the upper band.

Table 5.2 Simulated results for Fan shaped FSSs

First pass band (GHz)	Second pass band (GHz)	Band width for 1st band	Bandwidth for 2nd band
1.44 GHz-4.64 GHz	6.32 GHz-12.17 GHz	3.2 GHz	5.85 GHz

The proposed FSS sheet to be practically applicable for microwave filter applications to filter out the unwanted interferences from nearby bands of 'S' and 'X' bands, typically for the efficient working of WLAN , Bluetooth, ZIGBEE and Satellite communications .

- Third objective (section 3.3) is complimentary of the second design (objective) and it is optimized to obtain the transmission characteristics that stop the entire S and X band of wireless communication. Proposed FSSs is designed and optimized using CST Microwave Studio version 2016.Proposed FSS structure offers the stop band transmission parameters from frequency range of 2.06 GHz- 4.4 GHz (S band) and 7.93 GHz-12.45 GHz (X band) for first and second band respectively. As the proposed FSS structure is dual stop band hence can be practically applicable to filter out the unwanted signals from the nearby frequency bands such as L band, C band and K band, typically for efficient working of WLAN, ISM band, Bluetooth ,ZIGBEE, military areas, weather monitoring ,air traffic control, radar, satellite communication etc.

Table 5.3 Simulated results for complimentary of pass band (Stop band) FSSs

First pass band (GHz)	**Second pass band (GHz)**	**Band width for 1st band**	**Band width for 2nd band**
2.06 GHz- 4.4 GHz	7.93 GHz-12.45 GHz	2.34 GHz	4.52 GHz

- Fourth objective was based on the fractal geometry that offers the ultra-wide stop band (3.48 GHz – 12.24 GHz) transmission characteristics and covers the bandwidth of 8.76 GHz at normal angle of incident with resonance peak of frequency at nearly 8.2 GHz. It also shows angle of independency for incoming wave for TM mode only.

Table 5.4 Simulated results for Fractal geometry based Ultra wide stop band

Frequency band (GHz)	Bandwidth (GHz)
3.48-12.24	8.2

- In the fifth objective a CPW fed MPA is designed and simulated using CST Microwave Studio version 2016.Ultra wide stop band FSS that explained in section 3.5 is used as reflector to enhance the gain of the CPW fed MPA by an average of 2.25 dB.

Table 5.5 comparison of the antenna parameters with and without FSS reflector:

	Resonant frequency in GHz	Return loss in dB	Bandwidth (GHz)	Maximum peak Gain (dB)
Simulated results (without FSS reflector)	5.6 ,8.9	-33.04, 27.97	9.59	7.24
Simulated results (with FSS reflector)	3.52 ,5.36, 8.85	-34.44, -20.498, -37.77	9.717	8.048

- In the 4 chapter two dual band FSSs for both pass and stop band are fabricated and tested. Simulated and measured results of both the FSSs has been well matched with the simulated ones. Dual pass and stop band offers pass and stop transmission characteristics for S and X bands wireless communication. For pass band dual band covers from 2.01 GHz-4.96 GHz and 6.76 GHz-10.9 GHz respectively. In addition to this, complimentary structure of FSS offers dual band stop transmission characteristics for frequency range of 2.48 GHz-4.85 GHz and 8.32 GHz-12.45 GHz respectively.
- In chapter 5 conclusion of the each and every chapter has been mentioned.

5.2 DIFFERENT OPEN AREAS IN WHICH WORK CAN BE DONE IN FUTURE

1) In this thesis FSS design have a negligible thickness of the metallic pattern that is single square loop ($t << \lambda$), however it plays a very important role over the circuit parameters and consequently opens the door for 3-dimensional FSS.
2) More work can be done to make this FSS structure a conformal FSS structure.
3) Using fractal approach proposed FSS can be further miniaturized.
4) Duel or triple band FSS structure can be design using different number of Square loops.

5) More work can be done in the Mathematical analysis and modified the proposed FSS for getting better performance in terms of return loss and bandwidth.
6) FSS design can be extended to make a microwave absorber and use it for practical application of interest.

REFERENCES

[1] Theodore. S. Rappaport (2012).*Wireless Communication and practice*, 2nd Edition.

[2] Goldsmith Andrea (2005).*Wireless communications*, Cambridge University Press.

[3] Ic-pyo Hung (2015). Paper based frequency selective surface for stable angle of incidence, *IEICE Electronic express*, 12(7), 1-6.

[4] Yahya Rabia, Nakamura Akira and Itami Makoto (2016). Compact UWB frequency selective surfaces with angular stability, *IEICE Electronics Express*, 5, 39-43.

[5] Li Wei *et al.* (2017). A FSS of hybrid combined elements for dual-band operations, *IEICE Electronics Express*, Vol.14, pp.1–6.

[6] Zhao Zhenzhen *et al*. (2017).An Incident Angle Insensitive Band-Pass Frequency Selective Surface with Flat Top, *IEEE*, 273-274.

[7] Schennum G. H. (1973). Frequency Selective surfaces for multiple frequency antennas, *Microwave Journal*, 16, 55-57.

[8] Munk B.A. *Frequency selective surface - theory and design*. Wiley, New York, 2000.

[9] Wu T.K. *Frequency selective surfaces and grid array*, Wiley, New York, 1995.

[10] Balanis C. A. *Modern Antenna Handbook*, John Wiley & Sons, Inc. 2008.

[11] Marconi G. and franklin C.S. Reflector for use in wireless telegraphy and telephony, U.S. Patent, 1919.

[12] Fernandez J. J. S. Frequency Selective Surface for Terahertz Applications, Ph.D. Thesis, The University of Edinburgh, United Kingdom, 2012.

[13] Hui-Hsia Sung, "Frequency Selective Wallpaper for Mitigating Indoor Wireless Interference'', University of Auckland, 2006.

[14] Salvatore Celozzi, Rodolfo Araneo and Giampiero Lovat. *Electromagnetic Shielding*, John Wiley & Sons, Inc., 2008.

[15] Singh D., Kumar A., Meena S., and Agarwala V. (2012). Analysis of Frequency Selective Surfaces for radar absorbing materials, *Progress In Electromagnetics Research B*, 38, 297-314.

[16] C. Mias, C. Tsakonas and C. Oswald. *An Investigation into the Feasibility of designing Frequency Selective Windows employing periodic structures (Ref. AY3922),* Final Report for the Radio communications Agency, The Notting-ham Trent University, U.K.

[17] S. Islam *et al*. (2010). Effect of inter-element spacing variation on the performance of linear grounded frequency selective surface arrays in W-band, *Microwave and Optical Technology Letters*, 52, 155-160.

[18] Sung H.H. Frequency selective wallpaper for mitigating indoor wireless interference, PhD. Thesis, Electrical and Electronic Engineering, University of Auckland, 2006.

[19] T. Larsen (1962). A survey of the theory of wire grids, *IRE Transection on Microwave Theory and Techniques*, 10(3), 191-201.

[20] Langley R. J. and Drinkwater A. J. (1982). Improved empirical model for the Jerusalem cross, *IEE Proc. H (Microwaves, Optics and Antennas)*, 129, 1-6.

[21] Marcuvitz N., "Waveguide Handbook", Peter Peregrinus Ltd.: New York, vol.21, 1986.

[22] G. I. Kiani et al (2008). Angle and polarization-independent bandstop frequency selective surface for indoor wireless systems, *Microwave and Optical Technology Letters*, 50, 2315–2317.

[23] Natarajan R. et al. (2013).A compact frequency selective surface with stable response for WLAN applications", *IEEE Antennas and Wireless Propagation Letters*, 12, 718-720.

[24] Sesay M., Jin X. and Ouyang Z. (2014). Frequency selective surface with arbitrary shapes and its application to filter design, *Progress In Electromagnetics Research B*, 57, 75–85.

[25] Mizeikis V. (2010). Fabrication of frequency selective surface structures by femtosecond laser ablation of gold films, *Journal of Laser Micro/Nano engineering*, 5, 115-120.

[26] Dmitriev V. and Kawakatsu M. N. (2012). Microwave switchable frequency selective surface with high quality factor resonance and low polarization sensitivit, *Journal of Microwaves, Optoelectronics and Electromagnetic Applications,* 11, 263-268.

[27] Mohammed T. Al Haddad, Design of Frequency Selective Surface (FSS) for Mobile Signal Shielding, Master of engineering in electronics and communication, The Islamic University Of Gaza, Palestine,2016.

[28] Yadav Sanjeev, Jain Chandra Prakash, Mohan Sharma Mahindra (2018) Polarization independent dual-band pass frequency selective surface for Wi-Max applications. International Journal of RF Microwave Computer Aided Engineering 28(6), 1-7.

[29] Egemen Yilmaj Asim, Mustafa Kuzuoglu (2009). Design of the Square Loop Frequency Selective Surfaces With particle swarm optimization via the equivalent circuit model. *Radio engineering*, 18(2), 95-102.

[30] Barlevy Alon S. and Rahmat-Samii Yahya (1999). Control of Resonant Bandwidth in Frequency-Selective Surfaces by tilting the Periodic Elements, *Microwave and Optical Technology Letters*, Vol. 21.

[31] Guorui Chen, Ma Jinping Sz Li Chunhui and Yilin Chen (2000). Study on Frequency Selective Surfaces with Square Loop Slots, *Journal of Systems Engineering and Electronics*, 11(4), 11-16.

[32] Chun Yu, Cai-Cheng Lu (2005). Analysis of finite and curved frequency-selective surfaces using the hybrid volume-surface integral equation approach, *Microwave and Optical Technology Letters, Vol*. 45.

[33] Campos A. L. P. S., Oliveira E. E. C. de, and Silva P. H. F. (2009). Miniaturisation of frequency selective surfaces using fractal Koch curves, *Microwave and Optical Technology Letters, Vol*. 51.

[34] Egemen Yilmaz Asim and Mustafa Kuzuoglu (2009). Design of the Square Loop Frequency Selective Surface with Particle Swarm Optimization via the Equivalent Circuit Model, *Radio engineering*, vol. 18, 2009.

[35] Kiani Ghaffer I. et al (2010). Switchable Frequency Selective Surface for Reconfigurable Electromagnetic Architecture of Buildings, *IEEE transactions on antennas and propagation*, 58(2), 581-584.

[36] Yang Y., Wang X.-H., and Zhou H. (2012). Dual band frequency selective surface with miniaturized elements in low frequencies, *Progress In Electromagnetics Research Letters*, 33,167-175.

[37] In-Gon Lee, Ie-Pya Hong (2013). Frequency Selective Surfaces design for blind application, *European Conference on Antennas and Propagation*, pp.1-3.

[38] Costa Filippo, Monorchio Agostino and Manara Giuliano (2014). An overview of equivalent circuit modelling techniques of frequency selective surfaces and metasurfaces, *ACES Journal*, Vol. 29, 2014.

[39] Silva M. W. B., Campos A. L. P. S., and Kretly L. C. (2014). Design of thin microwave absorbers using lossy frequency selective surfaces, *Microwave And Optical Technology Letters*, Vol. 57.

[41] Mohamad Zoinol Abidin Abd. Aziz (2015). The investigation of single, dual and tri-band Frequency Selective Surface", *IEEE*, 79, 1-14.

[42] Ic-pyo Hung (2015). Paper based frequency selective surface for stable angle of incidence, *IEICE Electronic express*, 12(7), 1-6.

[43] Kartal Mesut and Doken Bora (2016). A New frequency selective absorber surface at the unlicensed 2.4-GHz ISM band, *Microwave and Optical Technology Letters*, Vol. 58.

[44] Yadav Sanjeev, Aseri Kiran and Sharma M. M. (2016). A Novel Band Pass Frequency Selective Surface for the Augmentation in the Performance of Wi- Max 2.5 / 3.5 GHz, *Antenna Test & Measurement Society (ATMS India-16)*, vol.28.

[45] Yun Junsik and Choi Jaehoon (2017). An All-Dielectric Band-Stop Frequency-Selective Surface", *Microwave and Optical Technology Letters*, Vol. 59.

[46] Varittha Sanphuang, Niru K. Nahar, and John L. Volakis (2017). THZ spatial filter employing bimaterial switching for temperature sensing, *Microwave and Optical Technology Letters*, Vol. 59.

[47] Zhang Hou, Zhong Tao (2017). Miniaturized frequency selective surfaces based upon 2.5-Dimensional closed spiral loops with stable resonant frequency, *IEEE*.

[48] Rahzaani Mahdiye, Dadashzadeh Gholamreza and Khorshidi Mohammadreza (2018). New technique for designing wideband one layer frequency selective surface in X-band with stable angular response", *Microwave Optical Technology Latter*, 60, 2133–2139.

[49] Silva Neto VP and D'Assunção AG (2018). Reconfigurable and stable frequency selective surfaces on non-uniform and finite arrays, *Microwave and Optical Technology Letters*, 60, 508–514.

[50] Antonio Luiz P. S. Campos and Elder Eldervitch C. de Oliveira (2010). Design of Miniaturized Frequency Selective Surfaces Using Minkowski Island Fractal, *Journal of Microwaves, Optoelectronics and Electromagnetic Applications*, Vol. 9.

[51] Davi B. Brito et al. (2013). A Minkowski Fractal Frequency Selective Surface with High Angular Stability, *IEEE*.

[52] Kaur Amanpreet, Kumar Naveen and Dr. Prasad Basudeo (2013). A Study of Various Fractal Antenna Design Techniques for Wireless Applications, *International Journal of Electronics & Communication Technology*, Vol. 4, pp. 47-50.

[53] Clarissa de Lucena Nóbrega et al. (2013). A compact frequency selective surface with angular stability based on the Sierpinski fractal geometry, *Journal of Electromagnetic Waves and Applications*, pp.1-9.

[54] Anshika Khanna, Dinesh Kumar Srivastava, Jai Prakash Saini (2015). Bandwidth enhancement of modified square fractal microstrip patch antenna using gap-coupling, *Engineering Science and Technology, an International Journal*, pp.286-293.

[55] Kubacki Roman, Mirosław Czy˙zewski and Dariusz Laskowski (2018). Minkowski Island and Crossbar Fractal Microstrip Antennas for Broadband Applications, *Applied Science,* vol.8, pp.1-9.

[56] Romeu Jordi and Yahya Rahmat-Samii (2000). Fractal FSS: A Novel Dual-Band Frequency Selective Surface, *IEEE Transactions on Antennas and Propagation*, Vol. 48, pp.1097-1105.

[57] J.-Y. Kim, J.H. Choi and C.W. Jung (2012). Band-notched planar UWB antenna using unit cells of frequency selective Surfaces, *Journal of Electromagnetic Waves and Applications*, Vol. 26, pp.2291–2303.

[58] Clarissa de Lucena Nóbrega et al. (2013). A compact frequency selective surface with angular stability based on the Sierpinski fractal geometry, Journal of Electromagnetic Waves and Applications, pp.1-9.

[59] Irfan Sohail Syed and Zarar Mohammad (2015). Electromagnetic shielding by frequency selective surfaces", *ARPN Journal of Engineering and Applied Sciences*, 10.

[60] Yahya Rabia, Nakamura Akira and Itami Makoto (2016). Compact UWB frequency selective surfaces with angular stability, *IEICE Electronics Express*, 5, 39-43.

[61] Li Wei et al. (2017). A FSS of hybrid combined elements for dual-band operations, *IEICE Electronics Express,* 14, pp.1–6.

[62] Zhenzhen Zhao et al. (2017). An Incident Angle Insensitive Band-Pass Frequency Selective Surface with Flat Top, *IEEE*, pp.273-274.

[63] Lia Qingya *et al*. (2018). A novel miniaturized-element frequency selective surface with a second-order band pass response, *IEICE Electronics Express*, 15, 1–6.

[64] Ranga Y. *et al.* (2012). Increasing the Gain of a Semicircular Slot UWB Antenna Using an FSS Reflector, *IEEE*, 478-471.

[65] Moufida Bouslama et al (2014). High gain Patch Antenna using a Frequency Selective Surface (FSS), *International Journal Of Communications*, 8, 16-20.

[66] Chatterjee Ayan, Parui Susanta Kumar (2015). Gain Enhancement of a Wide Slot Antenna Using a Second-Order Band pass Frequency Selective Surface, *Radio engineering*, 24(2), 455-461.

[67] Yahya Rabia, Nakamura Akira and Itami Makoto (2016). Design of constant gain UWB planar antenna using FSS-based reflectors, *IEICE Communications Express*, 5(1), 27–32.

[68] Aly Aboul-Dahab Mohamed *et al.* (2016). High Gain Compact Microstrip Patch Antenna For X-Band Applications", *International Journal of Antennas (JANT)*, 2(1), 47-58.

[69] Chatterjee Ayan, Pauri Susanta Kumar (2016). A Dual Layer Frequency Selective Surface Reflector for Wideband Applications, *RADIOENGINEERING*, 25(1), 67-72.

[70] Ghorbani Mahdi and Ghorbaninejad Habib (2017).Design of a High Gain Bandwidth Improved Aperture Antenna Using a Frequency Selective Surface**,** *ACES JOURNAL*, 32 (4), 318-324.

[71] Orr R. *et al*. (2015). Circular polarization frequency selective surface operating in Ku and Ka band, *IEEE Trans Antennas Propagation*, 5194 – 5197.

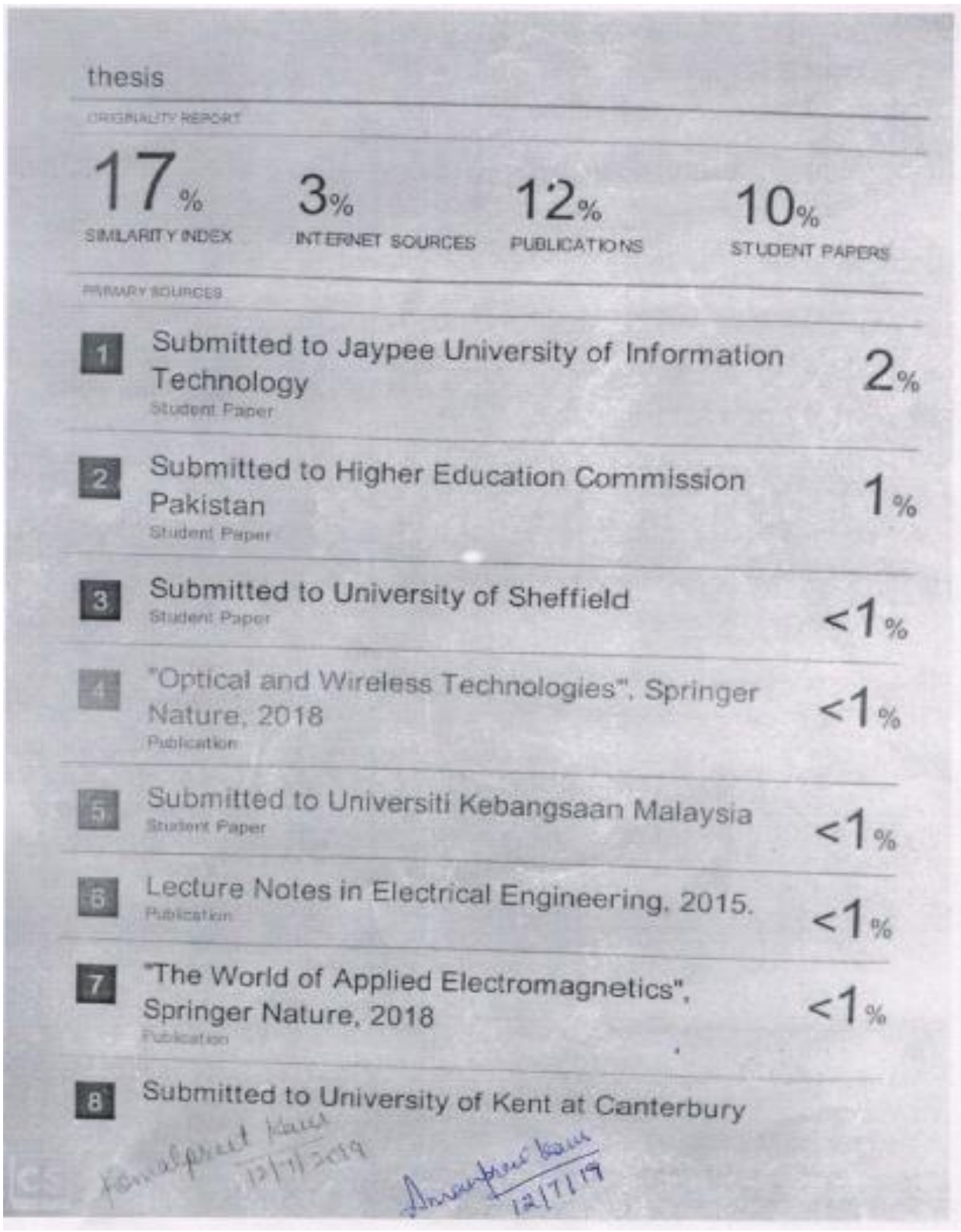

thesis

ORIGINALITY REPORT

17%	3%	12%	10%
SIMILARITY INDEX	INTERNET SOURCES	PUBLICATIONS	STUDENT PAPERS

PRIMARY SOURCES

1	Submitted to Jaypee University of Information Technology Student Paper	2%
2	Submitted to Higher Education Commission Pakistan Student Paper	1%
3	Submitted to University of Sheffield Student Paper	<1%
4	"Optical and Wireless Technologies", Springer Nature, 2018 Publication	<1%
5	Submitted to Universiti Kebangsaan Malaysia Student Paper	<1%
6	Lecture Notes in Electrical Engineering, 2015. Publication	<1%
7	"The World of Applied Electromagnetics", Springer Nature, 2018 Publication	<1%
8	Submitted to University of Kent at Canterbury	

Amanpreet Kaur 12/7/2019

Amanpreet Kaur 12/7/19